Safety Evaluation of Ship Operation in Coastal Area in terms of Optimal Ship Routing

LEE, SANGWON

(Degree)
博士（工学）

(Date of Degree)
2022-09-25

(Date of Publication)
2023-09-01

(Resource Type)
doctoral thesis

(Report Number)
甲第8473号

(URL)
https://hdl.handle.net/20.500.14094/0100477899

博　士　論　文

Safety Evaluation of Ship Operation in Coastal Area in terms of Optimal Ship Routing

（最適航法のための沿岸海域における船舶運航の安全性評価）

2022 年 7 月

神戸大学大学院海事科学研究科

LEE SANGWON

Safety Evaluation of Ship Operation in Coastal Area in terms of Optimal Ship Routing

Abstract

With the increasing demand for maritime transportation, optimal ship routing service has become an essential element in the shipping industry as well as the ship building fields. Many studies related to optimal ship routing are being conducted to achieve the most economical, environmentally friendly, and safe marine transportation around the world. However, there is relatively little interest in research on the ship operation that occur in coastal areas near ports, rather than ship navigation in the ocean. In particular, it is reported that more accidents occur during the ship operation such as berthing, mooring, and anchoring in the coastal area.

In many ports around the world, the safety measure and research have been continuously conducted to enhance the safety of these berthing, mooring, and anchoring operations for several decades. However, until now, ship accidents have continued in several ports. In spite of these efforts, there are still reports of ship accidents in coastal waters. It is essential to be more careful to prevent ship accidents in the coast because they can directly affect not only economic losses but also environmental pollution.

Recently, with the development of weather forecasting technology, ship accidents near ports have been decreasing. However, since errors in weather forecasts still occur, a complete reliance on weather forecasts can result in hazardous conditions for port and ship operations. Therefore, it is essential for smooth port management and safe ship operation to establish safety measures in preparation for failure in weather forecasting.

Therefore, in this study, the methodologies of safety evaluation for ship operation were proposed within berthing, mooring, and anchoring in coastal areas near ports. In this context, this study tried to suggest a novel methodology for safety reinforcement by approaching from three parts of ship operation, which is berthing, mooring, and anchoring near the port terminal.

To evaluate the safe berthing process, the measurement of the berthing velocity was performed. It was proposed to calculate the proper berthing velocity for the relevant terminal by statistically analyzing the measured data. As the size of the vessel increases, the size of the port terminal has become huge,

with the enhanced port facilities. However, the standard of the berthing velocity is still in use with the past standard that does not fit the reality without considering the change of recent size of ship. In addition, 'PIANC' (Permanent International Association of Navigation Congresses) is trying to set new standards by recognizing that past data such as 'Brolsma's curve' is not in conformity with the current navigation condition. Therefore, presenting the cases on the analysis of actual data about berthing velocity in each country, analysis was performed on collected data of berthing velocity from tanker terminals in Korea equipped with a DAS (Docking Aid System) which is a vessel speed measuring device. This measured data was classified by each vessel size and each jetty in this study. Through the analyzed results, it was compared and analyzed by plotting normal distribution, lognormal distribution, and Weibull distribution. In order to verify each distribution, visual confirmation was made using a Q-Q plot, and R-squared values were compared and verified. The linear regression was used to confirm the relationship between DWT and the berthing velocity of the ship. Finally, it was estimated to get the probability of exceedance for each distribution and propose a criterion for berthing velocity. It could provide navigators with basic data for safe berthing operation and to utilize it as basic data for efficient harbor and fender system design. This not only increases the durability of the marine structures but also reduce the maritime accidents where the vessel collides with the pier.

During the berthing process, the ship is moored using mooring facilities such as ropes, fenders, and bollards to conduct the cargo operations in port terminal. To ensure safe port operations, it is important to solve mooring problems. In particular, the many ports that face open seas have difficulties with long-period waves. As a countermeasure, the installation of a breakwater is proposed for mooring safety. However, this often cannot be put into practice because of financial issues. Instead, port terminals control berthing schedules with weather forecasting. However, mooring problems remain unsolved, because of inaccurate wave forecasting. To quantify the current situation, numerical simulations are presented with ship motions, fender deflections, and rope tensions. In addition, novel simulations for mooring ropes are proposed considering tension, friction, bending fatigue, and temperature. With this novel simulation, the optimal mooring method in terms of safety and economic efficiency was confirmed. In terms of safety, the optimal mooring method is verified to minimize dangerous mooring situations. Moreover, the optimal mooring method shows economic benefits and efficiency. It can help to reinforce the safety of port terminals and improve the efficiency of port operations.

The next area to examine is the safety operation for the anchored ship. In recent years, the number of waiting ships in offshore anchorage has increased owing to several reasons, such as the port lockdown and increased cargo volumes in maritime transportations. Moreover, port terminals have ordered ships to stay outside the harbor to prevent mooring accidents when rough waves are forecasted. Anchored

ships have been exposed to dangers owing to dragging anchors under rough sea conditions, especially those facing the open seas. In this study, we perform a numerical simulation of anchored ship motions to reproduce the dragging anchor. Additionally, we further evaluated the anchored ship motions based on underestimated wave conditions. Lastly, we constructed a novel risk assessment technique for anchored ships to assess the stranding risk, damage to marine structures, and risk of collision. The stranding risk was evaluated based on the relationship between the vertical displacement and Under Keel Clearance (UKC). Damaging risk can be identified from the information of harbor charts. The risk of collision was quantitatively assessed considering the main influential factors such as Closest Point of Approach (CPA), and the Ship Domain Overlapping Index (SDOI). Results showed that the proposed methodology can contribute to port safety and ship operation in terms of optimal ship routing.

This study was conducted to evaluate the safety of berthing, mooring, and anchoring processes for the prevention of the accidents during ship operation in the coast. The framework and methodology developed in this thesis could provide the enhanced safety guideline to manage and operate the ship as well as the port terminal. The proposed methodology in each operation still has many limitations and needs to be improved. Especially, there was insufficient data on the actual measurement of each ship's operation process. In order to broadly apply the methodology in this study, it is necessary to measure actual operational data for various types of ports and ships. Further research should use more abundant measurement data to identify differences from the results of this study.

Since ship accidents cause huge casualties and serious environmental pollution problems, it is necessary to further strengthen port and ship safety by using the methodology of this study before accidents occur. The practical and novel approach in this study can greatly contribute to prevention of accidents from the perspective of safe ship operation near the coastal water. In addition, it is expected that the results of the studies carried out in this thesis can help identify the causes of previous accidents by showing an approach from a new perspective to related operations and managers.

CONTENTS

List of Figures

List of Tables

1. Introduction

1.1 Background

The amount of maritime cargo is predicted to increase up to 15 billion tons in 2050 (Qinetiq et al., 2013). It means that maritime transportation will be the dominant means of transportation in the global era for years to come (Corbett et al., 2010; Ducruet, 2020). Numerous studies on optimal ship routing for the safe operation of ships have been performed, in accordance with the interest of the energy savings and sustainability. Safety maneuvering in the ocean is one of the main purposes of a ship. However, the ship must enter a port to achieve its own purpose of maritime transportation for the cargo transportation. The ship operation must include the non-nautical operation such as the mooring and anchoring near the port, as well as the maneuvering in the ocean.

When a ship arrives in the port, it goes through the procedures of entering the port through several steps.

(A) Upon arrival, the vessel will report to the port authority and check whether it is possible to berth directly or not. If there is enough berthing area with the proper weather conditions, there is no waiting period through anchoring in the offshore anchorage, and immediate berthing takes place. There is a possibility waiting in the offshore anchorage for several hours to days until the berthing site is assigned.

(B) After getting the berthing assignment, the pilot boards the ship for berthing operation at the pier. A pilot who understands the topographical characteristics of the port will conduct safe berthing together with the captain. As the finishing work of berthing, the captain checks whether the vessel is well moored with the mooring facilities of the pier.

(C) While mooring for several hours or days in the port through mooring facilities such as mooring lines, fenders, and bollards, the cargo operation will be carried out. During the cargo operation, the moored ship motions should be under control within the safe range.

All these operation in port must be carried out safely, so that the ship can continue the maneuvering and maritime transportation. The period of each operation could vary depending on the type, size of vessel, characteristics of the port, etc. In particular, the number of ships which had to stay in offshore anchorage, are extremely increased due to the recent impact of COVID-

19. In addition, there is a risk of mooring accidents due to unreasonable work planning in the port during bad weather.

As mentioned, the ship operations in port except for maneuvering can be divided into three perspectives; Anchoring for waiting, berthing process, mooring for cargo operation. According to Ventikos et al. (2015) and EMSA (2020), approximately 50-70 % of ship accidents have been reported to occur in port or coastal waters. These accidents have mainly been caused by the influence of rough weather during the anchoring, berthing and mooring operation. Therefore, it is necessary to develop the safety evaluation for each operations. To proceed the safety evaluation, the potential risk must be identified for each operation.

1.2 Introduction to the Ship Operation in the Coastal Area

1.2.1 Safety Evaluation for the Anchored Ship

Many studies have been carried out for the evaluation of anchored ship motions with dragging anchor. The anchored ship located in offshore anchorage exposed to the open sea could encounter the various risks. Due to the anchorage's location, the ship motions can be large with the long-period waves and rough waves. The large ship motions with dragging anchor caused by the rough waves can directly affect the accident of the anchored ship. Some studies have evaluated the anchored ship motions to simulate the dragging anchor, which occurs under strong winds during the offshore harbor refuge for typhoons (Inoue, 1981; Kikutani et al., 1983). However, these studies only considered wind forces. Zou et al. (2012) simulated anchored ship motions considering wave forces besides wind forces; however, the dragging anchors under stormy conditions were not analyzed. Sasa and Incecik (2012) studied the anchored ship motions for a stranded accident offshore harbor facing the Pacific Ocean during the offshore harbor refuge from a big typhoon. The ship stranded after it had drifted into the coast with the dragging anchor of long distances. Additionally, the dynamic model of anchor chain forces and the lumped mass method were introduced to accurately evaluate the mooring forces. Wave forces are considered as the dominant factor in causing ships to be stranded, given that stranding occurs due to vertical motions, and the dragging anchor, other than wind forces, can occur due to long periods of drift forces in irregular sea. The anchored ship motions are compared in each combination of external forces, such as wind forces, linear and non-linear wave forces in time domain motion analysis. It was observed that stranding accidents can occur due to combined external forces among wind

forces, and linear and non-linear wave forces. However, these studies are not widely applied to the safety analysis of ships in coastal sea areas, indicating that the emergency operation still depends on the intuition of ship masters (Sharpey-Schafer, 1954; Zhang and Zhao, 2013; Lu and Bai, 2015).

Anchored ship motions with dragging anchor are the key factor for evaluating safety for ships in coastal areas. It is important to reproduce the following points, which are vertical ship motions when stranding in shallow waters, damaging structures under the seabed such as cables or pipes by the anchor motion, and collisions with other ships. In the field of maritime transportation, many studies have been conducted on ship domains to analyze the risk of collision (Fujii and Tanaka, 1971; Kearon, 1977; Coldwell, 1983; Pietrzykowski and Uriasz, 2009; Hansen et al., 2013; Wang and Chin, 2016). Im and Luong (2019) proposed Potential Risk Ship Domain (PRSD) to evaluate the potential risk of collision in real time within the Collision Assessment zone. Further, Luong et al. (2021) developed the Marine Traffic Hazard Index (MaTha Index) to represent the dynamic waterway risk. The MaTha Index shows the high-risk collision area of the waterway using the Harbour Traffic Hazard Map. Pietrzykowski and Wielgosz (2021) determined the impact of ship size and speed to ship domain area based on simulation tests. Various risk assessment models of autonomous ships in actual seas have been derived to avoid collision of ships (Tam and Bucknall, 2010; Chai et al., 2017; Liu and Shi, 2020). As mentioned, congestion of ships in the offshore anchorage should be considered given that most collisions occur in coastal areas, especially in the vicinity of anchorage (Yeo et al., 2007; Debnath and Chin, 2016). Burmeister et al. (2014) proposed a collision model for marine risk assessment in offshore anchorages. The model estimated the risk of collision based on the function of collision frequency and consequence loss.

In most related models, the ship domain have shown as the ellipse shape due to the effect of the forward speed of the ship. However, it is not appropriate to analyze the collision risk of anchored ships with the same ship domain, because the anchored ships have almost zero speed in case of no drift due to dragging anchors. Liu et al. (2020) proposed a model to identify the risk of collision in offshore anchorage using the Automatic Identification System (AIS) database to derive the collision risk index (CRI) between ships in offshore anchorages. To evaluate the index, parameters such as the Distance at Closest Point of Approach, DCPA, Time to Closest Point of Approach, TCPA, and the SDOI were considered the main risk factors.

1.2.2 Safety Evaluation for Berthing Velocity

When the ship docks to the port facility, the berthing energy is generated according to the classification of the ship, the berthing method, angle and the velocity. In particular, the berthing velocity is a factor that has a great influence on the berthing energy, and the proper berthing velocity is determined at the time of the design of the pier according to the characteristic of the corresponding pier such as whether or not it is exposed to natural external force (Cho et al., 2018). If the ship's berthing velocity is excessive, it leads to accidents such as destruction of port facilities and damage to the ship hull. In the event of such an accident, it may lead to national economic damage due to the temporary closure of the pier as well as the repair cost of the pier and the ship's facilities.

For the proper berthing velocity, Brolsma's curve has been referenced in many countries since it was proposed in the 1970s, but has not been revised for a long time, requiring revision due to several limitations (Berkett Rankine, 2010; British Standards Institution, 2014). In addition, research on the automatic berthing has been conducted with the demand of safety berthing operation, however, there are little studies about proper berthing velocity (Bae et al, 2008; Nguyen and Jung, 2007; Park et al., 2006; Qiang et al., 2019). Meanwhile, PIANC (Permanent International Association of Navigation Congresses), an international organization, conducted the study on fenders that absorb berthing energy through the analysis of berthing velocity (PIANC, 2002), and recently presented the guideline for the berthing velocity in the concept of excess probability (PIANC, 2017). Yamase et al. (2013) confirmed that the berthing velocity is suitable for the log-normal distribution in the berthing energy calculation. In addition, it was confirmed that the correlation between the berthing velocity and DWT is not relative. Roubos et al. (2016) analyzed the measured berthing velocity data collected at Rotterdam Port in the Netherlands to identify the factors affecting the berthing. The berthing velocity of ships was analyzed by classifying by ship type and size, the UKC (Under-Keel Clearance), the conditions of natural external force, and the influence of the tugboat. It showed that the berthing velocity was greatly influenced by the pilot's proficiency, and the berthing assistance device, showing the Weibull distribution than the log-normal distribution. Perkovic et al. (2017) developed an integrated laser distance system that can monitor the safe berthing by synthesizing data such as berthing velocity and angle using a laser system, in a container terminal.

1.2.3 Safety Evaluation for the Moored Ship

Many studies have investigated the behavior of moored ships through physical experiments, numerical simulations, and field observations (Kubo and Barthel 1992; PIANC 1995; Kubo and Sakakibara 1997; Shiraishi et al. 1999). In this process, the influence of waves, such as long-period waves and harbor resonance has been identified as the main cause of large ship motions. Kubo and Sakakibara (1999) proposed the expansion of breakwaters and improvement of the mooring system as countermeasures to mooring issues. With countermeasures, such as the expansion of breakwaters, it was expected that mooring problems could be solved. However, the economic slowdown in the 2000s, such as in the global economic crisis, hindered the progress of measures that incur large scale construction costs. Even after 20 years, many ports suffer from mooring difficulties due to long-period waves (Van der Molen, Monárdez, and van Dongeren 2006; Kwak, Moon, and Pyun 2012; López and Iglesias 2014; Van der Molen et al. 2015; Sasa et al. 2018, 2019a). Sasa (2017) found that coastal passenger ships mooring at islands, which are exposed to the ocean, have been placed in dangerous conditions by long-period waves. Harbors exposed to dangerous situations have used the weather forecast system as an alternative to reduce mooring risks by evacuating ships from piers when rough weather is predicted. Despite these efforts, the nationwide questionnaire and field survey in this study show that various ports still have serious mooring problems. First, mooring arrangements have not been completely symmetrical at many port terminals. Based on the Schellin and Östergaard (1995) and Oil Companies International Marine Forum (OCIMF) (2018) recommendations, mooring arrangements should be as symmetrical as possible near the mid-part of the vessels. However, despite the recent trend of increasing ship size, port facilities and mooring arrangements have remained unchanged. This is the reason why the life cycle of ships (20 years) is much shorter than that of ports (50 years). Thus, the length of the quay wall has been insufficient for newly built larger ships. This eventually leads to an unbalanced mooring configuration. These incomplete mooring arrangements can cause the mooring force to be concentrated on a specific mooring rope, which increases the risk of accidents (ATSB 2008). Second, in these ports, the weather forecasting service is based on criteria such as allowable wave height (Shiraishi, 2009; Yoneyama, Minemura, and Moriya 2017). When forecasted rough weather, such as typhoons or long-period waves exceed the criteria of acceptability, the berthing of the ship would be delayed. However, weather forecasts cannot always be accurate, and these failures of forecasts have resulted not only in additional offshore anchoring, leading to additional losses, but also mooring accidents caused by unpredicted rough waves. Third, moored ship motions vary significantly depending on the

material of the mooring rope. To reduce ship motions, it is more advantageous to use high-modulus poly ethylene (HMPE) ropes or wire ropes, which have a low stretch of about 3–5%, rather than conventional synthetic fiber ropes, such as nylon and poly-propylene (PP) ropes with a high elasticity of about 20–30% (Villa-Caro et al., 2018). However, these HMPE ropes are not adopted by many shipping companies owing to various disadvantages, such as high price and vulnerability to high temperatures, especially for bulk carriers.

As these various effects and environmental forces act in combination, mooring accidents caused by mooring ropes have occurred in many ports. These mooring accidents eventually result in hull damage and human accidents. The main causes of rope breakage are a sudden force over breaking load, repetitive moderate tension, and unusual situations, such as human error and chemical effects (Overington and Leech 1997; Ridge et al. 2015). Nevertheless, previous studies on mooring problems have only focused on the tension of the mooring rope, and not considered the friction (Van der Molen, Monárdez, and van Dongeren 2006; Sakakibara and Kubo 2009; Sasa et al. 2018, 2019a). However, several studies have confirmed heat generation due to friction when cyclic tension is applied to the rope (Karnoski and Liu 1988; Hearle et al. 1993; Overington and Leech 1997). Even if the applied tension does not exceed the safety threshold of the mooring rope, the repeatedly applied forces eventually damage the ropes with heat generation because of the accumulation of friction energy (Yamamoto et al. 2004; Yamamoto, Kubo, and Asaki 2006; Yamamoto 2007). This frictional heat can be divided into external friction through contact on the mooring line surface, and internal friction because of contact between the inner strands of the mooring rope during repetitive extension. In the case of internal friction, it is mainly affected by the elongation of ropes and the contact area between the strands (Yamamoto, Kubo, and Asaki 2006). In the case of external friction, friction occurs mainly when the fairlead of the ship and the surface of the rope come into contact with large ship motions (Black et al. 2012). The friction and fatigue militate more in the bending part than in the straight part. This bending fatigue mainly occurs in wire ropes. It also largely affects ropes, such as HMPE ropes (Hobbs and Burgoyne 1991; Nabijou and Hobbs 1995; Sloan, Nye, and Liggett 2003; Bossolini et al. 2016). Ning et al. (2019) investigated rope failure through an experiment on the thermal damage of the rope with this bending fatigue.

1.3 Uncertainty of the Weather Forecasting Technology

Weather forecasting is one of the most important tools in all ship operation situations and is the

fundamental part of optimal ship routing. The accuracy of weather forecasting has become inevitable in handling dangerous situations in port operation. Furthermore, many studies have been conducted on weather forecasting at seas, which have been used to operate ships and ports (Chen et al., 2020; Lee et al., 2021). Despite the various developments in the weather forecasting technology, it is impossible to be perfectly accurate, that is, some errors still exist (Natskår et al., 2015; Girolamo et al., 2017). Chen and Wang (2020) demonstrated that forecasted results are sometimes significantly underestimated against the measured values, by 1.5–2 times. Considering underestimated weather conditions can be very dangerous for ships; it is crucial to understand its influence on ships quantitatively.

1.4 Objective and Outline of This Thesis

1.4.1 Objective

The main objective of this study is the development of the safety evaluation technique for each ship operation in coastal area, with respect to ship safety, economic efficiency as the part of optimal ship routing. The safety evaluation for the ship operation in coastal area will be conducted with the each part. In particular, the failure of weather forecasting is considered for the worst case scenario.

The total study will be divided into three main aspects to accomplish the main objective:

1. Propose the proper berthing velocity
2. Construct the evaluation method for the moored ship
3. Construct the safety evaluation method for the anchored ship

1.4.2 Outline of the Thesis

This study is divided into the five chapters to describe the total solution for the ship operation in coastal area as the part of optimal ship routing. Therefore, it consists of a total of seven chapters including an introduction and a conclusion. The flowchart is constructed for this study as shown in Fig. 1.1.

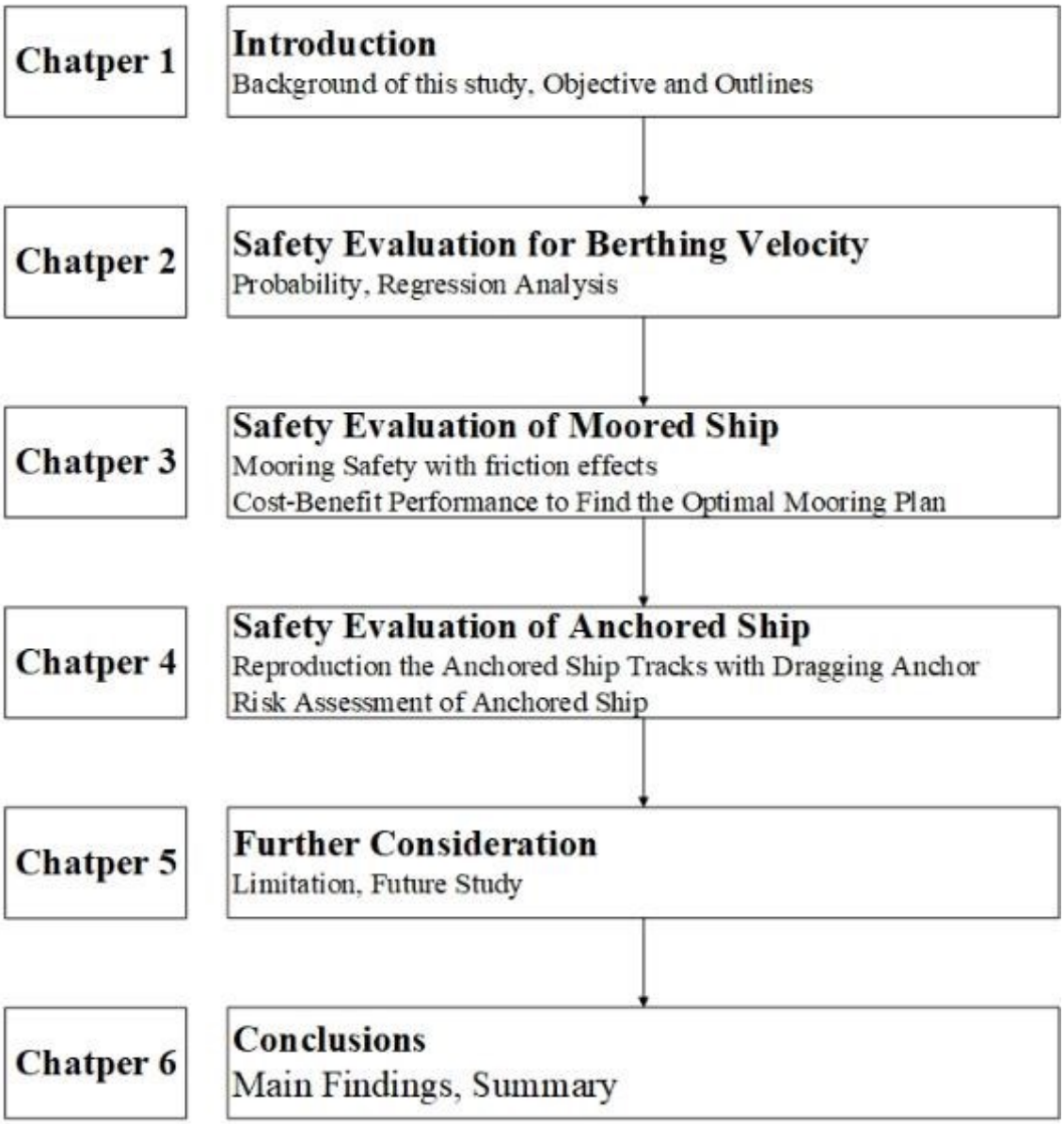

Fig. 1.1 Outline flowchart for the research work

Chapter 1 gives the brief introduction to the ship operation in coastal area. The background and necessity of this study has been described. In addition, the previous studies of the each part are described in this introduction.

Chapter 2 describes the analysis of the berthing velocity. To analyze the berthing velocity, the berthing velocity data were collected at a tanker jetty. The theoretical description for the estimating the berthing energy was presented in this chapter. For the statistical analysis using the

probability distribution function, the measured data was compared with the typical probability distribution function such as the normal, log-normal, and Weibull distribution function. The results with the probability distribution function were applied to the concept of probability of exceedance to calculate the predicted value at 1 / 1,000 and 1 / 10,000 probability. The regression analysis has been conducted to derive the relationship between ship size and berthing velocity by using the relationship. Relation curves for the berthing velocity were derived from measured data by linear regression analysis classified by confidence level.

Chapter 3 includes the numerical simulations of the moored ship motions. Safety evaluations of moored ships needs to consider the friction that leads to the point of mooring failure. In this study, a numerical model is developed for the temperature calculation of mooring ropes by considering the tension and friction caused by ship motions. First, the moored ship motions were calculated using measured wave data. These data show the effects of long-period waves, resulting in mooring problems. Subsequently, based on the 6 degrees-of-freedom of ship motions, the probability of breakage and temperature of the mooring rope is assessed with rope tension and elongation. Finally, the safety evaluation of moored ships could be modeled by considering force, friction, bending fatigue, and temperature as the main criteria. To confirm the effect of changing the mooring arrangement and the rope material for mooring safety, it was numerically simulated for case studies and evaluated using safety criteria. The results show that the proposed methods can reflect the actual situations and the effects of changing the mooring arrangement and rope material. In addition, the ships could stay in port with utmost safety and efficiency with the optimal mooring method.

Chapter 4 describes the safety evaluation methods for the anchored ships. To reproduce the anchored ship motions, the theoretical parts for the numerical simulation are described with the dynamic analysis for the anchor chain force. The description of onboard measurement systems against the 28,000-DWT class bulk carrier are summarized for approximately three years in global sea areas. The period of voyage, offshore anchoring, and stay inside the harbor was obtained from the measured data. It was noted that the ship was not on the voyage for approximately 40% of the operation time. The simulation results of anchored ship motions for each case and compares them with the ship motions from onboard measurement. The forecasting error should be considered to evaluate the emergency operation in the worst case scenario. Therefore, the simulation of anchored ship motion was conducted if the wave conditions were assumed as the underestimated results. Risk assessment for the anchored ship constructed including stranding, damaging, and collision accidents in anchorage. In particular, the risk of collision was evaluated by introducing

the relative risk factors with the AIS data.

Chapter 5 gives the limitation of this study and future developments direction of this study. This study tried to make the solution for the ship operation under the rough waves, especially under the failure of weather forecasting. The results of this study could be helpful for the several party related to port operations, such as ship operating companies (ship operators), port agencies (port operators), and local governments (port managers). However, there are still limitation of this study. The further discussion is described in this chapter.

Chapter 6 gives a brief conclusions with the main findings in this study.

References

ATSB (Australian Transport Safety Bureau). 2008. Independent investigation into the breakaway and grounding of the Hong Kong registered bulk carrier Creciente at Port Hedland, Western Australia on 12 September 2006. Canberra: ATSB. Accessed 31 May 2022. https://www.atsb.gov.au/publications/investigation_reports/2006/mair/mair232/.

Bae, C. H., Lee, S. K., Lee, S. E. and Kim, J. H., 2008. A Study of the Automatic Berthing System of a Ship Using Artificial Neural Network. Journal of Navigation and Port Research, Vol. 32, No. 8, pp. 589-596.

Beckett Rankine, 2010. Berthing velocities and Brolsma's curves. London, United Kingdom.

Black, K., S. J. Banfield, J. F. Flory, and I. M. L. Ridge. 2012. Low-Friction, Low-Abrasion Fairlead Liners. OCEANS 2012 IEEE/MTS Proceedings, Hampton Roads, USA, October 14–19, 1–11. https://doi.org/10.1109/OCEANS.2012.6405022.

Bossolini, E., O. W. Nielsen, E. Oland, M. P. Sørensen, and C. Veje. 2016. Thermal properties of Fiber ropes. Paper presented at European Study Group with In-dustry, Denmark: ESGI. https://orbit.dtu.dk/en/publications/thermal-properties-of-fiber-ropes.

British Standards Institution, 2014. Code of Practice for design of fendering and moorin g systems: BS6349 Part 4. BSI.

Burmeister, H. C., Walther, L., Jahn, C., Toter, S. and Froese, J., 2014. Assessing the fr equency and material consequences of collisions with vessels lying at an anchorage i n line with IALA IWrap MkII. *TransNav, the International Journal on Marine Navig ation and Safety of Sea Transportation*. Vol. 8, No. 1, pp. 61–68. https://doi.org/10.1 2716/1001.08.01.07

Chai, T., Weng, J. and Xiong, D., 2017. Development of a quantitative risk assessment model for ship collisions in fairways. *Safety Science*. Vol. 91, pp. 71–83. https://doi.org/10.1016/j.ssci.2016.07.018.

Chen, C., Sasa, K., Ohsawa, T., Kashiwagi, M., Prpić-Oršić, J. and Mizojiri, T., 2020. Comparative assessment of NCEP and ECMWF global datasets and numerical approaches on rough sea ship navigation based on numerical simulation and shipboard measurements. Applied Ocean Research. Vol. 101, 102219. https://doi.org/10.1016/j.apor.2020.102219.

Chen, S. T. and Wang, Y. W., 2020. Improving coastal ocean wave height forecasting during

typhoons by using local meteorological and neighboring wave data in support vector regression models. Journal of Marine Science and Engineering. Vol. 8, No. 3, 149. https://doi.org/10.3390/jmse8030149.

Cho, I. S., Cho, J. W., and Lee, S. W., 2018. A basic study on the measured data anal ysis of berthing velocity of ships. *Journal of Coastal Disaster Prevention*, Vol.5, No. 2,pp. 61-71, 2018. (in Korean)

Coldwell, T. G., 1983. Marine traffic behaviour in restricted waters. *Journal of Navigation*. Vol. 36, No. 3, pp. 430–444. https://doi.org/10.1017/S0373463300039783.

Debnath, A. and Chin, H., 2016. Modelling collision potentials in port anchorages: Appl ication of the Navigational Traffic Conflict Technique (NTCT). *Journal of Navigation*. Vol. 69, No. 1, pp. 183–196. https://doi.org/10.1017/S0373463315000521.

Ducruet, C., 2020. The geography of maritime networks: a critical review, *Journal of Tr ansport Geography*. Vol. 88, 102804. https://doi.org/10.1016/j.jtrangeo.2020.102824.

EMSA (European Maritime Safety Agency), 2020. Annual Overview of Marine Casualtie s and Incidents, Lisbon, Portugal, 147p. https://www.emsa.europa.eu/newsroom/latest-ne ws/item/4266-annual-overview-of-marine-casualties-and-incidents-2020.html.

Fujii, J. and Tanaka, K., 1971. Traffic capacity. *Journal of Navigation*, Vol. 24, No. 4, pp.543-552. https://doi.org/10.1017/S0373463300022384.

Girolamo, P. D., Risio, M. D., Beltrami, G. M., Bellotti, G. and Pasquali, D., 2017. The use of wave forecasts for maritime activities safety assessment. Applied Ocean Research. Vol. 62, pp. 18–26. https://doi.org/10.1016/j.apor.2016.11.006.

Hansen, M., Jensen, T., Lehn-Schioler, T., Melchild, K., Rasmussen, F. and Ennemark, F., 2013. Empirical ship domain based on AIS data. *Journal of Navigation*. Vol. 66, pp. 931–940. https://doi.org/10.1017/S0373463313000489.

Hearle, J. W. S., M. R. Parsey, M. S. Overington, and S. J. Banfield. 1993. Modelling the Long-Term Fatigue Performance of Fibre Ropes. Proceedings of the Third International Offshore and Polar Engineering Conference, Singapore, June 06–11, 377–383. https://www.onepetro.org/conference-paper/ISOPE-I-93-152.

Hobbs, R. E., and C. J. Burgoyne. 1991. Bending Fatigue in High-Strength Fibre Ropes. International Journal of Fatigue 13 (2): 174–180.

https://doi.org/10.1016/0142-1123(91)90011-m.

Im, N. and Luong T. N., 2019. Potential risk ship domain as a danger criterion for real-time ship collision risk evaluation. *Ocean Engineering*. Vol. 194, 106610.

https://doi.org/10.1016/j.oceaneng.2019.106610.

Inoue, K., 1981. An investigation on reducing cable tension caused by swing motion of ship moored at single anchor in wind-I: On the factors affecting the magnitude of cable tension. *The Journal of Japan Institute of Navigation*. Vol. 65, pp. 1–12.

https://doi.org/10.9749/jin.65.1. (In Japanese).

Karnoski, S. R., and F. C. Liu. 1988. Tension and Bending Fatigue Test Results of Synthetic Ropes. Proceedings of the Annual Offshore Technology Conference, Houston, USA, May 2–5, 343–350. https://doi.org/10.4043/5720-ms.

Kearon, J., 1977. Computer programs for collision avoidance and traffic keeping, *Conference on Mathematical Aspects on Marine Traffic*, London, United Kingdom, pp.229-242.

Kikutani, H., Tsuruta, S., Fukutani, T., 1983. Experimental and analytical study on the dynamic tension of mooring chain. *The Journal of Japan Institute of Navigation.* Vol. 69, pp. 17–23. https://doi.org/10.9749/jin.69.17. (In Japanese).

Kubo, M., and Barthel, V., 1992. Some Considerations How to Reduce the Motions of Ships Moored at an Open Berth. J. Japan Inst. Nav. 87, 47–58. http://doi.org/10.9749/jin.87.47.

Kubo, M., and Sakakibara, S., 1997. A time domain analysis of moored ship motions in a harbor considering harbor oscillations. Proceedings of the 7th International Offshore and Polar Engineering Conference, Honolulu, USA, May 25–30, 610–616. https://www.onepetro.org/conference-paper/ISOPE-I-97-345.

Kubo, M., and Sakakibara, S., 1999. A Study on Time Domain Analysis of Moored Ship Motion Considering Harbor Oscillations. In: Proc. 9th Int. Soc. Offshore Polar Eng. Conf. France, 574–581. https://www.onepetro.org/conference-paper/ISOPE-I-99-309.

Kwak, M., Y. Moon, and C. Pyun. 2012. Computer Simulation of Moored Ship Motion Induced by Harbor Resonance in Pohang New Harbor. Proceedings of 33rd Conference on Coastal Engineering, Santander, Spain, December 28, https://doi.org/10.9753/icce.v33.waves.68.

Lee, S. W., Sasa, K., Aoki, S., Yamamoto, K. and Chen C., 2021. New evaluation of ship mooring with friction effects on mooring rope and cost-benefit estimation to improve port safety. International Journal of Naval Architecture and Ocean Engineering. Vol. 13, pp. 306–320. https://doi.org/10.1016/j.ijnaoe.2021.04.002.

Liu, D. and Shi, G., 2020. Ship collision risk assessment based on collision detection al gorithm. *IEEE Access*. Vol. 8, pp. 161969–161980. https://doi.org/10.1109/ACCESS.2020.3013957.

Liu, Z., Wu, Z. and Zheng, Z., 2020. A novel model for identifying the vessel collision risk of anchorage. *Applied Ocean Research*. Vol. 98, 102130.

https://doi.org/10.1016/j.apor.2020.102130.

López, M., and G. Iglesias. 2014. Long Wave Effects on a Vessel at Berth. Applied Ocean Research 47: 63–72. https://doi.org/10.1016/j.apor.2014.03.008.

Lu, Y. and Bai, C., 2015. Dragging anchor event and theoretical verification of single m ooring ship. *Proceedings of the 9th International Conference on Frontier of Compute r Science and Technology, FCST 2015*, pp. 209–213.

https://doi.org/10.1109/FCST.2015.16.

Luong, T. N., Hwang, S. and Im, N., 2021. Harbour Traffic Hazard Map for real-time a ssessing waterway risk using Marine Traffic Hazard Index. *Ocean Engineering*. Vol. 239, 109884. https://doi.org/10.1016/j.oceaneng.2021.109884.

Nabijou, S., and R. E. Hobbs. 1995. Frictional Performance of Wire and Fibre Ropes Bent over Sheaves. The Journal of Strain Analysis for Engineering Design 30 (1): 45–57.

https://doi.org/10.1243/03093247V301045.

Natskår, A., Moan, T. and Alvær, P., 2015. Uncertainty in forecasted environmental conditions for reliability analyses of marine operations. Ocean Engineering. Vol. 108, pp. 636–647. https://doi.org/10.1016/j.oceaneng.2015.08.034.

Ning, F., X. Li, N. O. Hear, R. Zhou, C. Shi, and X. Ning. 2019. Thermal Failure Mechanism of Fiber Ropes When Bent over Sheaves. Textile Research Journal 89 (7): 1215–1223.

https://doi.org/10.1177/0040517518767147.

Nguyen, P. H. and Jung, Y. C., 2007. Automatic Berthing Control of Ship Using Adaptive Neural Networks. International Jouranl of Navigation and Port Research, Vol. 31, No. 7, pp. 563-568.

OCIMF (Oil Companies International Marine Forum). 2018. Mooring Equipment Guidelines. 4th ed. London: Oil Companies International Marine Forum.

Overington, M. S., and C. M. Leech. 1997. Modelling Heat Buildup in Large Polyester Ropes. International Journal of Offshore and Polar Engineering 7 (01): 63–69. https://www.onepetro.org/journal-paper/ISOPE-97-07-1-063.

Park, S. H., Cho, D.J. and Oh, S. W., 2006. A Study on Pseudolite-augmeted Positioning Method for Automatic Docking. Jouranl of Korean Navigation and Port Research, Vol. 30, No. 10, pp. 839-845.

PIANC (World Association for Waterborne Transport Infrastructure), 1995. Criteria for

movements of moored ships in harbor: A practical guide. Brussels: PIANC General Secretariat.

PIANC (World Association for Waterborne Transport Infrastructure), 2002. Guidelines for the design of fenders systems. Report of working group 33 of the MARITIME NAVIGATION COMMISSION.

PIANC (World Association for Waterborne Transport Infrastructure), 2017. Berthing velocities and fender design, Report of working group 145 of the MARITIME NAVIGATION COMMISSION.

Pietrzykowski, Z. and Uriasz, J., 2009. The ship domain – A criterion of navigational s afety assessment in an open sea area. *Journal of Navigation*. Vol.62, pp. 93–108. https://doi.org/10.1017/S0373463308005018.

Pietrzykowski, Z. and Wielgosz, M., 2021. Effective ship domain – Impact of ship size and speed. *Ocean Engineering*. Vol. 219, 108423. https://doi.org/10.1016/j.oceaneng.2020.108423.

Perkovic, M., Gucma, M., Luin, B., Gucma, L. & Brcko, T., 2017. Accomodating larger container vessels using an integrated laser system for approach and berthing. Microprocessors and Microsystems, Vol. 52, pp.106-116

Qiang, Z., Guibing, Z., Xin, H. and Renming, Y., 2019. Adaptive neural network auto-berthing control of marine ships. Ocean Engineering, Vol. 177, pp. 40-48.

Qinetiq, Lloyd's Register, and Univ. of Strathclyde, 2013. Global marine trends 2030. pp. 1–144.

Ridge, I. M. L., P. Wang, O. Grabandt, and N. O'Hear. 2015. Appraisal of Ropes for LNG Moorings. Proceedings of the OIPEEC Conference 5th International Stuttgart Rope days, Stuttgart, Germany, March 24–26. https://oipeec.org/products/appraisal-of-ropes-for-lng-moorings

Roubos, A., Groenewegen, L. and Peters, D. J., 2016. Berthing Velocity of Large Seagoing Vessels in the Port of Rotterdam. Marine Structures, Vol. 51, pp. 202-219.

Sakakibara, S., and M. Kubo. 2009. Initial Attack of Large-Scaled Tsunami on Ship Motions and Mooring Loads. Ocean Engineering 36 (2): 145–157. https://doi.org/10.1016/j.oceaneng.2008.09.010.

Sasa, K. and Incecik, A., 2012. Numerical simulation of anchored ship motions due to wave and wind forces for enhanced safety in offshore harbor refuge. *Ocean Engineering*. Vol. 44, pp. 68–78. https://doi.org/10.1016/j.oceaneng.2011.11.006.

Sasa, K. 2017. Optimal Routing of Short-Distance Ferry from the Evaluation of Mooring Criteria.

Proceedings of the International Conference on Offshore Mechanics and Arctic Engineering-OMAE 6 (2): 1–8. https://doi.org/10.1115/OMAE201761077.

Sasa, K., M. Mitsui, S. Aoki, and M. Tamura., 2018. Current Analysis of Ship Mooring and Emergency Safe System. Journal of Japan Society of Civil Engineers, Ser. B2 (Coastal Engineering) 74 (2): 1399–1404. https://doi.org/10.2208/kaigan.74.I_1399. (in Japanese).

Sasa, K., S. Aoki, T. Fujita, and C. Chen. 2019. New Evaluation for Mooring Problem from Cost-Benefit Effect. Journal of Japan Society of Civil Engineers, Ser. B2 (Coastal Engineering) 75 (2): 1243–1248. https://doi.org/10.2208/kaigan.75.I_1243. (in Japanese).

Schellin, T. E., and C. Östergaard. 1995. The Vessel in Port: Mooring Problems. Marine Structures 8 (5): 451–479. https://doi.org/10.1016/0951-8339(95)97304-Q.

Sharpey-Schafer, J. M., 1954. Anchor Dragging. *Journal of Navigation*. Vol. 7, No. 3, p p. 290–300. https://doi.org/10.1017/S0373463300020968.

Shiraishi, S., M. Kubo, S. Sakakibara, and K. Sasa. 1999. "Study on numerical simula-tion method to reproduce long-period ship motions." Proceedings of the 9th In-ternational Offshore and Polar Engineering, Brest, France, May 30–June 04, 536–543. https://www.onepetro.org/conference-paper/ISOPE-I-99-304.

Shiraishi, S. 2009. Numerical simulation of ship motions moored to quay walls in long-period waves and proposal of allowable wave heights for cargo handling in a port. Proceedings of the 19th International Offshore and Polar Engineering Conference, Osaka, Japan, July 21–26, 1109–1116. https://www.onepetro.org/conference-paper/ISOPE-I-09-232.

Sloan, F., R. Nye, and T. Liggett. 2003. Improving Bend-over-Sheave Fatigue in Fiber Ropes. OCEANS 2003 IEEE/MTS Proceedings, San Diego, USA, September 22–26, 1054–1057.

https://doi.org/10.1109/oceans.2003.178486.

Tam, C. and Bucknall, R., 2010. Collision risk assessment for ships. *Journal of Marine Science and Technology*. Vol. 15, No. 3, pp. 257–270. https://doi.org/10.1007/s00773-010-0089-7.

Van der Molen, W., P. Monárdez, and A. P. van Dongeren. 2006. Numerical Simula-tion of Long-Period Waves and Ship Motions in Tomakomai Port, Japan. Coastal Engineering Journal 48 (1): 59–79. https://doi.org/10.1142/S0578563406001301.

Van der Molen, W., D. Scott, D. Taylor, and T. Elliott. 2015. Improvement of Mooring

Configurations in Geraldton Harbour. Journal of Marine Science and Engineer-ing 4 (3). https://doi.org/10.3390/jmse4010003.

Ventikos, N. P., Koimtzoglou, A. and Louzis, K., 2015. Statistics for marine accidents in adverse weather conditions. Maritime Technology and Engineering – Guedes Soares & Santos (Eds). Taylor & Francis Group, London. pp. 243–251. https://doi.org/10.1201/b17494

Villa-Caro, R., J. C. Carral, J. Á. Fraguela, M. López, and L. Carral. 2018. A review of ship mooring systems. Brodogradnja 69 (1): 123–149. https://doi.org/10.21278/brod69108.

Wang, Y. and Chin, H., 2016. An empirically-calibrated ship domain as a safety criterion for navigation in confined waters. *Journal of Navigation*. Vol. 69, pp. 257–276. https://doi.org/10.1017/S0373463315000533.

Yamamoto, K., M. Kubo, K. Asaki, and Y. Kanuma. 2004. An Experimental Research on Internal Stress of Ropes Under Repeated Load. The Journal of Japan Institute of Navigation 112: 353–359. https://doi.org/10.9749/jin.112.353. (in Japanese).

Yamamoto, K., M. Kubo, and K. Asaki, 2006. Comparison between Numerical Calcu-lation and Experimental Results of Temperature Rise on Rope under Repeated Load. The Journal of Japan Institute of Navigation 116: 269–275. https://doi.org/10.9749/jin.116.269. (in Japanese).

Yamamoto, K. 2007. Basic Research on Preventing Breakage of Mooring Ropes. PhD diss., Kobe University. (in Japanese).

Yamase, S., Ueda, S., Okada, T., Arai, A. and Shimizu, K., 2013. Characteristics of Measured Berthing Velocity and the Application for Fender Design of Berthing Ship. Annual Journal of Civil Engineering in the Ocean, Vol. 69, No. 2, pp. 67-72. (in Japanese)

Yeo, G. T., Roe, M. and Soak, S. M., 2007. Evaluation of the marine traffic congestion of north harbor in Busan port. *Journal of Waterway, Port, Coastal, and Ocean Engineering*. Vol.133, No.2, pp.87-93. https://doi.org/10.1061/(asce)0733-950x(2007)133:2(87).

Yoneyama, H., K. Minemura, and T. Moriya. 2017. A study on calculation methods of allowable wave heights of a moored ship in remote island ports. Journal of Japan Society of Civil Engineers 73(2): 803–808. https://doi.org/10.2208/jscejoe.73.I_803. (in Japanese).

Zhang, P. and Zhao, J., 2013. The obligations of an anchored vessel to avoid collision at sea. *Journal of Navigation*. Vol. 66, No. 3, pp. 473–477. https://doi.org/10.1017/S0373463313000088.

Zou, Y., Shen, C. and Xi, X., 2012, Numerical simulations on the motions of anchored

capesize ships. *Journal of Navigation*. Vol. 65, No. 1, pp. 145–158. https://doi.org/10.1017/S0373463311000580.

Chapter 2 Measured Data Analysis of Berthing Velocity for Safety Berthing

2.1 Background

When the ship arrives at the port and docks to the mooring facility, the berthing energy is determined according to the classification of the ship, the berthing method, angle and the velocity. In particular, the berthing velocity is a factor that has a great influence on the berthing energy, and the proper berthing velocity is determined at the time of the design of the pier according to the characteristic of the corresponding pier such as whether or not it is exposed to natural external force. (Cho et al., 2018)

There are three main procedures for berthing operations at ports and wharf facilities.

First, the ship approaches the dock facility and approaches at the approximate speed. (Approaching speed)

Second, the fender absorbs the berthing energy generated through the first contact (Berthing) to the mooring facilities such as the fender of the wharf, and performs the berthing operations. In this case, the vessel’s velocity at the time of the first contact of the ship with the fender can be defined as the berthing velocity.

Third, after the last berthing operations, mooring lines, fenders, bollards and so on are monitored until the departure of safe mooring status and mooring safety is evaluated.

It is imperative that all three of these procedures be completed safely so that the vessel can complete safe cargo loading and unloading operations at the pier and ensure that the vessel can maintain adequate access and proper speed during this approach and docking.

Especially, if the ship's berthing velocity is excessive, the mooring facilities of the wharf may be destroyed or the ship may be damaged. In the event of such an accident, it may lead to national economic damage due to provisional shutdown of the quayside as well as repair of the quays and vessels. If the oil carriers, such as a very large crude oil carrier, engaged in this contact accidents with pier, marine pollution from oil spills may occur. Therefore, it is necessary for the port manager to estimate and manage the proper berthing velocity.

Today's ships are becoming bigger due to the development of shipbuilding technology and the

maneuvering performance is also developing. As a result, the characteristics of vessels are changing differently from the past. Vessel mooring facilities are also changing, including fenders and other factors affecting mooring.

Recently, the importance and necessity of DAS (docking aid system) have been emphasized, and many equipments have been installed to measure the berthing velocity at many port dock facilities. In particular, this can help secure navigation by monitoring information on the speed and location of a ship visually docked by the pilot working in a berthing operation, a manager of the port facility. In addition, there is an effect that the research on the measurement and analysis of the berthing velocity of the ship is activated through the measuring device.

In accordance with this international trend, the installation of DAS is legally recommended and installation is completed at the main port terminals. However, there are no guidelines and researches on the berthing velocity due to the delay of the activation of the equipment capable of measurement. Therefore, it is necessary to verify the designed berthing velocity of each port by collecting and analyzing the berthing velocity directly in Korea.

Therefore, in this study, the actual data of berthing velocity was collected and analyzed. Based on the results of the analysis, the predicted berthing velocity in the concept of probability of exceedance is presented. In addition, in order to raise the level of confidence in the characteristic value of the berthing velocity, which is being discussed internationally recently, the relation between the berthing velocity and the ship size according to the confidence level is derived and the basic data that can be utilized for calculating the appropriate design berthing velocity is provided.

This paper is composed of 5 chapters in total. In Chapter 2.2, the description of berthing energy and velocity are presented with the standards related to the berthing velocity. In Chapter 2.3, the outline of the measurement for the berthing velocity is explained. The probability distribution function that is best fit to the actual data is evaluated through comparison in Chapter 2.4. In Chapter 2.5, the relationship between ship size and berthing velocity are compared with the confidence level by using the relationship between ship 's main specifications and ship size. Finally, in Chapter 2.6, the summary will be discussed with main findings in this chapter. Fig. 2.1 shows the flowchart of this study.

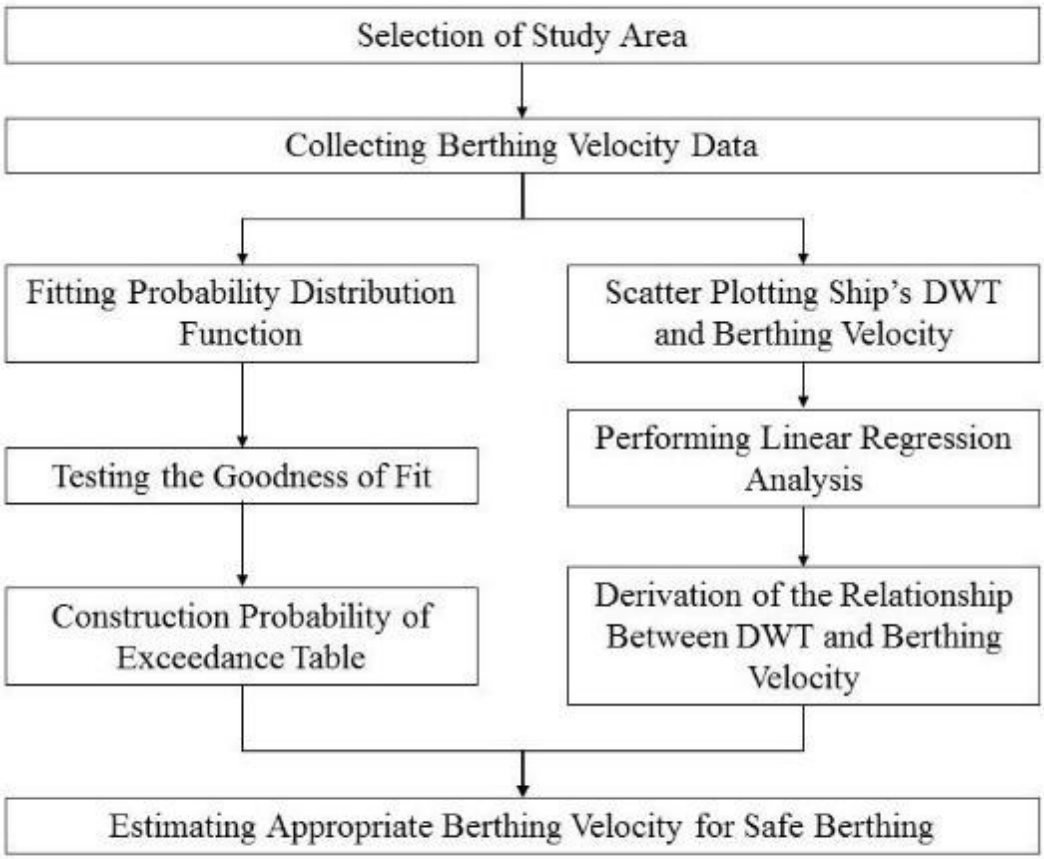

Fig. 2.1 Flow chart of the study

2.2 Overview of the Measurements for Berthing Velocity

2.2.1 Description of the Measurements System

DAS (Dock Mounted Docking Aid System) is installed in most tanker terminals and its arrangement is generally as shown in Fig. 2.2. As the size of vessels has recently become larger, the DAS's speedometer is measured with two laser sensors per berth, instead of the one measured, with a speed of 1 cm/s at a distance of 200 m from the berth. It is displayed on a large electric signboard so that when the ship is approached shore, the pilot and officers on board can identify the speed.

Fig. 2.2 Arrangement of Dock Mounted Laser System

2.2.2 Data Collection

Actual measured data for analyzing the characteristics of berthing velocity was measured in "Wharf A" classified by jetty 1 ~ 3 in single Korean port where DAS is installed. Data are collected from DAS measured from the ship berthed at the target quay for about 17 months from March 2017 to July 2018. The number of data classified by ship size and jetty is shown in Table 2.1. and Fig. 2.3. The maximum vessel capacity for each jetty is designed to be 80,000 DWT for jetty1, 120,000 DWT for jetty2, and 320,000 DWT for jetty3, and the maximum LOA is 295 m, 321 m, and 382 m respectively. The maximum berthing capacity for each jetty is determined by the size of the vessel. However, this does not determine the ship's berth size by the jetty, as seen in Table 2.1, it appears that vessels smaller than the maximum vessel berthed indiscriminately.

As seen in Table 2.1 and Fig. 2.3, the total number of berthing velocity data used in this study is 214, and there are 154 vessels under 100K DWT and 60 vessels over 100K DWT. In general, the berthing velocity is defined as the velocity of the first contact with the pier (Roubos et al., 2017 and 2018; MOF, 2014; Cho et al., 2018). The velocity of the ship is reduced to minimize the impact energy on the fender while the vessel is approaching to pier, and the velocity is also reduced due to the energy absorption by the fender after the first contact. The actual data used in this study, were the velocity measured from DAS of the front and back side at the time of contact with the ship. However, these two point data did not indicate which one of them is the first contact, since they were only displayed by numerical values without the time or distance from DAS to vessel. Since the velocity of the vessel might be reduced after the first contact with the pier and fender, larger velocity between contact velocity data measured from the bow and stern side of the vessel was assumed to be berthing velocity in this study.

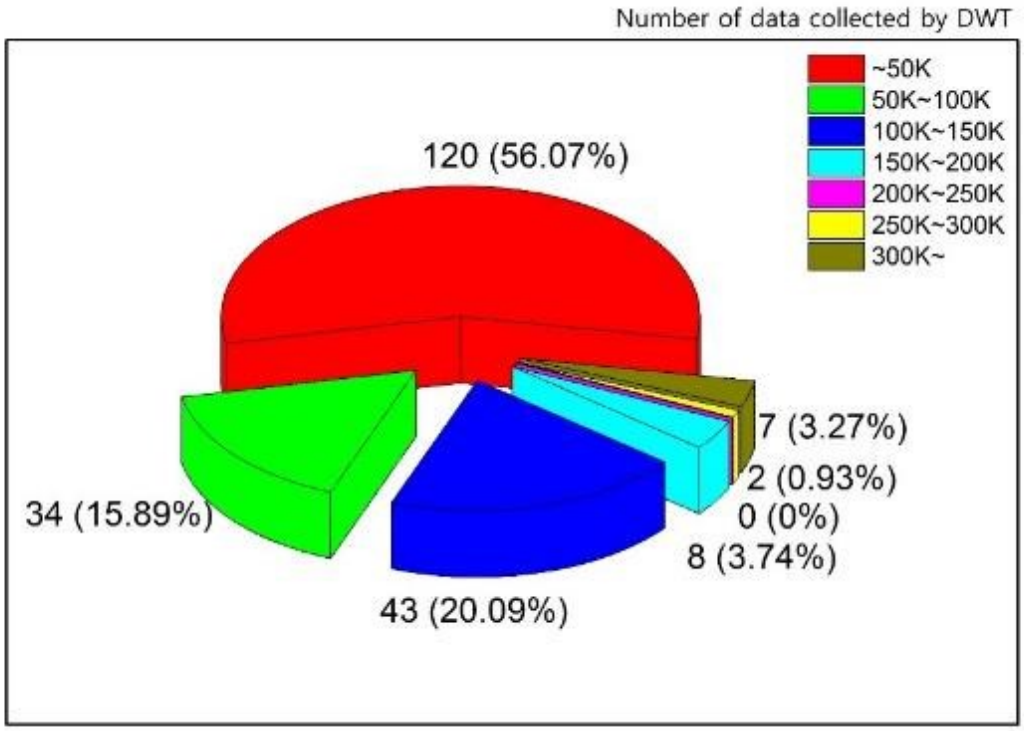

Fig. 2.3. Number of data collected by DWT

Table 2.1 Number of data collected by Jetty and DWT

DWT	Jetty 1	Jetty 2	Jetty 3	Total
~50K	65	55	-	120
50K~100K	24	5	5	34
100K~150K	-	4	39	43
150K~200K	-	-	8	8
200K~250K	-	-	-	0
250K~300K	-	-	2	2
300K~	-	-	7	7
All ships	89	64	61	214

The port was classified into Jetty 1 - 3 according to the maximum capacity of the berth. Jetty 1

was designed to have a berthing velocity of 12cm/s, and Jetty 2 and 3 was designed to have 15cm/s, respectively. Table 2.2 shows the characteristics of the port measuring the actual data collected in this study.

Table 2.2 Berth particular and operation regulations

	Jetty 1	**Jetty 2**	**Jetty 3**
Depth	17.0 m	18.0 m	19.5 m
Capacity	80,000 DWT	120,000 DWT	320,000 DWT
Max LOA	295 m	321 m	382 m
Berthing Velocity (Designed)	12 cm/s	15 cm/s	15 cm/s
Berthing Velocity (Operated)	Safety : 5cm/s, Warning : 6~10 cm/s, Dangerous : 11~15 cm/s		
Berthing Angle	Max 6 deg. within 30 m, Max 3 deg. at touching		

In general, the berthing velocity is based on the velocity at the time of first contact with the fender of the pier. When the ship is docked at the wharf, it is completely moored to the wharf. Even if the berthing operation is finished, the movement of the ship may be detected due to the characteristics of the ship and the wharf.

The DAS in this study is measured at two points in the direction of the fore and after part of the vessel, and measured the velocity of the vessel when the contact occurs. However, not only the measured value at any of the contact velocity measured at two points is not displayed as the initial contact but only the velocity at the time of contact with the fender located in each direction is displayed. Since the velocity of the ship decreases with the absorption of the berthing energy by the fender after impact, the data analysis is performed assuming that the maximum of the two

points of berthing velocity is the actual berthing velocity with the initial contact.

2.2.3 Basic Analysis of Measurement

For each jetty, the designed berthing velocity is specified when designing the jetty facility. Figs. 2.4 – 2.7 shows the scatter plot with the DWT of the ship and berthing velocity which berthed to each jetty. As shown in scatter plot of the berthing velocity and DWT, it can be confirmed that most of the ships are within the range of jetty designing velocity. In the case of 150,000 ~ 300,000 DWT ship, all vessels were berthed under the designed speed. The vessels exceeding the design value were mostly less than 50,000 tons, and the largest vessels exceeding the design value were identified as about 100,000 tons.

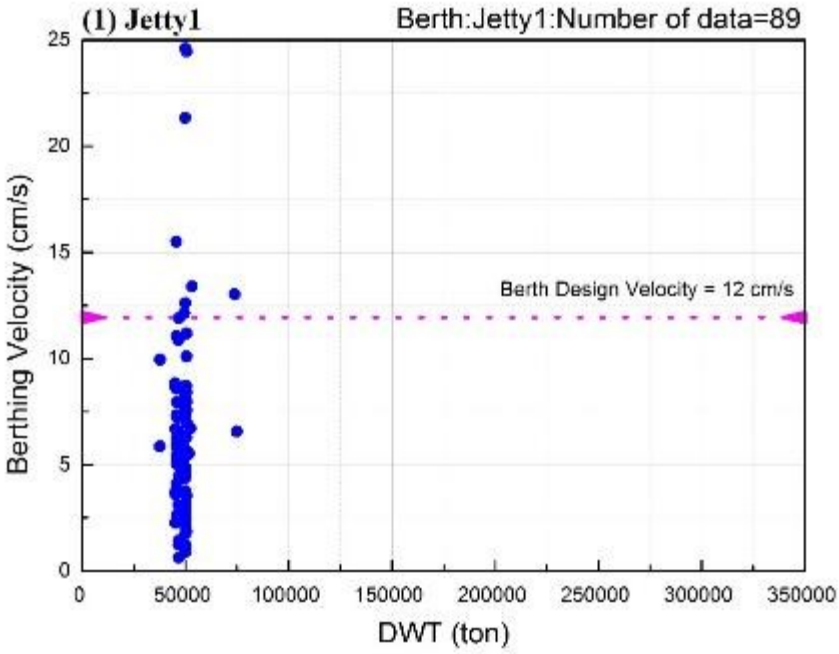

Fig. 2.4. Scattering map of berthing velocity versus DWT (Jetty 1)

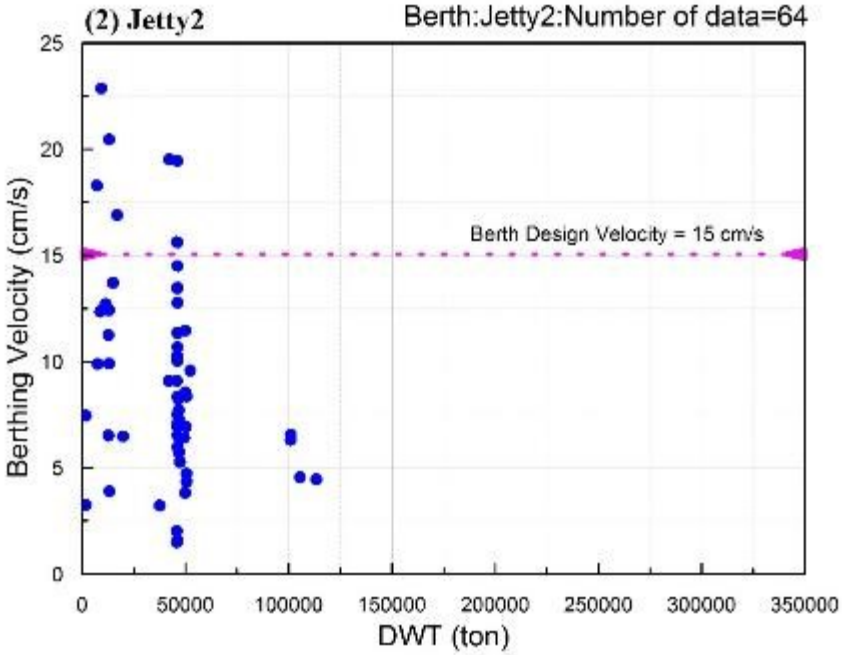

Fig. 2.5. Scattering map of berthing velocity versus DWT (Jetty 2)

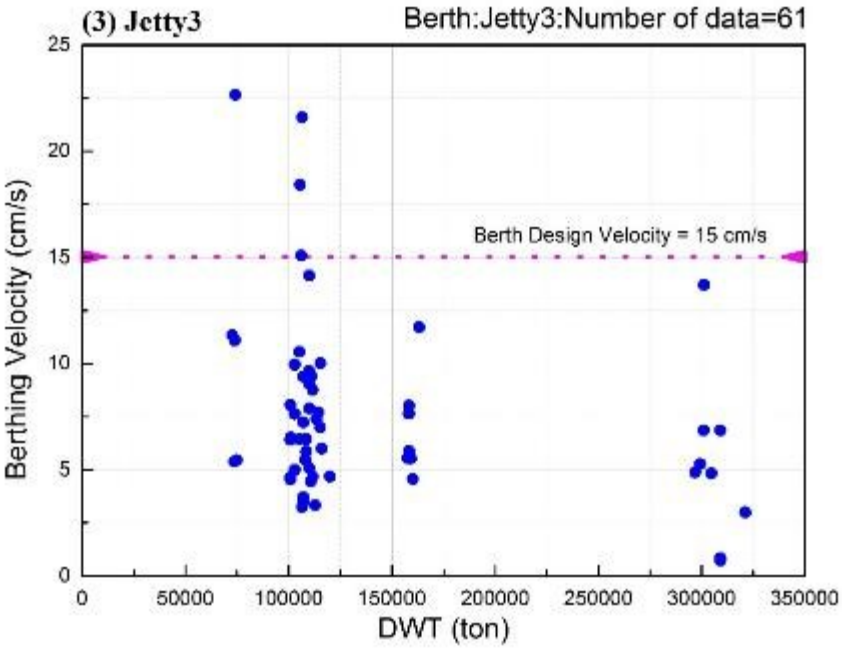

Fig. 2.6. Scattering map of berthing velocity versus DWT (Jetty 3)

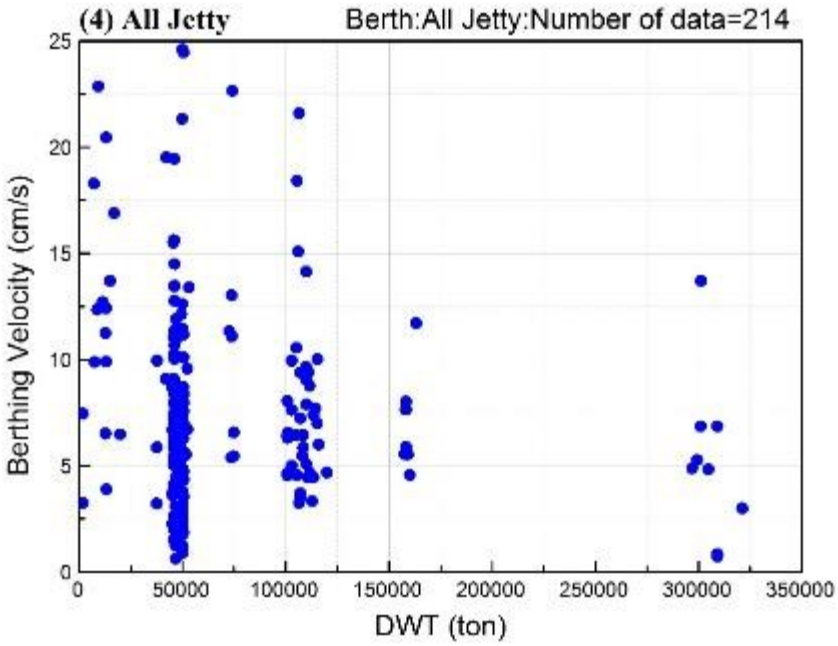

Fig. 2.7. Scattering map of berthing velocity versus DWT (All Jetty)

In the case of jetty1, most of the data consisted of vessels of about 50K DWT size in Fig. 2.4. Berth design velocity of jetty1 is set to 12 cm/s and most vessels were berthed within the berth design velocity range. Average berthing velocity of jetty1 was 6.631 cm/s, maximum berthing velocity was 24.6 cm/s as seen in Fig. 2.4. The size of vessel ranged from 37,000 DWT to 75,000 DWT. In jetty2 and jetty3, the maximum size of the berthing vessel is increased and the berth design velocity is designed to be 15 cm/s, which is larger than jetty1. Fig. 2.5 shows that in jetty2, vessels over 100K DWT are berthing, but the vessels smaller than 50K DWT have been confirmed to berthing and many vessels around 50K DWT have been identified. Average berthing velocity of jetty2 was 9.406 cm/s, maximum berthing velocity was 22.85 cm/s. Unlike other jetties, the size of the vessel has been confirmed to be in contact with vessels of various sizes from 1,750 DWT to 113,500 DWT. Fig. 2.6 shows that most ships larger than 100K DWT are berthing, and most of the data is berthing within the berth design velocity of 15 cm/s. Average berthing velocity of jetty3 was 7.576 cm/s, maximum berthing velocity was 22.65 cm/s. The size of vessels docking on jetty3 was dominated by vessels of large size from 72,700 DWT to 321,200 DWT. In all jetties as shown in Fig. 2.7, the average berthing velocity is in the berth design velocity range. However,

around 10 % of the ships were found to have berthing velocities exceeding this. This was a dangerous berthing, which had the potential to lead to damage to the berthing facility.

Table 2.3 shows the characteristics of berthing velocity for each jetty. The average value of total data was measured as 7.575 cm/s, the standard deviation was 4.494, and the maximum value of measured data was 24.60 cm/s. The average Jetty 1 is 6.631 cm/s, which is close to half of the design value of 12 cm/s. However, the maximum value of the measured data is 24.60 cm/s, which is about twice as large as the design velocity. Therefore, additional analysis on the cause analysis and the appropriateness of the design berthing velocity is necessary. In Jetty 2 and Jetty 3, mean values were 9.046 cm/s and 7.576 cm/s, respectively, and were within the range of 15 cm/s, which is the design value. However, the maximum values of measured data are 22.85 cm/s and 22.65 cm/s, exceeded the design berthing velocity.

Also, when comparing the average values of each jetty, the average value of Jetty 2 is 9.046 cm/s, which is more than 6.631 cm/s of Jetty 1 and 7.576 cm/s of Jetty 3. This is due to the fact that there are many ships less than 50,000 DWT in Jetty 2 and that the velocity of the ships is excessive, so that the average value is higher in Jetty 2 where many small vessels are docked than other jetties.

Table 2.3 Characteristic of Berthing Velocity Values for each Jetty

Velocity(cm/s)	Jetty 1	Jetty 2	Jetty 3	Total
Average	6.631	9.046	7.576	7.575
Standard deviation	4.505	4.422	4.235	4.494
Coefficient of variance	0.679	0.489	0.559	0.593
Max observed value	24.60	20.45	22.65	24.60
No. of data	89	57	61	207

2.3 Probability Distribution Function for Berthing Velocity

2.3.1 Types of Probability Distribution Functions

It is generally known that the frequency of the berthing velocity follows a lognormal distribution (NILIM, 2015; Yamase et al., 2013). In this study, I try to identify the best fit probability distribution function by comparing the frequencies of the normal distribution, the lognormal distribution, and the Weibull distribution function and the actual berthing velocity data among the probability distribution functions.

In this study, the probability distribution function (PDF) was used for the analysis of measured data. Among them, the analysis was performed with the histogram of the frequency of berthing velocity using the three probability distributions, normal distribution, lognormal distribution, and Weibull distribution. The formula corresponding to each probability distribution is as follows.

$$f(x) = \frac{1}{\sigma\sqrt{2\pi}} exp\left(-\frac{(x-\mu)^2}{2\sigma^2}\right), \tag{2.1}$$

$$f(x) = \frac{1}{x\sqrt{2\pi}\sigma} exp\left(-\frac{(\ln x-\mu)^2}{2\sigma^2}\right), \tag{2.2}$$

$$f(x) = \frac{k}{\lambda}\left(\frac{x}{\lambda}\right)^{k-1} exp(-\left(\frac{x}{\lambda}\right)^{k}), \tag{2.3}$$

where:

$f(x)$: Probability distribution function (PDF)

x : Berthing velocity (cm/s)

μ : Mean (cm/s)

σ : Standard deviation (cm/s)

λ : Scale parameter Weibull distribution (cm/s)

k : Shape parameter Weibull distribution

In general, the berthing velocity is known to follow the lognormal distribution and is often assumed to be analyzed (Ueda et al., 2002; Yamase et al., 2013; Murakami et al., 2015). However, in this study, it was analyzed that the berthing velocity also follows the Weibull distribution as well as the lognormal distribution. In the case of Weibull distribution, it is often used when analyzing the failure rate, but even in the case of berthing velocity, it is considered appropriate to approach the concept of accident rate.

2.3.2 Application of Probability Distribution Function by each Jetty

Figs. 2.8 – 2.11 show the frequency of the berthing velocity represented by the histogram and overlaid by probability distribution function curves of normal, lognormal and Weibull distribution. In all jetty's case, the normal distribution seems to not follow much. In jetty1, it is difficult to distinguish between the lognormal distribution and the Weibull distribution because both data distribution curves are close to the histogram of the berthing velocity. The histogram of jetty2 is close to the lognormal distribution, but the Weibull distribution is the closest, and the histogram in jetty3 is found to follow the lognormal distribution best. When the entire data set is identified, the Weibull distribution appears to best describe the histogram.

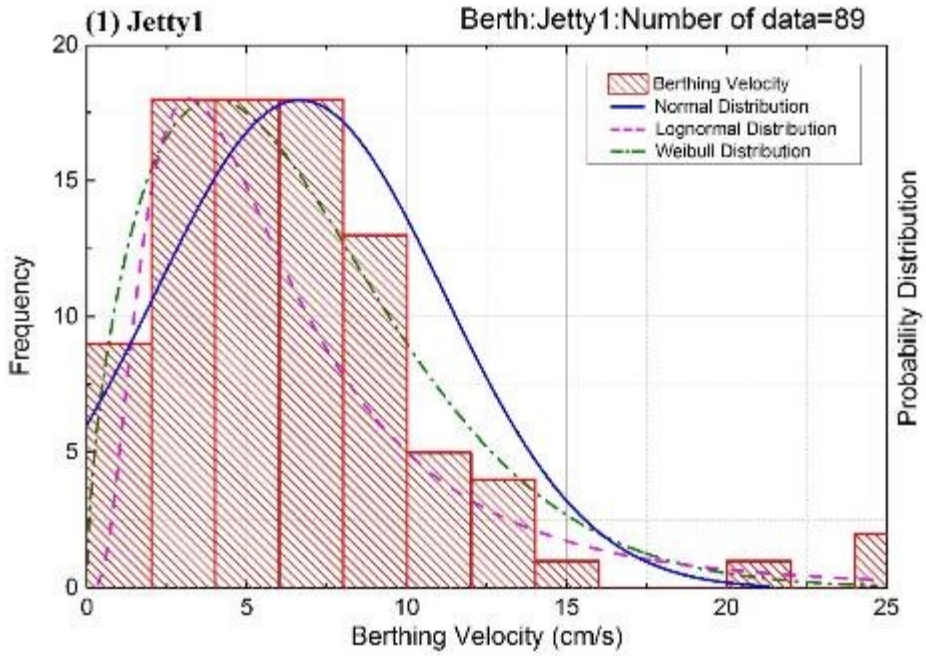

Fig. 2.8. Frequency distribution of berthing velocity (Jetty 1)

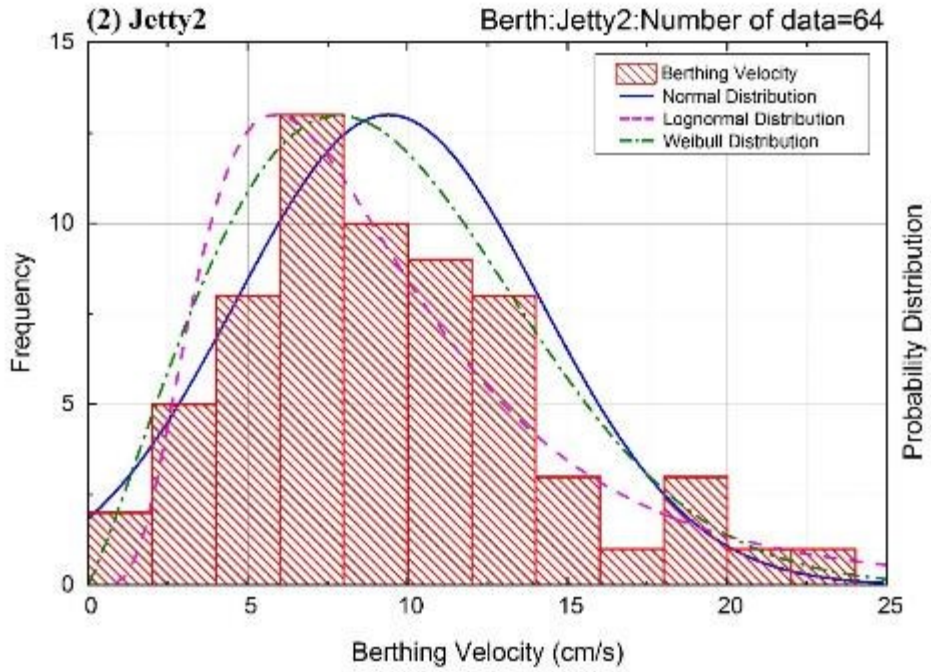

Fig. 2.9. Frequency distribution of berthing velocity (Jetty 2)

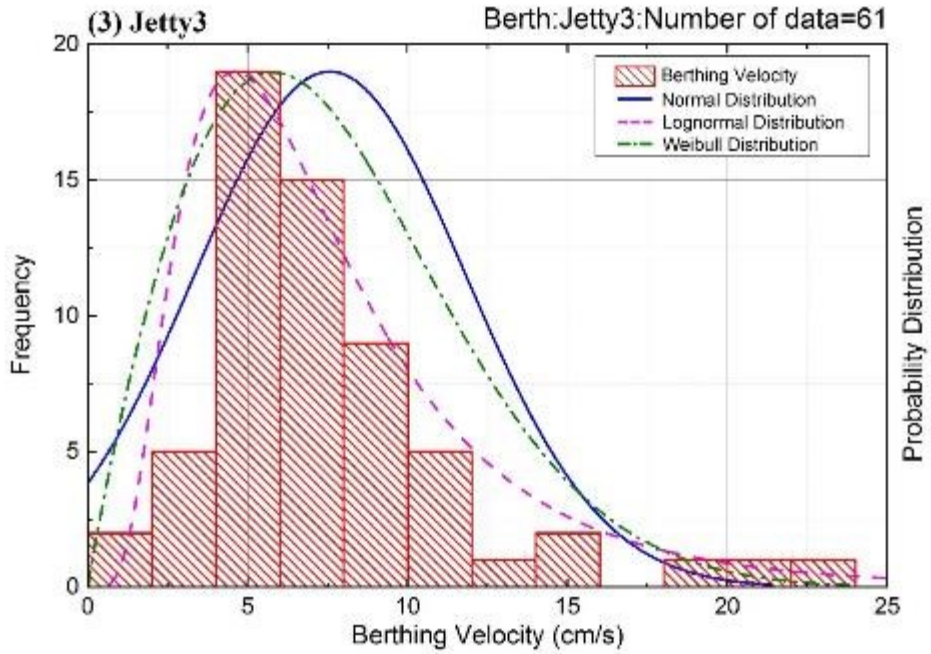

Fig. 2.10. Frequency distribution of berthing velocity (Jetty 3)

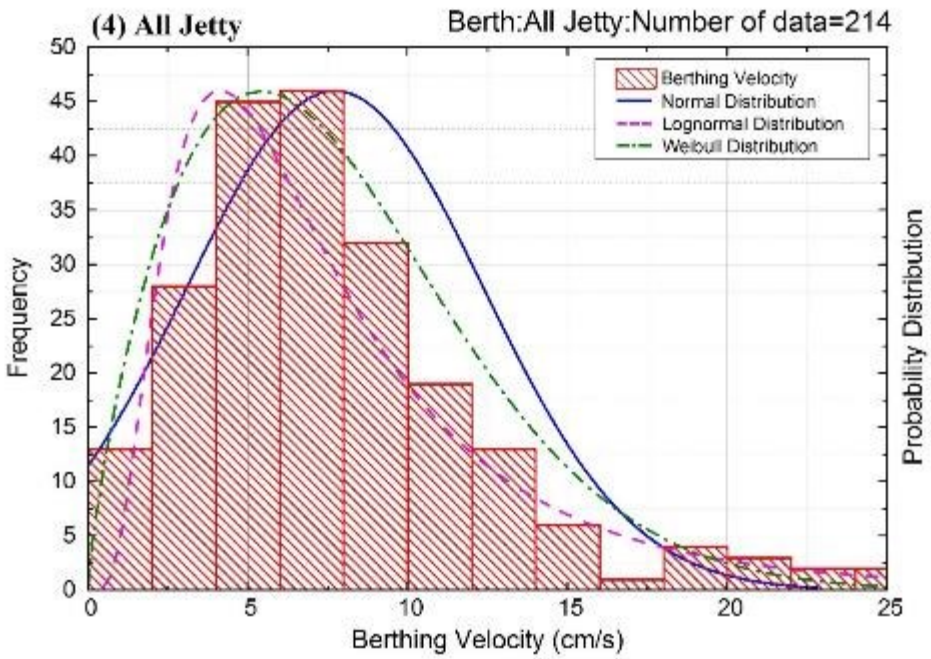

Fig. 2.11. Frequency distribution of berthing velocity (All Jetty)

As mentioned in previous studies about berthing velocity, some of the frequency for berthing velocities appears to follow the lognormal distribution, but seems to be closer to the Weibull distribution as shown in previous figures.

To accurately assess the goodness of fit for this probability distribution, Q-Q plot was used to visually check the probability distribution. As can be seen in Figs. 2.8 – 2.11 of the frequency histograms, there is some data that can easily identify which probability distribution follows the histogram, but there is clearly a case where it is difficult to ascertain which distribution fits best. There are several methods to confirm this, but in this study, the Q-Q plot was used to visually confirm it.

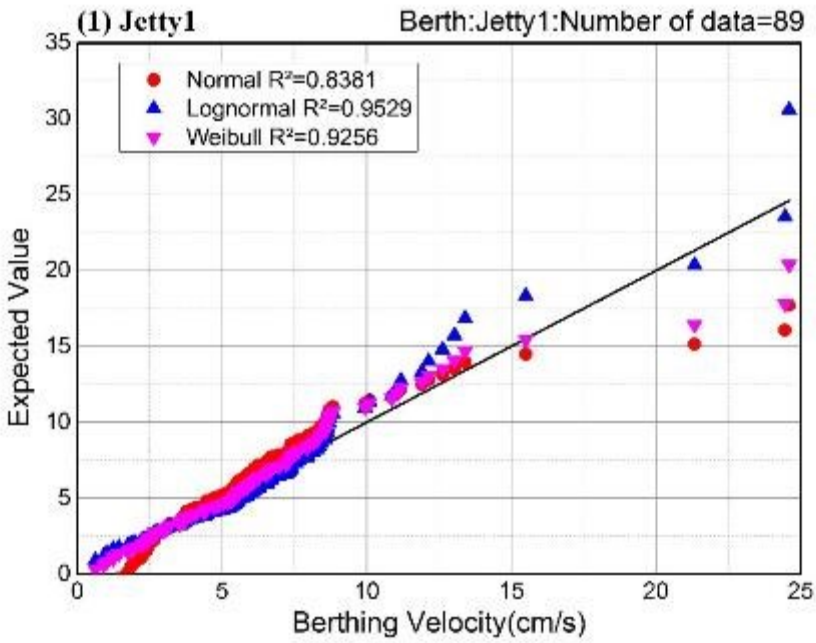

Fig. 2.12. Q-Q probability plot (Jetty 1)

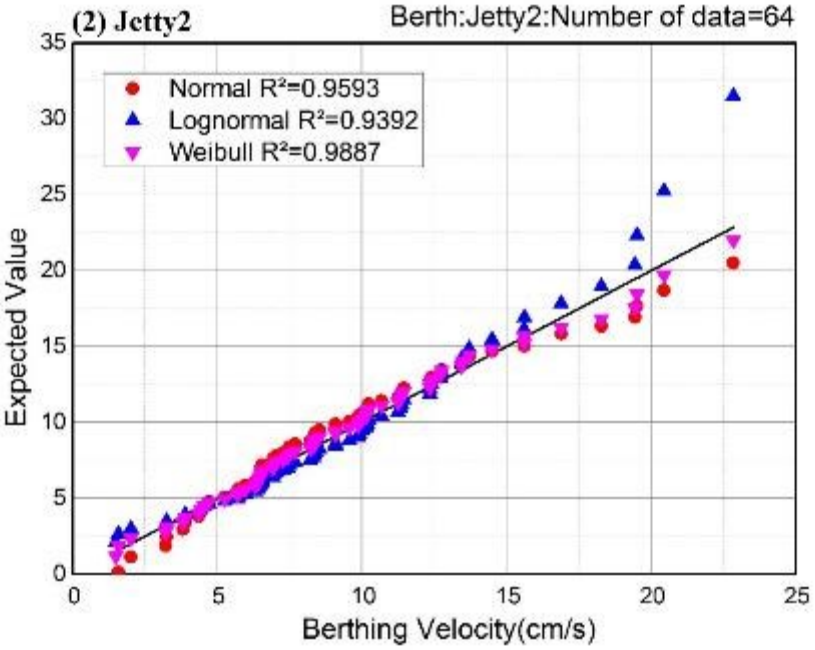

Fig. 2.13. Q-Q probability plot (Jetty 2)

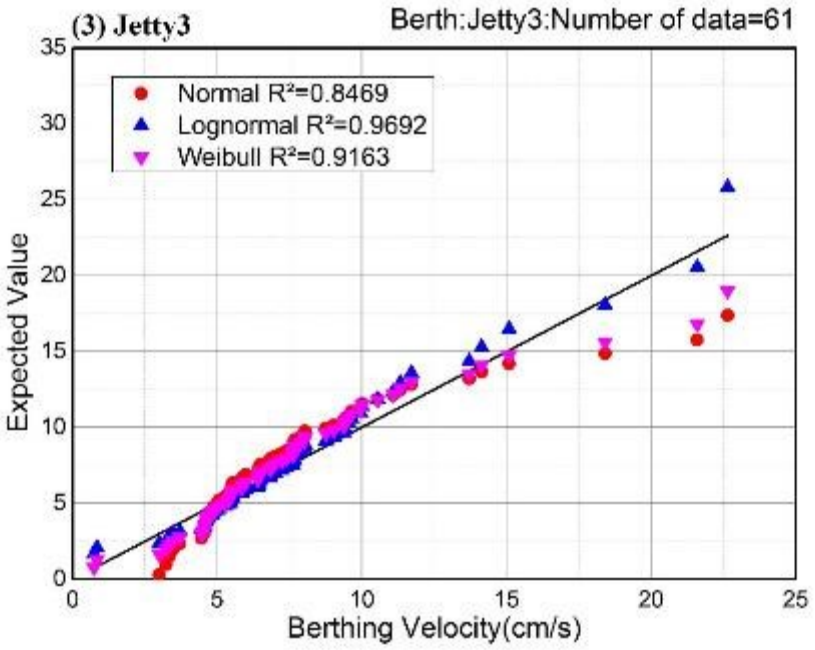

Fig. 2.14. Q-Q probability plot (Jetty 3)

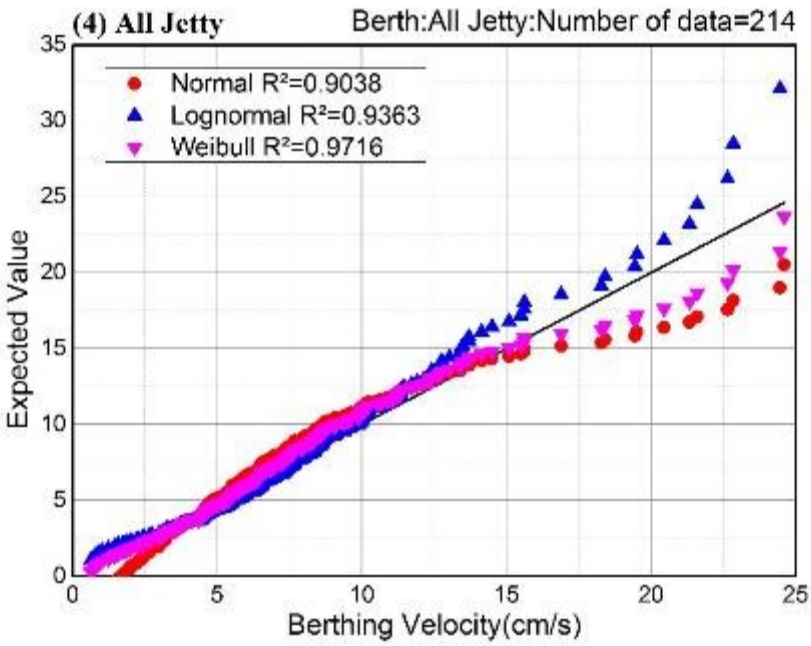

Fig. 2.15. Q-Q probability plot (All Jetty)

Figs. 2.12 – 2.15 show the graph of Q-Q plots plotted for each jetty, and it is possible to visualize the most probable probability distribution that was difficult to distinguish from the histogram. Fig. 2.12 shows the lognormal distribution seems to follow the last value of 24.6 cm/s in jetty1. In Fig. 2.13 for jetty2, the lognormal distribution deviates from about 20 cm/s and Weibull distribution is best observed. In case of jetty3, the distribution which is located nearest to the last value can be confirmed by the lognormal distribution as shown in Fig. 2.14. In Fig. 2.15, showing the whole data set, the lognormal distribution deviates from the end, and Weibull distribution is the best fit distribution.

The R-squared value was calculated and analyzed to find out exactly which probability distribution accurately follows. R-squared is a correlation coefficient that measures the difference between the estimated linear regression and the actual value. The value has a value between 0 and 1, and if it has a value close to 1, it can be said that it has a more correlation. As a result, in jetty1, lognormal distribution was the most suitable as shown in Fig. 2.12 (R-squared: 0.9529). In Fig.

2.13 for jetty2, Weibull distribution (R-squared: 0.9887) and jetty3 had lognormal distribution as shown in Fig. 2.14 (R-squared: 0.9692). The total data set in Fig. 2.15 was found to be Weibull distribution (R-squared: 0.9512). It can be confirmed that the proper distribution by executing the Q-Q plot differently from simply confirming with the histogram.

Through the Q-Q plot in Fig. 2.15, the expected value tends to deviate from the line of $y = x$, from the point about 14 ~16 cm/s. It means that is about 94.4 % of the total data is distributed in the vicinity of the straight line as shown in Table 2.4.

By using the Q-Q plot, it was possible to visually check which distribution is most suitable among the individual probability distributions, or to compare R-squared values to find the most appropriate distribution. In addition to the Q-Q plot, the most fit distribution can be checked using goodness of fit such as the chi-square test, K-S test(Kolmogorov-Smirnov test), A-D test(Anderson-Darling test), or Shapiro-Wilk test that verify the normality.

Table 2.4 Frequency count of berthing velocity

Velocity (cm/s)	Count	Cumulative count	Relative Frequency	Cumulative Frequency
0~2	13	13	6.1 %	6.1 %
2~4	28	41	13.1 %	19.2 %
4~6	45	86	21.0 %	40.2 %
6~8	46	132	21.5 %	61.7 %
8~10	32	164	15.0 %	76.6 %
10~12	19	183	8.9 %	85.5 %
12~14	13	196	6.1 %	91.6 %
14~16	**6**	**202**	**2.8 %**	**94.4 %**
16~18	1	203	0.5 %	94.9 %
18~20	4	207	1.9 %	96.7 %
20~22	3	210	1.4 %	98.1 %
22~24	2	212	0.9 %	99.1 %
~24	2	214	0.9 %	100.0 %

2.3.3 Application of Probability Distribution Function by ship's size (DWT)

As shown in Fig. 2.5, the vessel's size was distributed from small ships less than 10K DWT to 100K DWT in jetty2. In addition, the size of ship varied from 100K DWT to 300K DWT for jetty3 as shown in Fig. 2.6. Therefore, for the analysis of berthing velocity by ship size, additional analysis was carried out by dividing the ship size based on 100K DWT and this scattering map shows in Figs. 2.16 and 2.17.

Figs. 2.16 – 2.21 show scattering map, frequency distribution and Q-Q plot divided by 100K DWT. Previous studies on berthing velocity and berthing energy have examined the berthing velocity depending on the vessel DWT. Therefore, in this study, the analysis was performed by dividing by 100K DWT, and the frequency distribution of berthing velocity was different as shown in Figs. 2.18 and 2.19.

Q-Q plot was performed as shown in Figs. 2.20 and 2.21 because it is difficult to accurately confirm the fit of histogram and each probability distribution in Figs. 2.18 and 2.19. As a result,

Weibull distribution was found to be the most suitable distribution for ships less than 100K DWT as shown in Fig. 2.20, but the lognormal distribution was found to be the most suitable distribution for ships over 100K DWT as shown in Fig. 2.21.

Table 2.5 Characteristic berthing velocity values by DWT

Berthing velocity(cm/s)	Under 100K DWT	Over 100K DWT	Total
Average	7.963	7.135	7.731
Standard Deviation	4.931	3.735	4.633
Coefficient of Variance	0.619	0.523	0.599
Max observed Value	24.6	21.6	24.6
Data Number	154	60	214

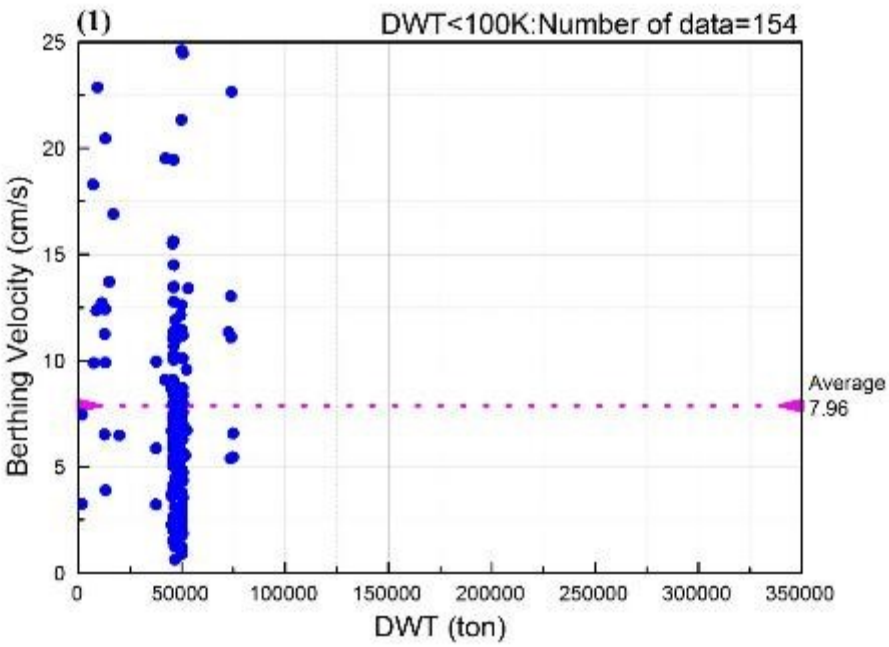

Fig. 2.16. Scattering map of berthing velocity versus DWT (less than 100 K DWT)

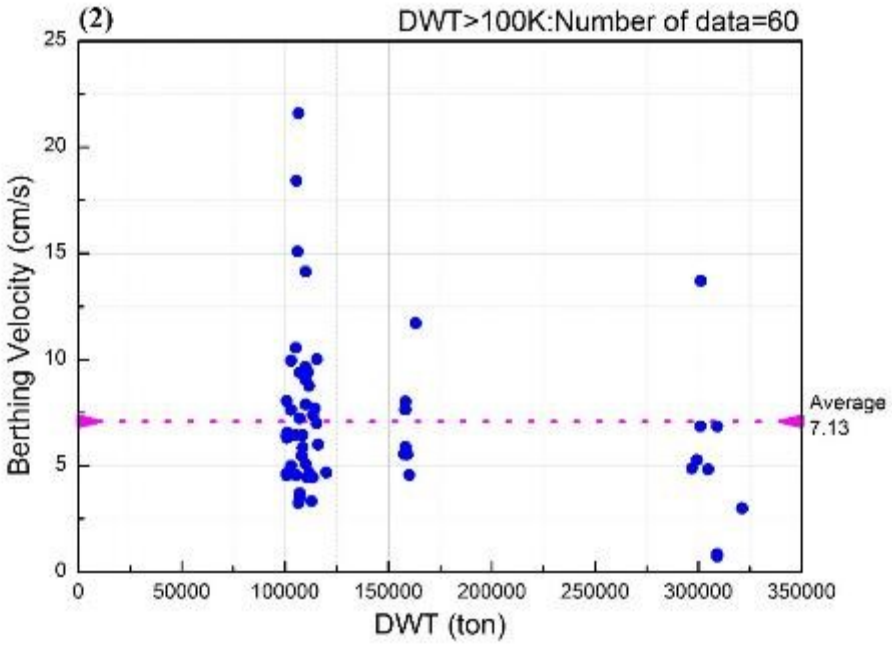

Fig. 2.17. Scattering map of berthing velocity versus DWT (more than 100 K DWT)

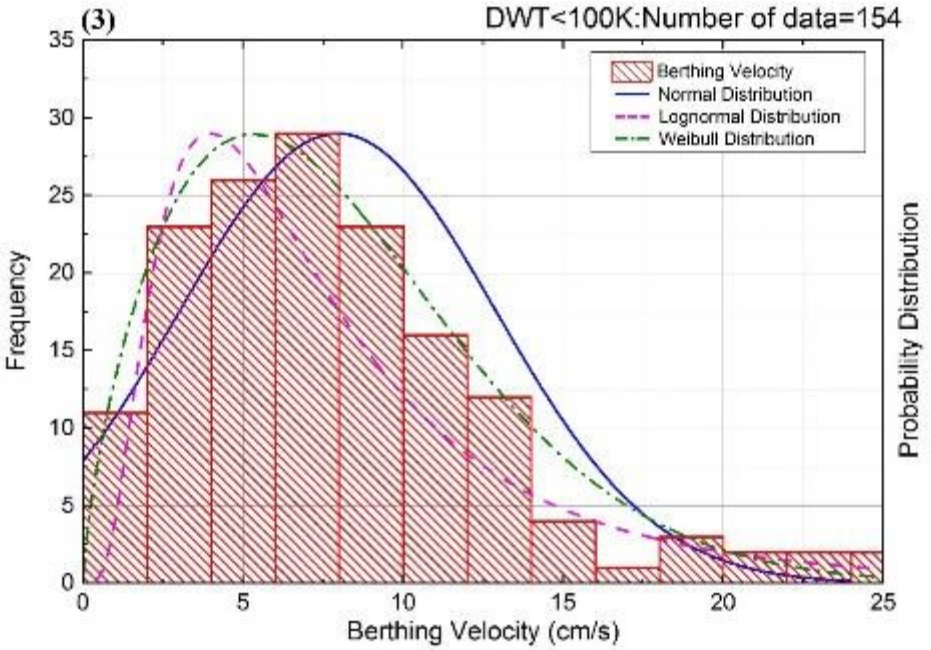

Fig. 2.18. Frequency distribution of berthing velocity (less than 100 K DWT)

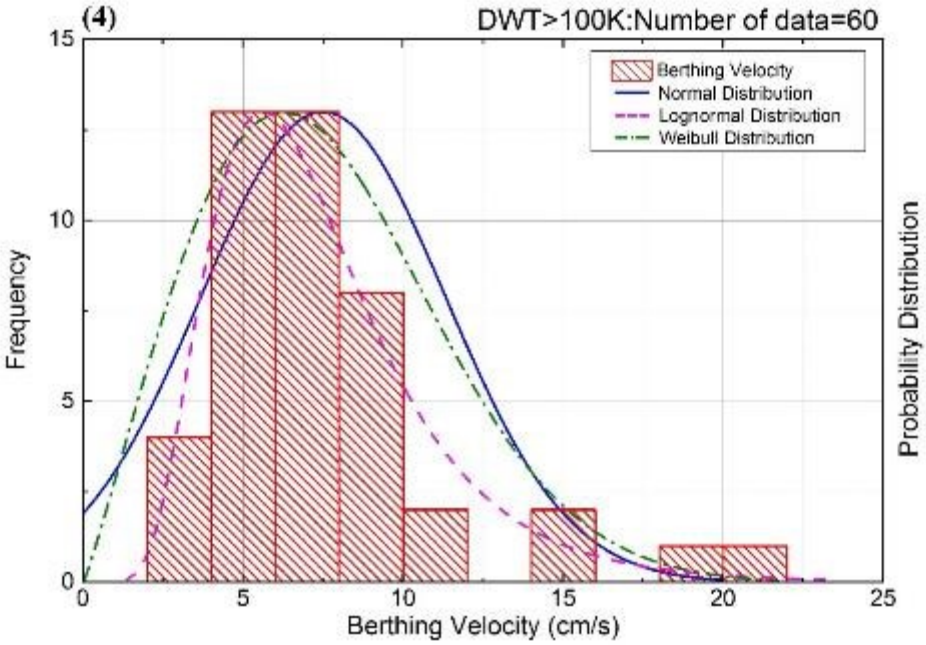

Fig. 2.19. Frequency distribution of berthing velocity (more than 100 K DWT)

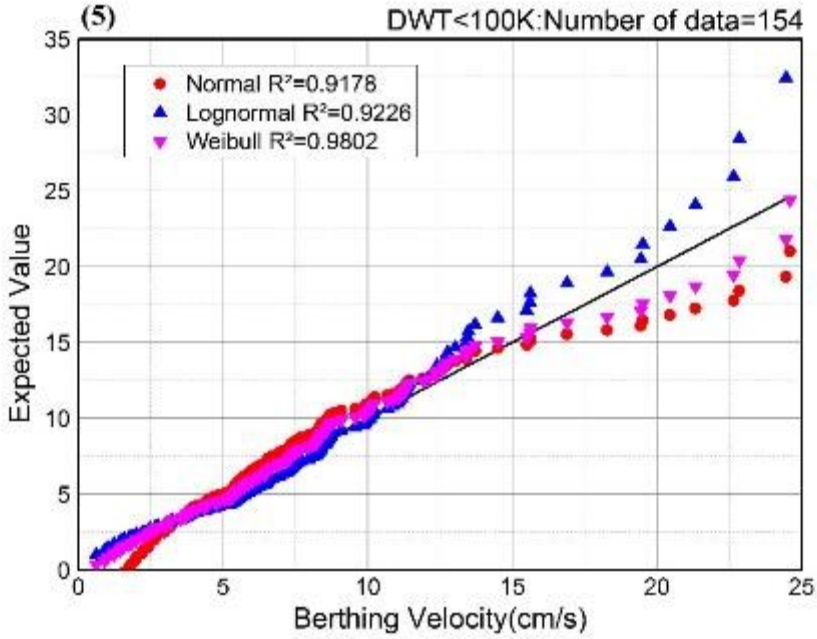

Fig. 2.20. Q-Q probability plot (less than 100 K DWT)

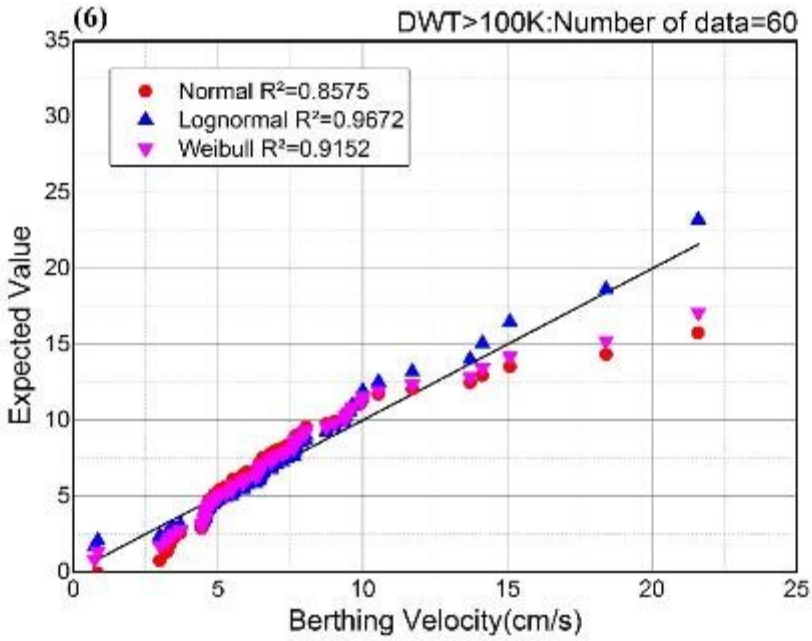

Fig. 2.21. Q-Q probability plot (more than 100 K DWT)

Table 2.5 shows that the average berthing velocity was 7.963 cm/s for vessels less than 100K DWT and the average velocity for vessels over 100K DWT was 7.135 cm/s. The difference between these two mean values shows that the berthing velocity decreases as the vessel size increases. Fig. 2.22 shows the linear regression analysis between DWT and berthing velocity. As a result of the linear regression analysis as shown in Fig. 2.22, although the slope of the difference and the linear regression analysis are not so large, the berthing velocity decreases as the vessel size increases like Table 2.5. As each jetty analysis, the histogram of the probability distribution by ship size was shown to follow lognormal distribution and Weibull distribution rather than normal distribution. As a result of checking with Q-Q plot, under 100K DWT data were followed by Weibull distribution (R-squared: 0.9802) and over 100K DWT were followed by the lognormal distribution (R-squared: 0.9672), similar to the jetty analysis.

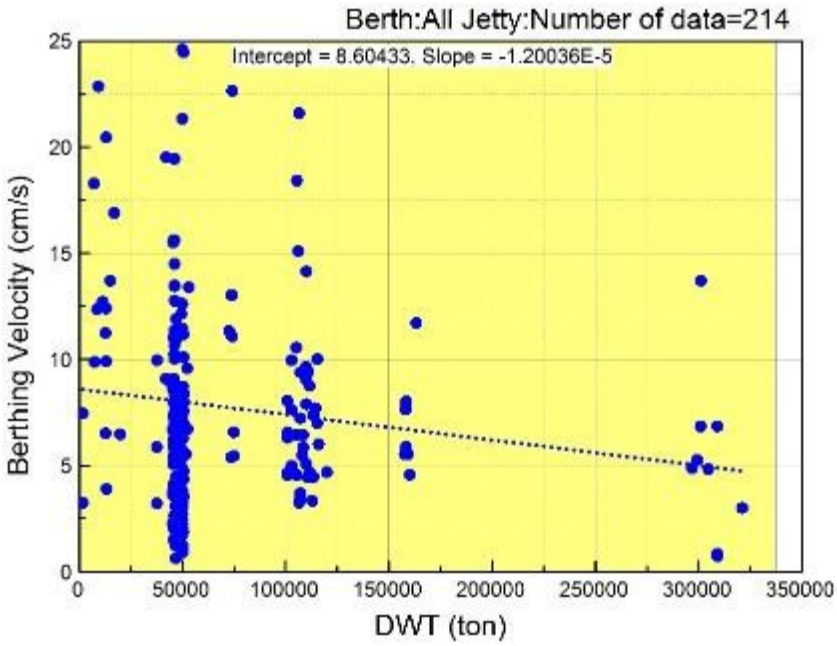

Fig. 2.22. Linear regression analysis between DWT and berthing velocity

2.4 Application of the concept of Probability of Exceedance

Design values for berthing velocities shall be based on very lower probabilities of exceedance. International design codes for marine structures are being made through various stochastic analyzes. In this study, we only propose an estimate of the probability of exceedance for the berthing velocity through the measured data. This does not mean that it is part of the assessment of the safety of the marine facility.

The berthing velocity corresponding to a probability of 1/1,000 and 10,000 was predicted by using the probability of exceedance concept. The median rank concept is used to derive a graph for the probability of exceedance. Fig. 2.23 is a graph overlaid extrapolated berthing velocity corresponding to measured data and normal distribution, lognormal distribution, and Weibull distribution. As can be seen in Fig. 2.23, the measured values are generally analyzed as if they follow the Weibull distribution.

Estimates based on each probability distribution for each probability of exceedance are shown in Table 2.6. Since the measured data is found to be the most compliant with the Weibull

distribution, the berthing velocity of the excess probability concept seems to be applied to the value of the Weibull distribution in Table 2.6.

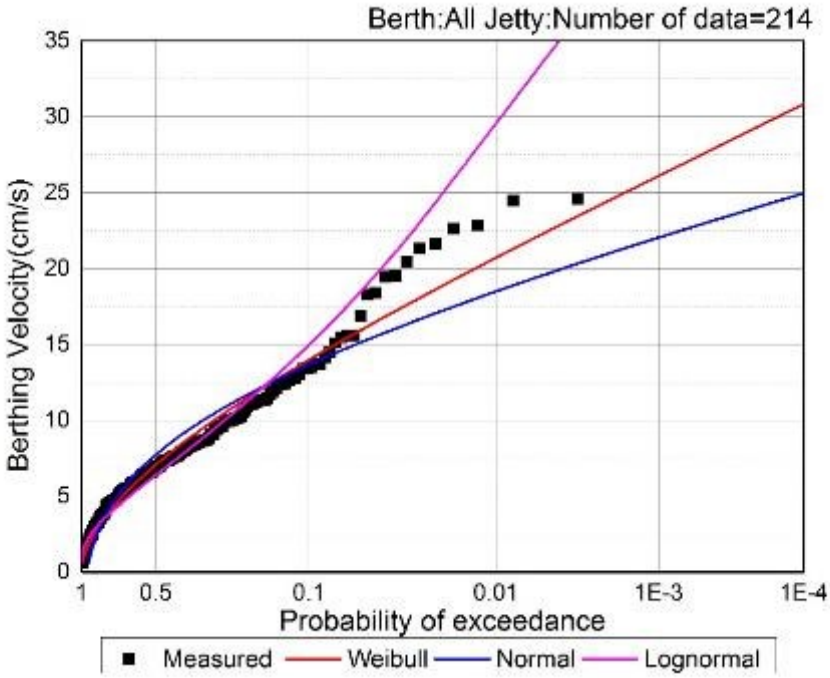

Fig. 2.23. Probability of exceedance for berthing velocity

Table 2.6 Extreme value estimates of the berthing velocity

Extreme value estimates of the berthing velocity (cm/s)				
Probability of exceedance	***1/10***	***1/100***	***1/1,000***	***1/10,000***
Normal distribution	13.573	18.472	22.001	24.881
Lognormal distribution	14.978	29.534	43.599	55.978
Weibull distribution	13.994	20.790	26.215	30.763

2.5 Summary

The berthing velocity, which has an absolute effect on the berthing energy that occurs when a ship berths at a wharf, is based on observations in the target area or past literature such as Brolsma's curve. However, these data have not been revised for a long time. Therefore, new

revisions are needed through the latest berthing statistics data. In this study, international standards and studies related to berthing velocity were compared and analyzed. The actual data of berthing velocity was collected from a tanker dock equipped with DAS (Dock Mounted Docking Aid System) in Korea, which is a berthing velocity measuring device. Based on this data, the statistical analysis of berthing velocity, which is divided into each jetty and size of vessels, was performed from various perspectives.

The frequency of berthing velocity was known to follow the lognormal distribution in previous studies. However, as a result of this study, it was analyzed to be closer to the Weibull distribution than the lognormal distribution. Since most of the existing research results are based on the assumption that the berthing velocity follows the lognormal distribution, further studies on the assumption that it follows the Weibull distribution are needed. Also, it is necessary to revise the berth design velocity of many ports by introducing the berthing velocity in the concept of probability of exceedance following the Weibull distribution.

The limitation of this study is that only the actual data measured by only one wharf (Jetty 1-3) of tanker carrier located in Korea is analyzed. Further studies are needed on the actual data measured on different types of vessels and other quays. It is necessary to develop a new curve to replace Brolsma's curve by deriving the relationship between berthing velocity and size of vessels (DWT) by the confidence interval.

References

Bae, C. H., Lee, S. K., Lee, S. E. and Kim, J. H., 2008. A Study of the Automatic Berthing System of a Ship Using Artificial Neural Network. Journal of Navigation and Port Research, Vol. 32, No. 8, pp. 589-596.

Beckett Rankine, 2010. Berthing velocities and Brolsma's curves. London, United Kingdom.

British Standards Institution, 2014. Code of Practice for design of fendering and mooring systems: BS6349 Part 4. BSI.

Brolsma, J. U., Hirs, J. A., and Langeveld, J.M., 1977. On fender design and berthing velocities. Proc. International Navigation Congress, Section II, Subject 4, pp. 87-100.

Cho, I. S., Cho, J. W., and Lee, S. W., 2018. A basic study on the measured data analysis of berthing velocity of ships. Journal of Coastal Disaster Prevention, Vol.5, No.2,pp. 61-71. (in Korean)

Korea Maritime Safety Tribunal, 2015. Special Investigation Report on the Contact Accidents of M/T WU YI SAN. (in Korean)

Ministry of Oceans and Fisheries, 2014. Harbour and fishery design criteria. (in Korean)

Murakami, K., Takenobu, M., Miyata, M., and Yoneyama, H., 2015. A Fundamental Analysis on the Characteristics of Berthing Velocity of Ships for Design of Port Facilities. Technical note of National Institute for Land and Infrastructure Management, No.864. (in Japanese)

National Institute for Land and Infrastructure Management (NILIM), 2015. A fundamental analysis on the characteristics of berthing velocity of ships for design of port facilities. Techinical note of national institute for land and infrastructure management, Japan:NILIM. (in Japanese)

Nguyen, P. H. and Jung, Y. C., 2007. Automatic Berthing Control of Ship Using Adaptive Neural Networks. International Jouranl of Navigation and Port Research, Vol. 31, No. 7, pp. 563-568.

Park, S. H., Cho, D.J. and Oh, S. W., 2006. A Study on Pseudolite-augmeted Positioning Method for Automatic Docking. Jouranl of Korean Navigation and Port Research, Vol. 30, No. 10,

pp. 839-845.

Perkovic, M., Gucma, M., Luin, B., Gucma, L. & Brcko, T., 2017. Accomodating larger container vessels using an integrated laser system for approach and berthing. Microprocessors and Microsystems, Vol. 52, pp.106-116.

PIANC (World Association for Waterborne Transport Infrastructure), 2002. Guidelines for the design of fenders systems. Report of working group 33 of the MARITIME NAVIGATION COMMISSION.

PIANC (World Association for Waterborne Transport Infrastructure), 2017. Berthing velocities and fender design, Report of working group 145 of the MARITIME NAVIGATION COMMISSION.

Qiang, Z., Guibing, Z., Xin, H. and Renming, Y., 2019. Adaptive neural network auto-berthing control of marine ships. Ocean Engineering, Vol. 177, pp. 40-48.

Roubos, A., L. Groenewegen, and D.J. Peters, 2017. Berthing velocity of large seagoing vessels in the ports of Rotterdam. Marines Structures, vol. 51, pp. 202-219.

Roubos, A., D. J. Peters, L. Groenewegen, and R. Steenbergen, 2018. Partial safety factors for berthing velocity and loads on marine structures. Marines Structures, vol. 58, pp. 73-91.

Shin, C. S., 2007. Evaluation techniques on collision force between ship and port structure. Journal of the Korean Society of Civil Engineers, vol. 25, pp. 111-118, (in Korean)

Trelleborg, 2016. Fender application design manual. Trelleborg Marine Systems.

Ueda, S., Hirano, T., Shiraishi, S., and Yamase, S., 2002. Reliability design method of fender for berthing ship. Proc. Of the 30th PIANC, pp. 692-707.

Yamase, S., Ueda, S., Okada, T., Arai, A., and Shimizu, K., 2013. Characteristics of measured berthing velocity and the application for fender design of berthing ship. Annual Journal of Civil Engineering in the Ocean, JSCE Vol.69, pp. 67-72. (in Japanese)

Chapter 3 Safety Evaluation of Moored Ship and Cost-Benefit Estimation

3.1 Introduction

Around the 1990s, with cargo volume increasing around the world, port efficiency and the safety of ships in ports became important. As such, many studies have investigated the behavior of moored ships through physical experiments, numerical simulations, and field observations (Kubo and Barthel, 1992; PIANC, 1995; Shiraishi et al., 1999). Kubo and Sakakibara (1999) proposed the expansion of breakwaters and improvement of the mooring system as countermeasures to mooring issues. With countermeasures, such as the expansion of breakwaters, it was expected that mooring problems could be solved. However, the economic slowdown in the 2000s, such as in the global economic crisis, hindered the progress of measures that incur large-scale construction costs.

In addition, the influence of waves, such as long-period waves and harbor resonance has been identified as the main cause of large ship motions. By controlling of the natural period and spring constant between mooring lines and fenders, it can reduce ship motions. it is more advantageous to use high-modulus poly ethylene (HMPE) ropes, which have a low stretch of about 3–5%, rather than conventional synthetic fiber ropes, such as nylon and poly-propylene (PP) ropes with a high elasticity of about 20–30% (Foster, 2002; Villa-Caro et al., 2018). However, these HMPE ropes are not adopted by many shipping companies yet owing to various disadvantages, such as high price and vulnerability to high temperatures.

Even after 20 years, many ports suffer from mooring difficulties due to these reasons (Van der Molen et al., 2006, 2015; Kwak et al., 2012; López and Iglesias, 2014; Sasa et al., 2018, 2019). Sasa (2017) found that coastal passenger ships mooring at islands, which are exposed to the ocean, have been placed in dangerous conditions by long-period waves.

Harbors exposed to dangerous situations have used the weather forecast system as an alternative to reduce mooring risks by evacuating ships from piers when rough weather is predicted (Shiraishi, 2009; Yoneyama et al., 2017). However, weather forecasts cannot always be accurate, and these failures of forecasts have resulted not only in additional offshore anchoring, leading to additional losses, but also mooring accidents caused by unpredicted rough waves.

Previous studies on mooring problems have only focused on the tension of the mooring rope (Van der Molen et al., 2006; Sakakibara and Kubo, 2009; Sasa et al., 2018, 2019). However,

several studies have confirmed heat generation when cyclic tension is applied to the rope (Karnoski and Liu, 1988; Hearle et al., 1993; Overington and Leech, 1997; Black et al., 2012), especially in the HMPE rope. Even if the applied tension does not exceed the safety threshold of the mooring rope, the repeatedly applied forces eventually damage the ropes with heat generation because of the accumulation of friction energy (Yamamoto et al., 2004, 2006; Yamamoto, 2007). In addition, the bending fatigue largely affects ropes. (Hobbs and Burgoyne, 1991; Nabijou and Hobbs, 1995; Sloan et al., 2003; Bossolini et al., 2016; Ning et al., 2019).

In this study, we developed a new evaluation of cost-benefit performance to plan an optimal mooring method that satisfies the safety and economic efficiency for port operations. For more accurate safety evaluation of mooring ropes, an improved temperature evaluation method considering frictions and bending fatigues was used instead of the tension evaluation method. Subsequently, new parameters such as demurrage, initial investment cost, and maintenance cost were introduced to verify the economic efficiency. The results show that the proposed methods can reflect the actual situations and the effects of changing the mooring arrangement and rope material. Hence, this paper presents numerical methods for evaluating mooring safety as well as practical applications. Specifically, this study can improve port efficiency from the viewpoint of both safety and economic efficiency.

Following this introductory information, Section 3.2 presents a nationwide questionnaire and current berthing operations to understand and identify actual mooring problems. In Section 3.3, we describe the methods used to calculate the moored ship motions and the detailed process to assess mooring safety developed. In Section 3.4, we introduce simulation conditions such as the target vessel, mooring arrangements and the weather conditions in the study area. The results and application for moored ship safety in rough sea conditions are discussed in Section 3.5, and concluding remarks, key findings from this study, and suggested directions for future research are presented in Section 3.6. Fig. 3.1 illustrates the flowchart of how mooring methods is evaluated on the viewpoint of safety and economic efficiency in this study. Various parameters should be included in the design of mooring methods.

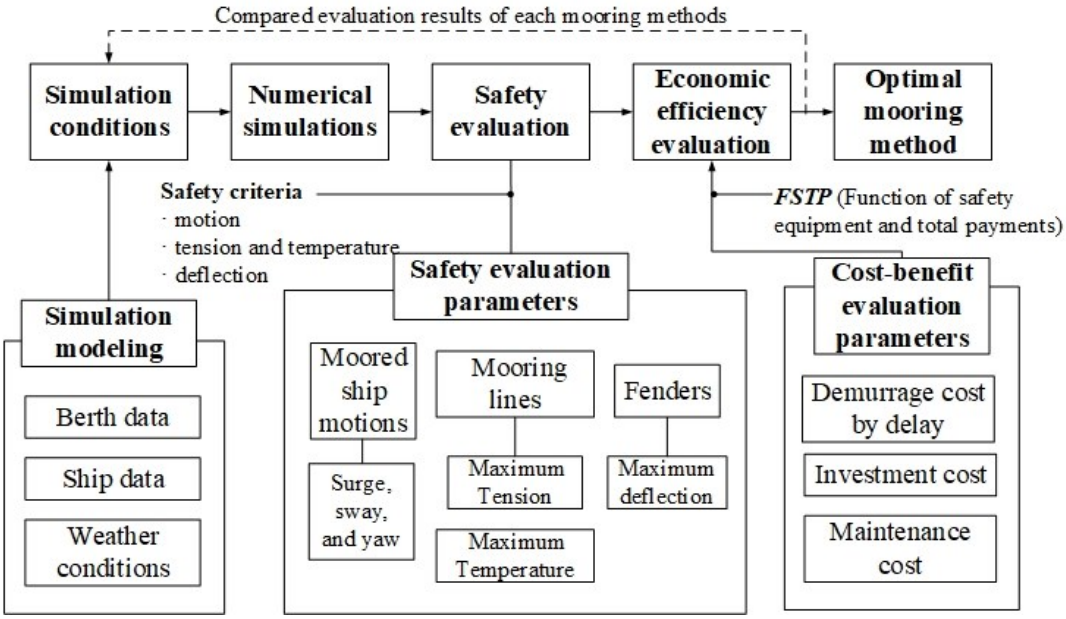

Fig. 3.1. Flowchart of the optimal mooring method process

3.2 Investigation of Current Mooring Problems

3.2.1 Nationwide Questionnaire and Survey on Mooring Problem

In the 1990s, mooring accidents were reported in ports worldwide. Many studies have shown that these accidents are mainly caused by long-period waves (Sasa et al., 2001; Hashimoto and Kawaguchi, 2003; Van der Molen et al., 2006, 2015; González-Marco et al., 2008; Shiraishi, 2009; Ikeda et al., 2011; Van Essen et al., 2013; López and Iglesias, 2014). Thus, the following methods are proposed as countermeasures: (1) Construction of additional breakwaters, (2) Control of the spring constants between mooring lines and fenders to reduce asymmetrical property of mooring, (3) Control the natural period of motions to avoid resonance phenomena.

These practical methods are expected to be used for the safety of port operations. However, they cannot be put into practice because of the large budget required for construction costs. It is necessary to study this current situation on mooring problems from the viewpoint of port operation. A nationwide survey was conducted to accurately identify the current mooring problems. The survey was conducted by mailing a questionnaire sheet. The questionnaire was administered to 120 organizations related to port operations, such as ship operating companies, port agencies, and local governments. The number of responders is 42 (35%). The total number

of questions is 8, including the main questions (Q1)–(Q4), which were as follows:

•(Q1) Have you ever experienced difficulties or dangers in port operation caused by rough seas?

•(Q2) Are you aware of research related to mooring problems conducted over the decades?

•(Q3) Do you use the weather forecast service for port safety management?

•(Q4) Do you think current management is sufficient for the safe operation of moored ships?

Fig. 3.2 shows the answers to questions (Q1)–(Q4). In (Q1), 63% of the respondents said they experienced mooring difficulties due to large ship motions caused by waves. In (Q2), nearly 70% of the respondents were not aware of related studies on moored ship motions. Moreover, it was found that most of the respondents misunderstood the definition of long-period waves (30–300 s of wave periods) with swells (10–16 s). As an alternative to the countermeasure, 62% of the respondents use weather forecast services, as shown in (Q3). This means that nearly 40% of respondents still operate ships without weather forecasts for mooring safety. Regarding (Q4), 59% of the respondents feel insufficiently equipped for the current situation of moored ship motions.

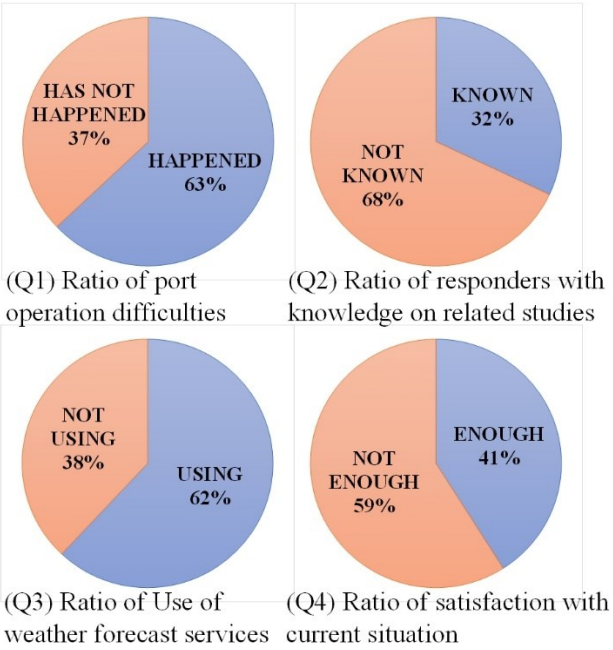

Fig. 3.2. Questionnaire results

As a result of the nationwide survey, the relevant operators are still struggling with the

problems of moored ships. Accordingly, it is necessary to prepare more realistic countermeasures. It is evident that related studies have not been applied to improve the safety of mooring ship operations in ports. In addition, it indicates that mooring problems are not being resolved from a political and economic perspective. Therefore, it is necessary to conduct further research from this point of view.

3.2.2 Current Berthing Operation in T Port

A specific port should be selected to analyze moored ship motions with long-period waves. The selected port is T Port, which is one of the main ports facing the Pacific Ocean with breakwaters to prevent wave effects (Fig. 3.3). The visiting survey in T Port was conducted three times—in October 2017, March 2018, and March 2019—to investigate the real mooring problems. The breakwaters were to be expanded as per a decision of the local committee to maintain port safety. However, the construction has not been affected due to financial deficits. One of the operators of this port, which has problems with the influence of long-period waves, has been using weather forecasting services as an alternative to breakwater expansion since 2011.

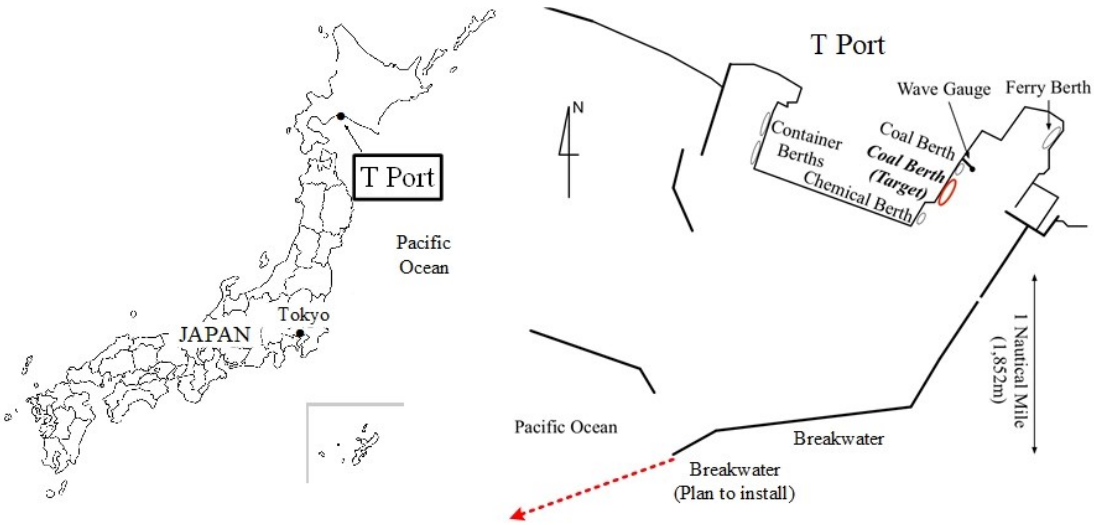

Fig. 3.3. Study area facing the open sea (Pacific Ocean) and the detailed port terminal status for breakwater installation and expansion plans

Waves and winds are continuously observed with an ultrasonic wave gauge and wind sensor at the end of the port. The height of the sea surface is recorded at 0.5 s intervals. Additionally, the time series in terms of the power spectrum is statistically analyzed. The heights of the significant and long-period waves can be obtained as follows:

$$H_{1/3} = 4.0\sqrt{\int_0^{\infty} S(f)df}\,, H_{L1/3} = 4.0\sqrt{\int_0^{0.03} S(f)df}\ , \tag{3.1}$$

where $H_{1/3}$ and $H_{L1/3}$ are the wave heights of the significant and long-period waves, respectively, $S(f)$ is the frequency spectrum of waves inside the harbor, and f is the frequency. Fig. 3.4 shows the (A) time history and (B) power spectrum of measured wave data inside the harbor. From the power spectrum graph in Fig. 3.4(B), it can be seen that a low frequency of 0.006–0.02 Hz (50–166 sec) has strong power spectrums inside the harbor. This shows the presence of the long-period waves near the mooring facilities.

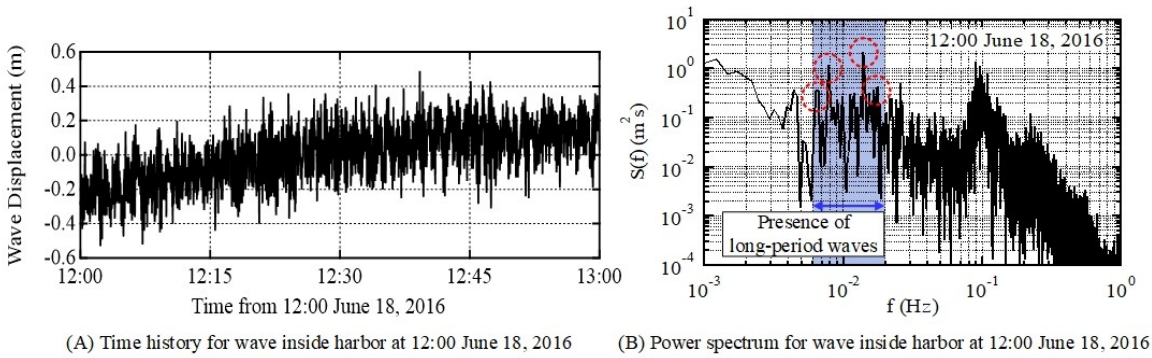

(A) Time history for wave inside harbor at 12:00 June 18, 2016 (B) Power spectrum for wave inside harbor at 12:00 June 18, 2016

Fig. 3.4. Time history and wave spectrum in terms of the power spectrum inside T Port

In this terminal, the berth masters, who have managed and operated the berthing of ships, determine the berthing schedule, and refer to the wave forecasting service. The Ministry of Land, Infrastructure, Transport and Tourism (MLIT) (2009) recommends the operation standards as a significant wave height in the 0.3–0.5 m range and long-period waves in the 0.1–0.2 m range. Based on these recommendations for weather forecasting, each wave condition is divided into three levels, as shown in Table 3.1.

In “Level 1,” the ships can stay inside the harbor with caution. In “Level 2” and “Level 3,” all ships in the port must immediately evacuate to offshore anchorage. With these berthing operation guidelines, serious accidents have been avoided. However, dangerous situations still occur because of incorrect forecasts.

Table 3.1 Berthing operation guidelines and standards for moored ships in T Port

Wave level	Action in the port	Decision by berth master
Level 1	Pay attention during cargo handling (Caution and additional mooring lines)	Staying inside harbor with caution
Level 2	Cargo handling impossible (Danger)	Offshore anchoring
Level 3	Dangerous and emergency evacuation is required (Urgency)	

3.3 Numerical Simulation of Moored Ship Motions

3.3.1 Analytical Theory of Moored Ship Motions

The numerical analysis for the motion of a ship moored to a quay wall induced by environmental forces was conducted by solving the equations of motion in Eq. (3.2) (Cummins, 1962). The time domain analysis was applied for this numerical analysis. In previous studies, this model was validated for multiple cases of measured ship motions with long-period waves at various ports with accuracy (Kubo and Sakakibara, 1999; Shiraishi et al., 1999). In this study, since the moored ship motion could not be measured in the T Port, the evaluation was conducted as the simulated ship motion. The ship motion was simulated based on the measured wave data inside the harbor. Moreover, it was confirmed that the estimated ship motion was reliable by comparing it with the visual report in T Port.

$$\sum_{i=1}^{6}\left(M_{ij}+m_{ij}\left(\infty\right)\right)\ddot{X}_j(t)+\sum_{i=1}^{6}\int_{-\infty}^{t}L_{ij}(t-\tau)\dot{X}_j(\tau)d\tau+\sum_{i=1}^{6}\left(C_{ij}+K_{ij}\right)X_j(t)=F(t)$$

$$(i,j=1,2,\cdots,6), \tag{3.2}$$

where M is the mass matrix (including the moment of inertia) of the hull; $m(\infty)$ is the invariant additional mass; $L(t)$ is the memory effect function; C is the stability matrix; K is the mooring force matrix; $F(t)$ is the external force vector at time t; X indicates the displacement vector of ship motion; and the subscripts i and j indicate the motion mode. Furthermore, $L(t)$ and $m(\infty)$ are expressed by the following equations:

$$L_{ij}(t) = \frac{2}{\pi}\int_0^\infty q_{ij}(\omega) cos\omega t d\omega \,, \tag{3.3}$$

$$m_{ij}(\infty) = p_{ij}(\omega) + \frac{1}{\omega}\int_0^\infty L_{ij}(t) sin\omega t dt \,, \tag{3.4}$$

where $p(\omega)$ and $q(\omega)$ are the added mass and the damping coefficient at the angular frequency ω. The wave existing force is a combination of wave components in each frequency and wave direction on the actual sea surface. They are computed using the three-dimensional Green function method (John, 1950) for arbitrary body shape in each angular frequency. This numerical model reproduces the accurate moored ship motions for some measured cases in long-period waves (Shiraishi et al., 1999). Eq. (3.2) is defined in the time domain and is numerically solved by the Newmark-β method.

Each case was solved for 3,600 s with a time interval of 0.2 s. The amplitude of ship motions is defined as the maximum amplitude using the zero-up crossing method. The tension of the mooring rope and fender deformation is evaluated as the maximum value in the computed time series.

The tension of the mooring rope is also an important parameter for evaluating the safety of a moored ship. The absolute value of the rope tension has been used as a parameter to discuss safety (Shiraishi et al., 1999). In OCIMF (2018), the safety working load (SWL) of synthetic fiber rope is defined as 50% of the minimum breaking load (MBL). The ratio of the applied tension to the MBL of the rope can be defined as the probability of breakage by tension, PBT, defined as

$$PBT\ (\%) = \frac{T_m}{T_{MBL}}, \tag{3.5}$$

where T_m is the maximum value of the affecting tension of the mooring rope, and T_{MBL} is the specific MBL of the rope, which denotes the allowable load. Referring to previous studies related to the rope-breaking mechanism (Karnoski and Liu, 1988; Hearle et al., 1993; Overington and Leech, 1997), friction is also an important factor in rope safety. The probability of breakage without consideration of friction can be underestimated. Therefore, it is necessary to develop the mooring evaluation method considering the friction.

3.3.2 Analysis of Mooring Rope Temperature

The tension of the mooring rope occurs periodically under the influence of waves. This repetitive tension can eventually lead to a temperature rise or breakage of the rope. The thermal calculation needs to divide the two parts of the rope: (1) straight part and (2) bending part, as shown in Fig. 3.5. In the straight part, friction occurs between strands inside the rope, so mainly internal friction is generated. In the bending part, however, in addition to the internal friction, external friction is generated because of contact between the structure, such as the fairlead and the surface of the rope. In addition, this bending part is subject to the effect of bending fatigue.

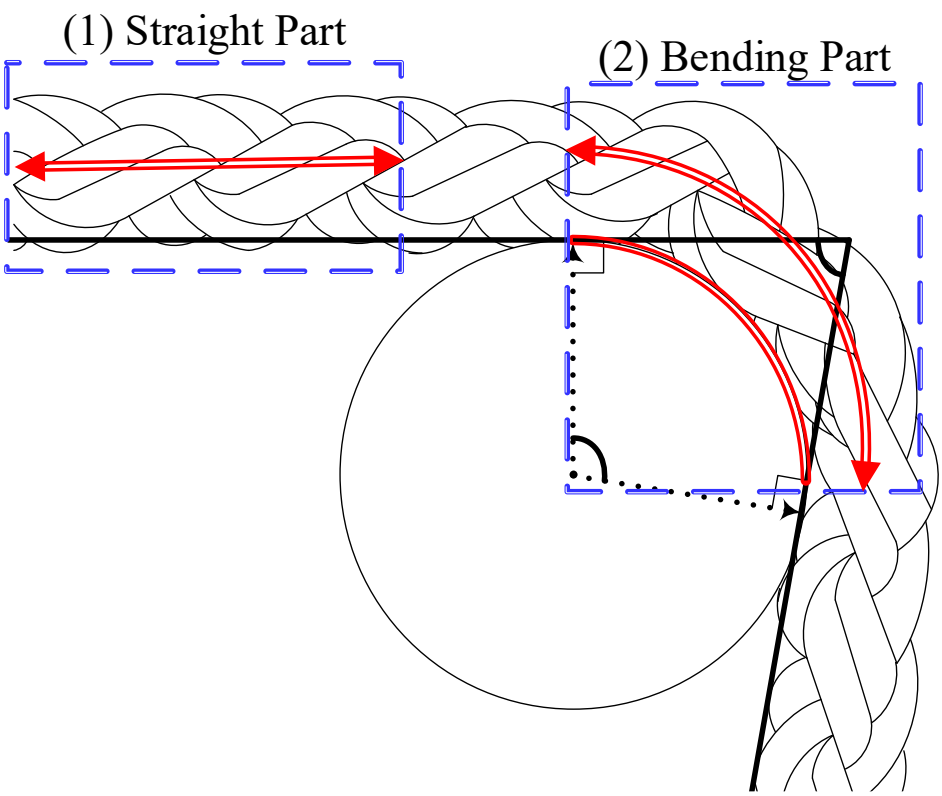

Fig. 3.5. Classification of parts subject to friction: (1) straight part and (2) bending part

First, it is possible to calculate the frictional energy of the straight parts based on previous experiments (Yamamoto et al., 2004, 2006; Yamamoto, 2007). For heat calculation by internal friction, it is necessary to use the thermal equilibrium equation as follows:

$$dQ_{i+1,j} = dQ_{i,j-1} - dQ_{i,j} + dQ_{fri,j}\,, \tag{3.6}$$

where $dQ_{i+1,j}$ is the accumulated heat quantity, $dQ_{i,j-1}$ is the inflow heat quantity, $dQ_{i,j}$ is the outflow heat quantity, and $dQ_{fri,j}$ is the heat quantity due to friction. i and j are the time and position from the inside of the rope, respectively. The accumulated heat quantity, inflow, and outflow heat quantity can be calculated by the equation for heat conductivity as follows:

$$dQ_{i+1,j} = c\rho V_j\left(\theta_{i+1,j} - \theta_{i,j}\right), \tag{3.7}$$

$$dQ_{i,j-1} = \lambda A_{j-1}\frac{\theta_{i,j-1}-\theta_{i,j}}{dr}dt, \tag{3.8}$$

$$dQ_{i,j} = \lambda A_j\frac{\theta_{i,j}-\theta_{i,j+1}}{dr}dt, \tag{3.9}$$

where c is the specific heat of the rope ($kcal/°C \cdot kg$), ρ is the density (kg/m^3), V_j is the volume of position j, and A_j is the area of the section. λ is the heat conductivity coefficient and $\theta_{i,j}$ is the temperature in time i and position j, r is the radius of the rope, dr is $r/10$, and dt is 0.5 s, which is the time interval used in this study. In addition, the internal frictional energy can be calculated by the following:

$$dQ_{fri,j} = \frac{k_1 \cdot k_2 \cdot k_3 \cdot \mu \cdot A_s \cdot p_i \cdot dl_i}{4.186\times10^3} \cdot \frac{V_j}{V}, \tag{3.10}$$

where k_1 is the coefficient of pressure, k_2 is the coefficient of elongation, and k_3 is the coefficient of internal friction. These coefficients were obtained from the experiments. μ is the coefficient of friction, A_s is the total area of the contact area (m^2), p_i is the internal pressure (N/m^2), dl_i is the line elongation, V_j is the volume of j position, and V is the total volume of the rope. The temperature of the rope by internal friction can be obtained by the following:

$$c\rho V_j\left(\theta_{i+1,j} - \theta_{i,j}\right) = \lambda A_{j-1}\frac{\theta_{i,j-1}-\theta_{i,j}}{dr}dt - \lambda A_j\frac{\theta_{i,j}-\theta_{i,j+1}}{dr}dt + \frac{k_1 \cdot k_2 \cdot k_3 \cdot \mu \cdot A_s \cdot p_i \cdot dl_i}{4.186\times10^3} \cdot \frac{V_j}{V}, \tag{3.11}$$

where $\theta_{i,j}$ is the calculated temperature in i time and j position. This equation for the internal friction has been verified by experiments (Yamamoto et al., 2004, 2006; Yamamoto, 2007).

However, this equation only explains for the straight part of the rope. Therefore, it is necessary to consider the additional frictional energy in the bending part of the rope. The additional frictional energy is generated by the external friction between the fairlead and the surface of the rope. It can be obtained by the Capstan equation, as shown in Eq. (2.12).

$$W_{ex} = T_m \cdot exp^{\mu\delta} \cdot dl\,, \tag{3.12}$$

where W_{ex} is the frictional energy of the external force between the fairlead and the rope, T_m is the tension of the rope, μ is the coefficient of friction, δ is the angle of the contact area, and dl is the elongation of the rope.

Finally, there is an effect of bending fatigue. Many studies have found that bending fatigue has a remarkable influence on the damage and heat of the rope (Nabijou and Hobbs, 1995; Sloan et al., 2003; Bossolini et al., 2016; Ning et al., 2019). Ridge et al. (2015) experimentally provided comparative results of the temperature rise through repeated load experiments on the bending part of synthetic fiber ropes. Through their experiments, the appropriate bending coefficient is added as k_4 to the equation of frictional energy in Eq. (3.13). The final result of the thermal model is summarized in Eq. (3.13), including both the internal friction, external friction, and bending fatigue.

$$c\rho V_j\left(\theta_{i+1,j} - \theta_{i,j}\right) = \lambda A_{j-1}\frac{\theta_{i,j-1}-\theta_{i,j}}{dr}dt - \lambda A_j\frac{\theta_{i,j}-\theta_{i,j+1}}{dr}dt$$

$$+\frac{k_1 \cdot k_2 \cdot k_3 \cdot k_4 \cdot \mu \cdot A_s \cdot p_i \cdot dl_i}{4.186\times10^3} \cdot \frac{V_j}{V} + T_m \cdot exp^{\mu\delta} \cdot dl, \tag{3.13}$$

The maximum temperature rises in the bending parts owing to the additional external friction and bending fatigue, while the temperature rise in the straight parts only depends on the internal friction. The temperature of the bending part was compared to the maximum temperature for the safety parameter in this study.

3.4 Conditions of Numerical Simulation

3.4.1 Modeling the Ship and Port

This coal terminal was originally designed for 60,000 DWT (Deadweight) class coal carriers. However, recently, 90,000 DWT class ships have mainly been docking because of the trend of increasing ship size. Current mooring arrangement is obviously unbalanced in Fig. 3.6. In particular, the relatively short lines can be a risk of accidents because the mooring force can be concentrated (ATSB, 2008; Van der Molen et al., 2015). Numerical simulations were performed for 90,000 DWT coal carriers that were mainly berthed at T Port. The main dimensions of the modeled ship are shown in Table 3.2.

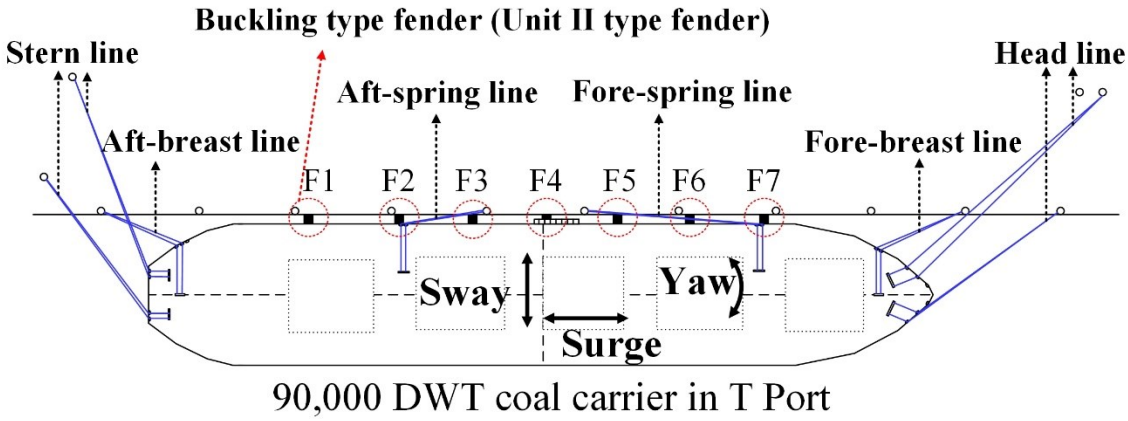

Fig. 3.6. Current mooring arrangements and description of the mooring facilities in T Port

Table 3.2 Main dimension of 90,000 DWT coal carrier

Classification	90,000 DWT coal carrier
Length overall (LOA)	235.00 m
Length between perpendiculars (LPP)	230.00 m
Breadth	43.00 m
Depth	18.40 m
Actual draft (half loaded)	10.76 m

When ships are moored in port or offshore, horizontal motions, such as surge, sway, and yaw

motions, become dominant. Thus, these three modes of motion are focused on in this study. In addition, the definition of the mooring line is determined by its location and role, as shown in Fig. 3.6.

The target vessel has usually used a 60 mm diameter PP ropes. The performance curve of ropes appears differently depending on the material of the rope. The load-elongation characteristics of each specific mooring rope of PP and HMPE are shown in Fig. 3.7. In addition, buckling type fenders are installed in this port to reduce the ship motions during cargo operation. The fenders were placed against the ship, with a height of 1,600 mm and a length of 1,100 mm. A total of seven fenders are located with an elastic limit for the reaction force of 1,253 kN at 60% deflection, as shown in Fig. 3.7.

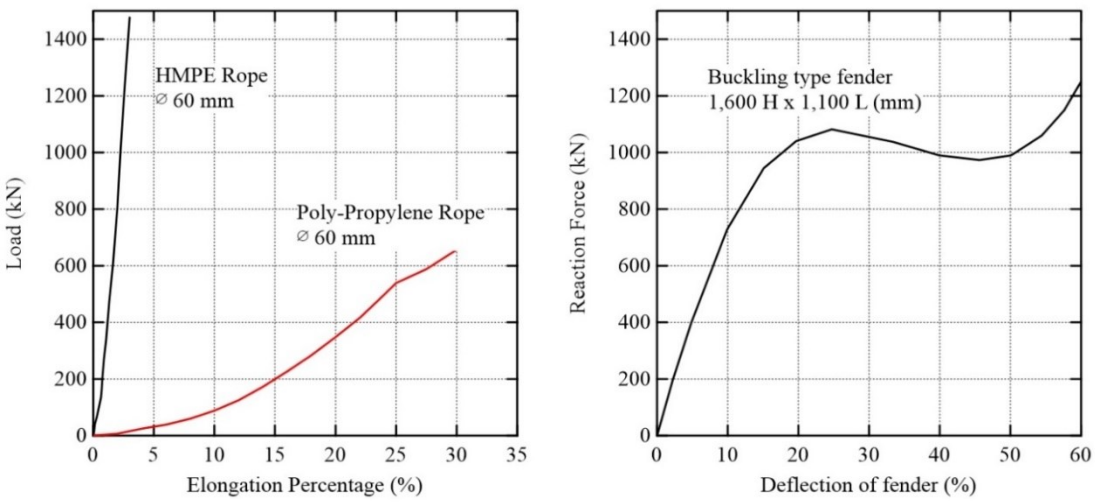

Fig. 3.7. Load-elongation characteristics of mooring ropes (HMPE and PP ropes) and reaction force-deflection of buckling type fenders

3.4.2 Rough Wave Condition

The records of offshore anchoring due to rough waves from 2015 to 2018 are summarized in Table 3.3. During the 4 years, there were 18 cases over 61 days. Offshore anchoring was considered necessary in these cases because the wave condition was forecasted to be Level 2 or 3. Therefore, it is possible to prevent dangerous situations.

Table 3.3 Record of offshore anchoring due to rough weather forecasting (2015–2018)

Case	Waiting period	Maximum $H_{1/3}$ (Inside harbor)	Maximum $H_{L1/3}$ (Inside harbor)	Weather condition
O-1	2015-11-26–2015-11-28	0.74 m	0.33 m	Low pressure
O-2	2016-01-15–2016-01-20	1.33 m	0.97 m	Low pressure
O-3	2016-05-02–2016-05-05	0.76 m	0.34 m	Low pressure
O-4	2016-08-06–2016-08-11	1.05 m	0.77 m	Typhoon
O-5	2016-08-29–2016-09-01	2.31 m	1.65 m	Typhoon
O-6	2017-03-13–2017-03-14	0.46 m	0.18 m	Low pressure
O-7	2017-04-17–2017-04-20	1.02 m	0.62 m	Low pressure
O-8	2017-09-19–2017-09-20	1.16 m	0.66 m	Typhoon
O-9	2017-10-07–2017-10-09	0.58 m	0.38 m	Low pressure
O-10	2017-12-12–2017-12-13	0.71 m	0.08 m	Low pressure
O-11	2018-01-22–2018-01-24	0.78 m	0.18 m	Low pressure
O-12	2018-03-02–2018-03-03	1.08 m	0.37 m	Low pressure
O-13	2018-03-09–2018-03-11	0.42 m	0.23 m	Low pressure
O-14	2018-03-21–2018-03-24	0.25 m	0.14 m	Low pressure
O-15	2018-04-12–2018-04-13	0.55 m	0.13 m	Low pressure
O-16	2018-05-02–2018-05-04	0.25 m	0.14 m	Low pressure
O-17	2018-05-17–2018-05-20	0.23 m	0.12 m	Low pressure
O-18	2018-10-25–2018-10-30	1.01 m	0.23 m	Low pressure

Table 3.4 Record of dangerous cases with unexpected mooring risk (2015–2018)

Case	Staying period in port	Maximum $H_{1/3}$ (Inside harbor)	Maximum $H_{L1/3}$ (Inside harbor)	Weather condition	Visual report (Ship motions)
P-1	2015-11-15–2015-11-17	0.63 m	0.22 m	Low pressure	Small
P-2	2015-12-11–2015-12-13	0.48 m	0.26 m	Low pressure	Small
P-3	2016-02-21–2016-02-23	0.97 m	0.25 m	Low pressure	Small
P-4	2016-04-13–2016-04-15	1.04 m	0.19 m	Low pressure	Small
P-5	2016-04-15–2016-04-17	1.04 m	0.37 m	Low pressure	Small
P-6	2016-04-27–2016-04-29	0.54 m	0.22 m	Low pressure	Small
P-7	2016-06-18–2016-06-21	0.71 m	0.34 m	Low pressure	Large
P-8	2016-07-31–2016-08-02	0.43 m	0.23 m	Typhoon	Small
P-9	2016-09-22–2016-09-24	0.51 m	0.25 m	Typhoon	Small
P-10	2016-12-13–2016-12-15	1.45 m	0.24 m	Low pressure	Small
P-11	2017-02-06–2017-02-08	0.49 m	0.23 m	Low pressure	Middle
P-12	2017-02-24–2017-02-26	1.17 m	0.22 m	Low pressure	Middle
P-13	2017-07-23–2017-07-25	0.50 m	0.31 m	Typhoon	Small
P-14	2017-07-25–2017-07-27	0.44 m	0.27 m	Typhoon	Small
P-15	2017-09-29–2017-10-01	1.11 m	0.16 m	Typhoon	Small
P-16	2017-10-29–2017-10-31	0.87 m	0.30 m	Low pressure	Small
P-17	2018-08-01–2018-08-03	0.25 m	0.08 m	Low pressure	Small
P-18	2018-08-16–2018-08-18	0.19 m	0.13 m	Low pressure	Small
P-19	2018-08-26–2018-08-28	0.45 m	0.16 m	Typhoon	Small
P-20	2018-12-05–2018-12-07	0.58 m	0.11 m	Low pressure	Small

Table 3.4 shows the records of dangerous cases with unexpected mooring risk from 2015 to 2018. This study defines “unexpected mooring risk” as the probabilistic risk associated with

mooring accidents when forecasted in Level 1. During this period, 20 cases with unexpected mooring risk occurred over 60 days. These cases were expected to allow safe cargo operation. However, they were reported to have mooring difficulties due to unexpected rough seas in reality.

Furthermore, there was an emergency evacuation due to large ship motions in Case P-7. In an emergency situation, the assistance of tug boats is immediately necessary. However, the tugboats are located an hour away from this port, so the only safety measure is to add mooring ropes in this port. However, since these measures are not sufficient, additional countermeasures are essential for safe port operation. The relation of wave heights between long-period waves and significant waves for the T Port is summarized in Fig. 3.8.

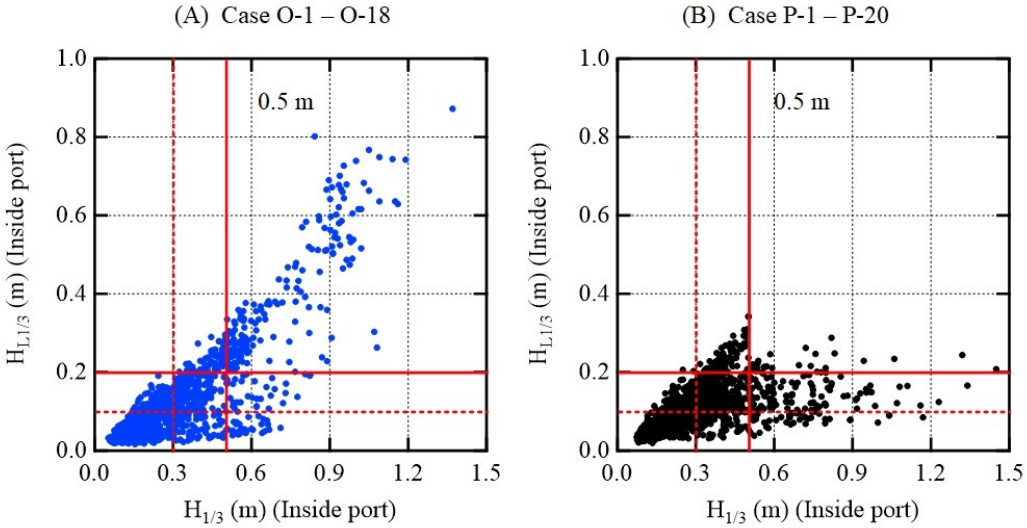

Fig. 3.8. Relation between the long-period and significant waves in 2015–2018

It is obvious that $H_{L1/3}$ exceeds 0.1–0.2 m, which makes large ship motions, even if $H_{1/3}$ is below 0.3–0.5 m inside the harbor in Fig. 3.8(B). In Fig. 3.8(A), wave heights exceed the safety criteria in many cases. However, it is obvious that many records of the wave heights are below the safety range, owing to the overestimated forecasting in this port. Therefore, it is possible to increase the efficiency of port operation by reducing such inappropriate mooring delays.

Among the total cases affected by the rough waves in Tables 3.3 and 3.4, the typical cases are selected. Fig. 3.9 shows the time history for the height of significant waves and long-period waves for the typical cases. The significant wave height is about 0.43–1.33 m, and the long-period wave

height is about 0.23–0.97 m. The wave height of these cases exceeds the operational criteria of wave height. Therefore, it is shown that mooring difficulties could occur during these periods.

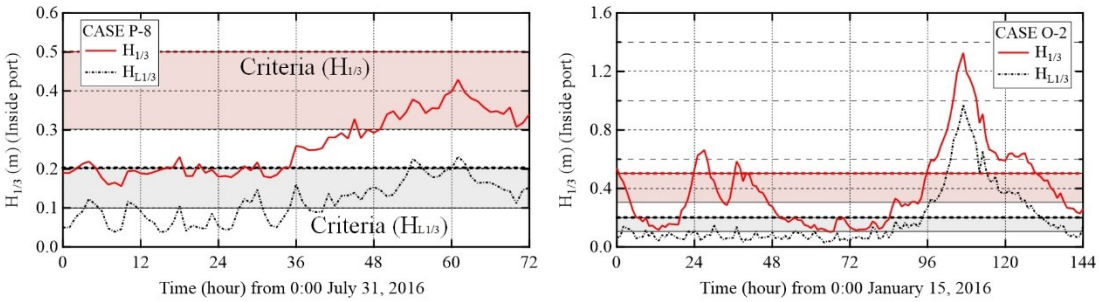

Fig. 3.9. Time history of the significant wave height in typical cases (Case P and Case O)

3.4.3 Mooring Arrangement

In this study, numerical simulations of moored ship motions were conducted for the suggested mooring Methods (A)–(C) with the present method, as shown in Fig. 3.10.

The present method refers to the unbalanced condition of the current mooring arrangement with synthetic fiber ropes. Method (A) indicates the mooring method using the synthetic fiber rope with the revised mooring arrangement as the symmetrical one. In Method (B), although the mooring arrangement is the same as that in the present method, the HMPE is used instead of the synthetic fiber rope. As the HMPE rope has very little elongation, the end-part of the HMPE rope is connected to the 11 m nylon tail rope to absorb the tension. Method (C) refers to the symmetrical mooring arrangement using the HMPE rope with a nylon tail rope. Comparing the present method with each suggested mooring Methods (A)–(C), the main purpose of the simulation is to verify the optimal mooring method in terms of safety and economic efficiency.

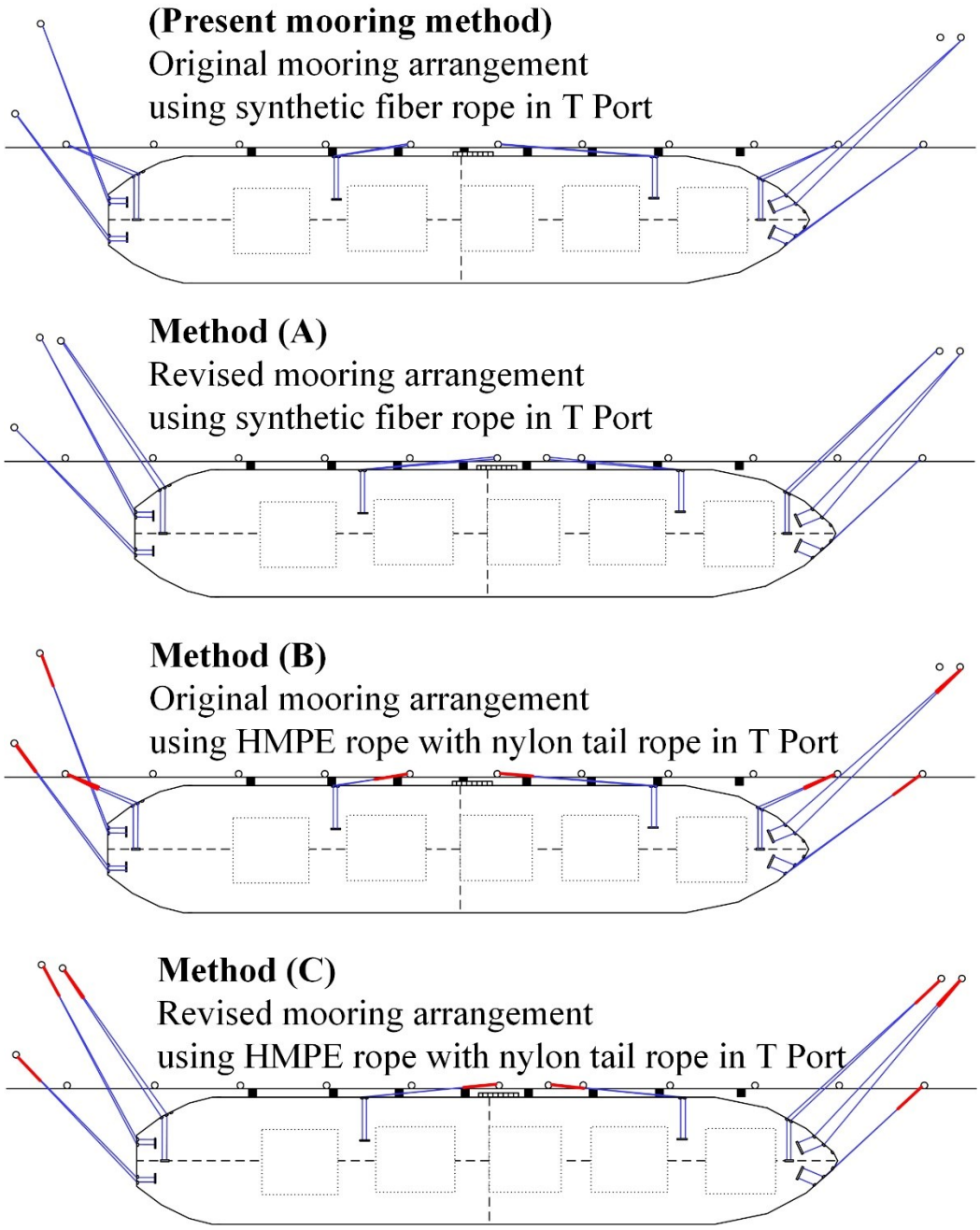

Fig. 3.10. Present mooring method and the suggested mooring methods

3.5 Results and Discussion

3.5.1 Analyzed Results of Moored Ship Safety

In this study, the total cases affected by rough waves (20 cases with unexpected mooring risk,

and 18 cases for offshore anchoring) were simulated and analyzed for verification of mooring safety. Here, the simulation results of typical cases are shown as examples. The heights of the significant wave and long-period waves for the typical examples (Case O and Case P) are shown in Fig. 3.9.

Case O is one of the cases of offshore anchoring due to rough sea forecasting. The ship arrived at the T Port on January 15, 2016. However, because rough waves were forecasted, the berthing schedules were delayed according to the berthing operation guidelines. In this study, the simulation was conducted for the first 72 h under the assumption that there is no offshore anchoring.

Variations of moored ship motions and fender deflections are analyzed in January 15–20, 2016, as shown in Fig. 3.11. The World Association for Waterborne Transport Infrastructure (PIANC) guidelines for criteria of moored ship motions for bulk carriers with a conveyer belt operation are 5 m for surge, 2.5 m for sway, and 3° for yaw (PIANC, 1995). These criteria for each parameter are represented by the red line in the figure.

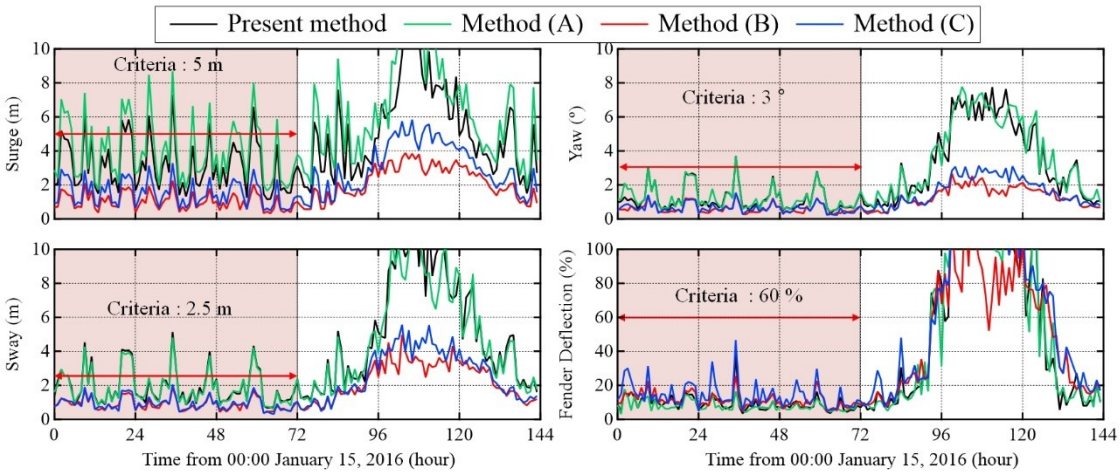

Fig. 3.11. Variations of moored ship motions (surge, sway, and yaw) and fender deflections for January 15–20, 2016 (CASE O)

In Fig. 3.11, the maximum amplitudes of surge, sway, and yaw motions exceed the criteria in the present method and Method (A), while the maximum amplitude is under the criteria in Methods (B) and (C). This indicates that the application of the HMPE rope is effective in reducing

ship motions. However, the amplitude of motions did not significantly change according to the mooring arrangements. Meanwhile, the fender deflections do not exceed the safety criteria in all methods. Deflection of the fenders is not significantly different from mooring methods.

Variations in the safety parameters for mooring ropes, such as PBT and $TEMP$ are analyzed from January 15–20, 2016, as shown in Fig. 3.12. The safety criteria for a rope tension are set at 50% of the break strength (OCIMF, 2018). In addition, the safety criteria for temperature are set at 60 °C based on the studies of TTI and Nobel Denton (1999) and McKenna et al. (2004). PBT shows that the value of the fore-breast line only approaches the safety limit in Method (B). PBT of the other line is within the safe range. The reason for the high tension of the fore-breast line in Method (B) is related to the mooring arrangement. The mooring arrangement in Method (B) shows very short fore-breast lines. In order to reduce the large ship motions, the kinetic energy of ship motions generated from rough waves must be absorbed by the fore-breast lines consisting of HMPE ropes in Method (B).

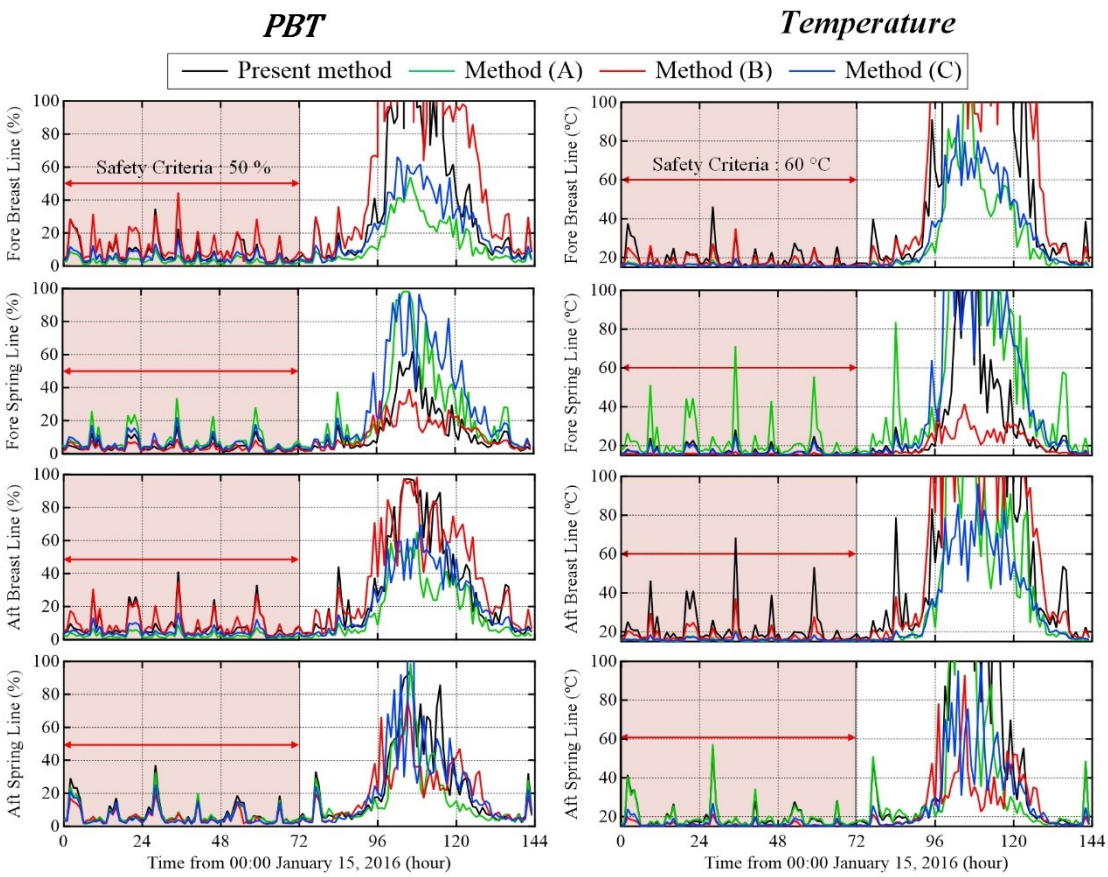

Fig. 3.12. Variations of the evaluation of mooring ropes for January 15–20, 2016(CASE O)

In addition, the variation in the maximum temperature of the rope is shown in Fig. 3.12. In the temperature analysis, the fore-spring line in Method (A) and aft-breast line in the present method are evaluated as dangerous because they exceed the safety range of 60 °C. Nevertheless, Method (C) is the only method evaluated as safe, as it meets all safety criteria. Comprehensively, Method (C) only shows the safe mooring in this example, Case O, resulting in the cancellation of offshore anchoring.

Case P is one of the cases with unexpected mooring risk. The ship arrived on July 31, 2016 and directly berthed at this port. The wave forecast services expected safe conditions. However, the wave conditions were rough enough to create dangerous mooring situations.

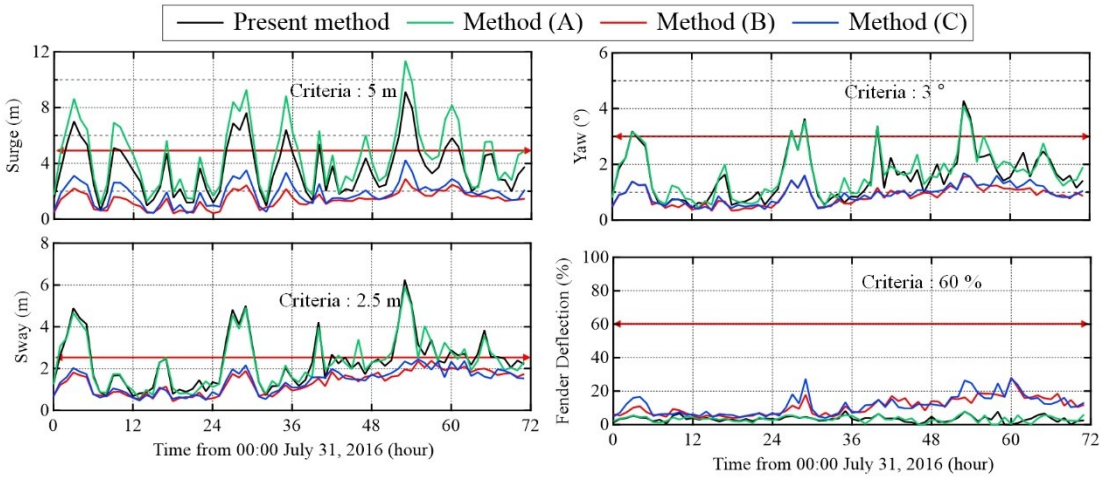

Fig. 3.13. Variations of moored ship motions (surge, sway, and yaw) and fender deflections from July 31 to August 2, 2016 (CASE P)

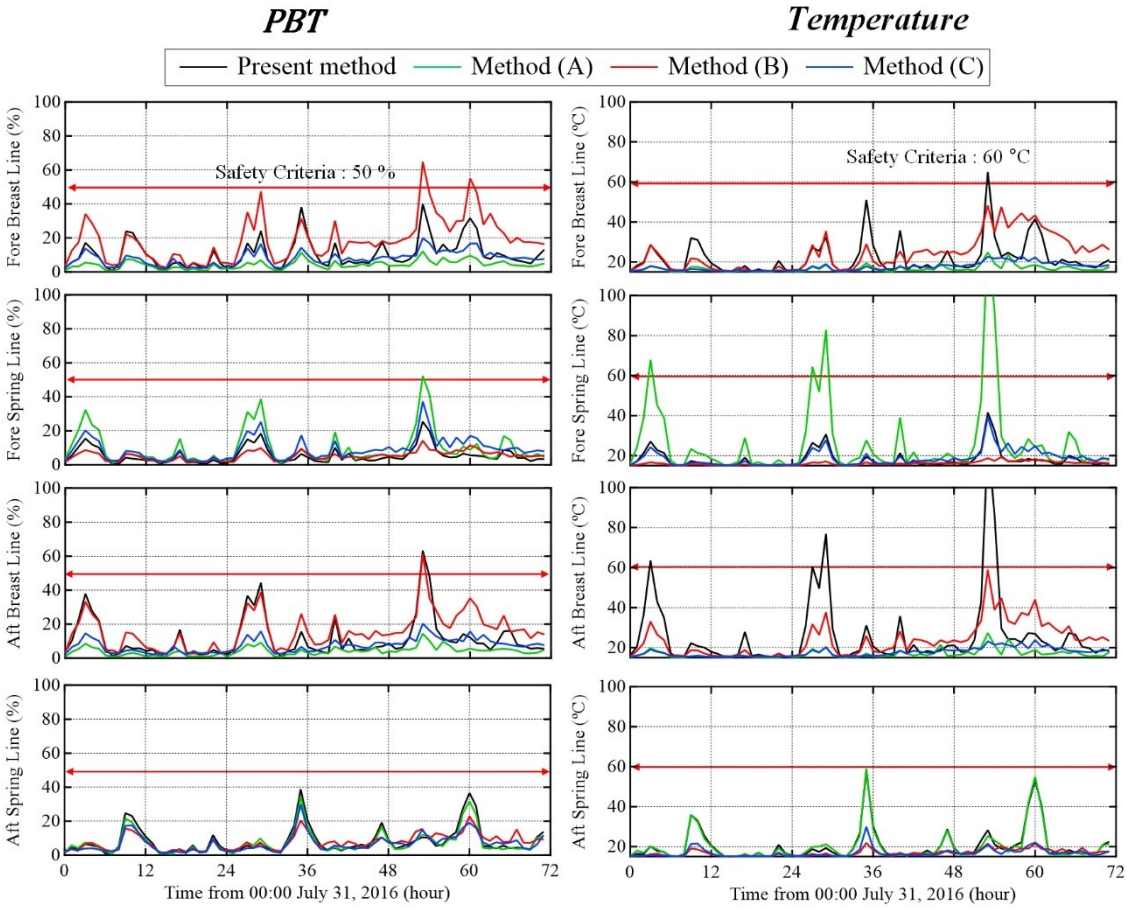

Fig. 3.14. Variations of evaluation of mooring rope from July 31 to August 2, 2016 (CASE P)

Variations in moored ship motions and fender deflections were analyzed from July 31 to August 2, 2016, as shown in Fig. 3.13. With the PIANC guidelines, the simulation shows that the present method and Method (A) using PP ropes exceeds the criteria. However, Methods (B) and (C) with HMPE rope show that the moored ship can stay within safety limits. Meanwhile, the fender deflections do not exceed the safety criteria in any of the methods. Variations of safety parameters for mooring ropes from July 31 to August 2, 2016, are analyzed in Fig. 3.14. It is clear that the tension of the fore-breast and aft-breast lines exceed the safety criteria in Method (B), and the tension of the aft-breast line exceeds the safety criteria in the present method. However, the values are less than the safety criteria in Method (C).

With the effects of friction and bending fatigue, the value of $TEMP$ is higher when using

synthetic fiber rope than when using HMPE rope. It is shown that the value of $TEMP$ is related to rope materials. Although the values of PBT and $PBTF$ of the fore-breast line exceed the criteria in Method (B), the value of $TEMP$ is less than the criteria. In addition, the value of $TEMP$ of the fore-breast line exceeds the criteria in the present method. The elongation of the ropes with ship motions is significantly reduced when using the HMPE ropes, which helps to maintain the low temperature of the ropes. For this reason, it is obvious that the adoption of HMPE ropes can be advantageous for safety from the viewpoint of temperature.

3.5.2 Evaluation from the Viewpoint of Safety

The decision of berthing is based on reliable wave forecasting in the case of the T Port. However, the wave forecast cannot be perfect and sometimes leads to incorrect decisions. These inappropriate mooring situations occur when the wave force is underestimated or not considered. Therefore, it is necessary to verify the optimal mooring method from a safety point of view by analyzing these mooring situations.

The simulation results are analyzed and compared with the present method and suggested mooring Methods (A)–(C). The relationships between long-period wave heights and maximum amplitude from the simulated results of 2736 h (=38 cases × 72 h) for 38 cases in 2015–2018 are shown in Fig. 3.15. In addition, the red lines in the figure indicate the safety criteria, which are 50% for tension and 60 ℃ for temperature. In Fig. 3.15, it is obvious that the least dangerous mooring situations that exceed safety criteria are in Method (C). However, Methods (A) and (B) are not significantly different from the present method.

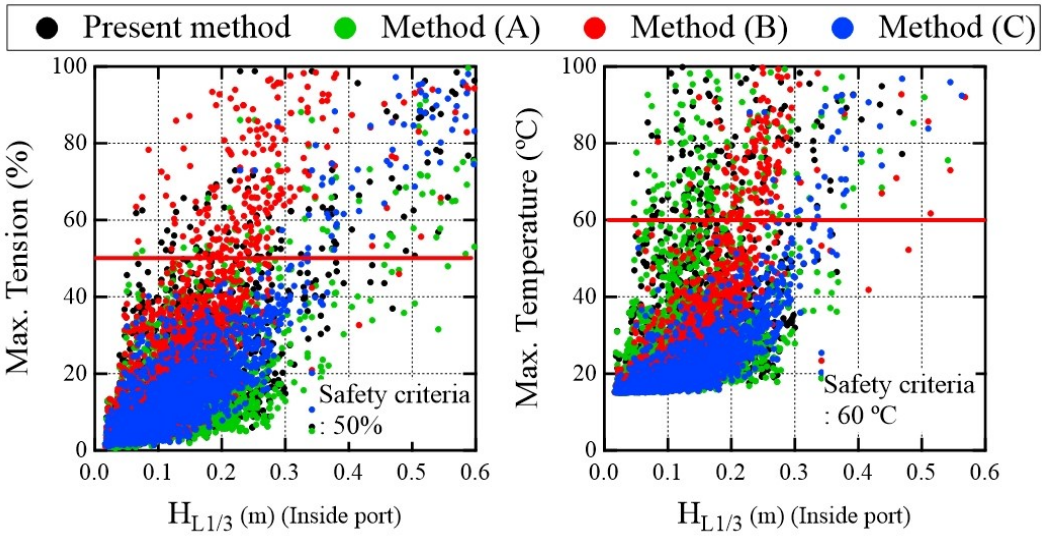

Fig. 3.15. Relations between the long-period wave heights and maximum amplitude of tension and temperature of mooring ropes in 2015–2018

In terms of safety, the maximum amplitude of each evaluation method is compared with the safety criteria. If the simulated value of each operation hour exceeds the safety criteria, the operation hours are defined as the dangerous hours with mooring risk. For the 72 hours of every case, it is analyzed whether the operation is dangerous or not. The portion of dangerous hours with mooring risk within total operation hours, PDM, can be obtained as follows:

$$PDM\ (\%) = \frac{H_d}{H_o}, \tag{3.14}$$

where H_o is the total operation hours in port, and H_d is the dangerous mooring hour with mooring risk, which exceeds the safety criteria. Comparing the value of PDM in each mooring method, it is possible to verify the low-risk mooring method. Using this concept, each mooring method can be compared objectively, and the optimal mooring methods in rough waves can be verified. The results of the mooring safety evaluation in all cases are shown in Fig. 3.16.

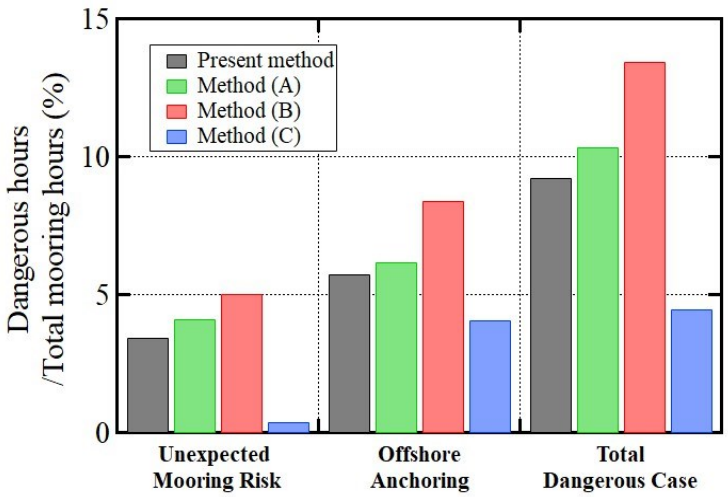

Fig. 3.16. Portion of dangerous hours from the total mooring period according to the suggested mooring Methods (A)–(C) in 2015–2018

The results of the present method and Method (A) are similar. It is shown that these two methods are nearly equal in the total portion of high risk (10%). However, Method (B) is the most dangerous in this evaluation because the result shows the largest proportion of high risk (13%). In contrast, the operation hours using Method (C) are only exposed to dangerous situations for less than 5% of the total operation hours. In particular, the dangerous hours are only 11 hours (0.4%) in the case with an unexpected mooring risk. The results show that Method (C) is most effective in terms of safety.

3.5.3 Evaluation from the Viewpoint of Cost-Benefit Performance

Based on the field survey, including literature review, the main priority of port operation can be categorized into two aspects. These are safety and economic efficiency. Safety is the standard for how safe the moored ship is to stay without any difficulties. Economic efficiency refers to how efficiently the moored ship can be operated without significant delay due to rough sea. However, there are no effective evaluation methods for the mooring facility that balance finance with safety. This point is very important to solve the mooring problem in the current situation. From these points of view, the berthing delay is validated by enhancing the mooring methods.

To verify the possibility of berthing, the evaluation of mooring safety is focused on checking whether the result exceeds the safety criteria during the first 72 hours. If the simulation result exceeds these safety limits, the demurrage cost cannot be reduced because the berthing is impossible. If the simulation result is less than these limits, the ship could reduce the demurrage cost because berthing is possible.

In fact, the actual berthing delay due to rough waves is a total of 61 days over 4 years in the T Port. However, this simulated result is different for each mooring method, as shown in Table 3.5. In addition, there is a difference of 20 days between the simulation results and reality in the present method. These 20 days of berthing delay are caused by overestimated weather forecasting. If the forecasting accuracy is 100%, the present method can reduce the berthing delay by 20 days. Through the difference of these 20 days, it can be estimated that the error of the current weather forecasting system is approximately 33% (0.33=1-41/61).

Table 3.5 Total delay in the actual and simulated result for suggested mooring Methods (A)–(C) in 2015–2018

Total delay	Present	Method (A)	Method (B)	Method (C)
Actual delay	61 days	-	-	-
Simulation result of delay (100% of forecasting accuracy)	41 days	43 days	52 days	22 days

Using the mooring Methods (A) and (B), the results show berthing delays of 43 and 52 days, respectively. This result indicates that the two methods for economic efficiency are not effective than the present method because they cannot reduce the berthing delay. Method (C) shows only 22 days of berthing delay, which is the only efficient from the economic aspect.

As mentioned, it is very important to discuss the reduced cost by enhancing the mooring systems, as shown here. Methods (A)–(C) require the cost of initial investment and an additional maintenance cost to introduce the new mooring system. However, it is shown that Methods (A) and (B) are not worth it to consider economic efficiency because both these methods increase the berthing delay. Therefore, the economic effect should be verified only for Method (C) by considering these investment and extra maintenance costs for additional facilities. Basically,

maintenance costs for the present method are required for other methods, too. However, the additional cost of maintenance is only evaluated here by introducing the new mooring system. To evaluate the relationship between the accumulated cost of demurrage and the total investment cost of the new mooring system, the function of safety equipment and total payments, *FSTP*, is newly defined here.

$$FSTP = \sum_{i=1}^{N} D_i + \sum_{i=1}^{N} (I_i + M_i)\ , \tag{3.15}$$

where D_i is the accumulated cost of demurrage (delay) per year, I_i is the investment cost of the initial construction and the renewal of the mooring system (every 20 years), and M_i is the additional maintenance cost due to the enhanced mooring system (every five years). N is the operation periods (years).

For the accumulated cost of demurrage, it is necessary to know the cost of demurrage per day. Based on the field survey in T Port, the daily cost of demurrage is set at \$40,000. Thus, the total accumulated cost of demurrage D_i can be obtained for the present method and Method (C) as in Table 3.6. For example, the present method shows 61 days of delays for 4 years in reality. This means that the delay occurs on an average for 15.25 days every year. Therefore, multiplying this average by the daily cost of demurrage (\$40,000), the annual loss D_i of the present method is \$0.61 million.

Method (C) requires investment cost I_i of bitt installation (\$0.5 million = 2 sets × \$250,000), rope replacement (\$0.44 million = 22 sets × \$20,000), and installation of a shore winch (\$2.4 million = 6 sets × \$400,000). The additional maintenance cost M_i is set to \$0.1 million per five years in Method (C). The parameter values of D_i, M_i, and I_i for the present method and Method (C) are summarized in Table 3.6.

Table 3.6 Parameter values for the function of safety equipment and total payments

Parameter	Present method	Method (C)
D_i (Current weather forecasting)	\$0.61 million /year	\$0.42 million /year
D_i (100% accuracy weather forecasting)	\$0.41 million /year	\$0.22 million /year
M_i	-	\$0.10 million /5 years
I_i	-	\$3.34 million /20 years

Variations in *FSTP* are compared between the present method and Method (C) if the life cycle of the port is assumed to be 60 years. Fig. 3.17 shows the result of *FSTP* with the current forecasting system. The black line shows the accumulated loss of the present method. The present method has an annual economic loss of \$0.61 million without any investment and additional maintenance cost, resulting in \$36.6 million after 60 years. Although Method (C) required initial investment costs due to the enhanced mooring system, the total cumulative loss was \$36.3 million. The investment cost is finally compensated for and leads to profits after 20 years.

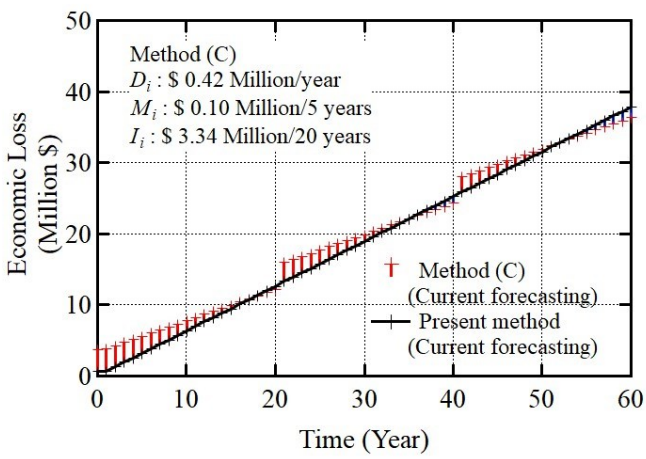

Fig. 3.17. Function of safety equipment and total payments with the current weather forecasting systems

In addition, if 100% of weather forecasting is possible with the development of a weather forecasting technology, the variations in *FSTP* can be described as shown in Fig. 3.18. Here, the

FSTP of Method (C) with 100% forecasting accuracy can be compared with two cases of the present method (current and 100% forecasting accuracy). In Fig. 3.18(A), since both the present method and Method (C) are assumed to have 100% forecasting accuracy, each mooring method shows the total accumulated loss of $24.6 million and $24.3 million, respectively. However, if compared with the present method including the current forecasting error (20 days, 33%), Method (C) with advanced forecasting shows admirable economic efficiency, as shown in Fig. 3.18(B). The cumulative economic benefits gradually increase over time, resulting in a total accumulated benefit of $12.6 million after 60 years. It shows that the enhanced mooring method with the improvement in weather forecast accuracy can contribute to significantly reducing the economic loss of a moored ship.

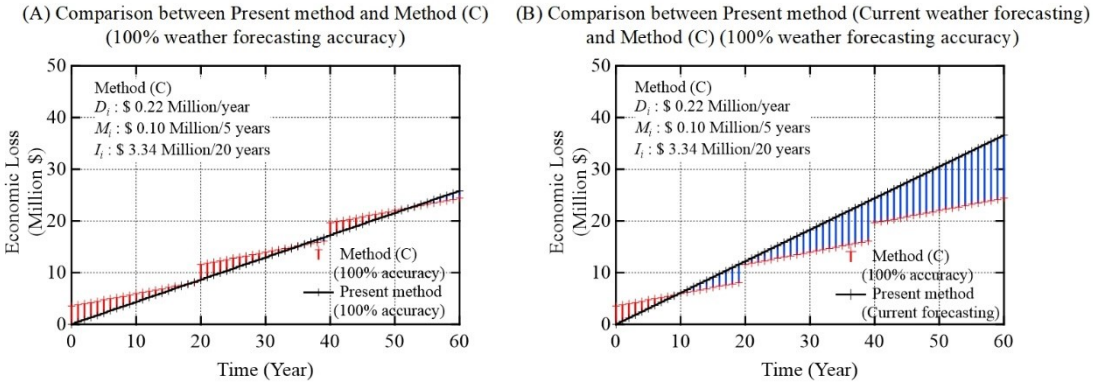

Fig. 3.18. Function of safety equipment and total payments with 100% accuracy of the weather forecasting systems

According to the field survey, some port operators do not hesitate to invest in safety as a top priority, regardless of how much the cost is necessary. However, many domestic port operators cannot afford to invest in the reinforcement of port facilities. In this study, Method (C) is verified as the optimal mooring method in the T Port. This proposed method requires a large budget for initial investment. However, this initial investment can be recovered by reducing the demurrage cost of offshore anchoring. Moreover, this improvement in port facilities can increase the allowable wave height, increasing the efficiency of port operations. In addition, the extra benefit can be expected from the development of weather forecasting technology.

In this study, the suggested mooring method (C) is verified to be effective and sufficiently applicable not only for the improvement of port safety but also for financial advantage in the long term. However, because these results are for the target terminal only, the results could be different depending on the mooring situation at other ports. Therefore, it is necessary to conduct additional analyses with other port terminals in future studies.

3.6 Summary

In this study, new evaluation methods were proposed to reduce the risk of a moored ship. Friction and bending fatigue were newly included in the analysis of mooring ropes. This method seems more effective and accurate because it considers the rope-breaking mechanism. In addition, optimal mooring methods were verified in terms of safety and economic efficiency. This study is summarized as follows.

(1) Simulated results show that accumulated friction generates heat and damages the rope. Therefore, it was necessary to analyze friction, bending fatigue, and temperature, in addition to a tension analysis.

(2) Moored ship motion was compared among mooring Methods (A)–(C). The optimal mooring method from the safety point of view is one that maintains the lowest dangerous mooring hours. As a result, since Method (C) had the lowest number of dangerous hours, it was considered optimal in terms of safety.

(3) The *FSTP* was newly introduced to confirm economic efficiency. It is defined as total costs including investment, maintenance, and demurrage. It enables one to estimate the amount of total costs. Methods (A) and (B) showed negative effects, which meant that their economic efficiency was not sufficient. Method (C) showed economic benefits among the three suggested mooring methods.

(4) As a result of checking with the proposed evaluation methods in terms of safety and economic efficiency, Method (C), a balanced mooring arrangement with a HMPE rope, was verified as the optimal mooring method. Moreover, economic efficiency can be expected to reach maximum benefit with the development of weather forecasting technology.

(5) This study is expected to help port terminals experiencing mooring problems in terms of economic efficiency and safety. It is necessary to verify these results through actual

measurements in further research. A further analysis of mooring safety must also be conducted for different port regions, weather conditions, ship types, etc.

References

ATSB (Australian Transport Safety Bureau), 2008. Independent investigation into the breakaway and grounding of the Hong Kong registered bulk carrier Creciente at Port Hedland, Western Australia on 12 September 2006. Canberra. https://www.atsb.gov.au/publications/investigation_reports/2006/mair/mair232/.

Black, K., Banfield, S.J., Flory, J.F., Ridge, I.M.L., 2012. Low-Friction, Low-Abrasion Fairlead Liners. In: Proc. OCEANS 2012 IEEE/MTS. USA, 1–11. http://doi.org/10.1109/OCEANS.2012.6405022.

Bossolini, E., Nielsen, O.W., Oland, E., Sørensen, M.P., Veje, C., 2016. Thermal properties of Fiber ropes. Paper presented at European Study Group with Industry, Denmark. https://orbit.dtu.dk/en/publications/thermal-properties-of-fiber-ropes.

Cummins, W.E., 1962. The Impulse Response Function and Ship Motions. Technical Report No. DTMB-1661, David Taylor Model Basin, USA.

Foster, G.P., 2002. Advantages of Fiber Rope over Wire Rope. J. Ind. Text. 32 (1), 67–75. http://doi.org/10.1106/152808302031656.

González-Marco, D., Sierra, J.P., Fernández de Ybarra, O., Sánchez-Arcilla, A., 2008. Implications of Long Waves in Harbor Management: The Gijón Port Case Study. Ocean Coast Manag. 51, 180–201. https://doi.org/10.1016/j.ocecoaman.2007.04.001.

Hashimoto, N., Kawaguchi, K., 2003. Statistical forecasting of long period waves based on weather data for the purpose of judgment of executing cargo loading. In: Proc. 13th Int. Soc. Offshore Polar Eng. Conf. Honolulu, USA, 697–704. https://www.onepetro.org/conference-paper/ISOPE-I-03-302.

Hearle, J.W.S., Parsey, M.R., Overington, M.S., Banfield, S.J., 1993. Modelling the Long-Term Fatigue Performance of Fibre Ropes. In: Proc. 3th Int. Soc. Offshore Polar Eng. Conf. Singapore, 377–383. https://www.onepetro.org/conference-paper/ISOPE-I-93-152.

Hobbs, R.E., Burgoyne, C.J., 1991. Bending Fatigue in High-Strength Fibre Ropes. Int. J. Fatigue. 13 (2), 174–180. http://doi.org/10.1016/0142-1123(91)90011-m.

Ikeda, H., Yasuda, D., Yoneyama, H., Otake, Y., Hiraishi, T., 2011. Development of mooring system to reduce long-period motions of a large ship. In: Proc. 21th Int. Soc. Offshore Polar Eng. Conf. Hawaii, USA, 1214–1221.

https://www.onepetro.org/conference-paper/ISOPE-I-11-317.

John, F., 1950. On the motion of floating bodies II. Commun. Pure Appl. Math. 3 (1), 45–101. http://doi.org/10.1002/cpa.3160030106.

Karnoski, S.R., Liu, F.C., 1988. Tension and Bending Fatigue Test Results of Synthetic Ropes. In: Proc. Annual Offshore Tech. Conf. Houston, USA, 343–350. http://doi.org/10.4043/5720-ms.

Kwak, M., Moon, Y., Pyun, C., 2012. Computer Simulation of Moored Ship Motion Induced by Harbor Resonance in Pohang New Harbor. In: Proc. 33rd Conf. Coast. Eng. Spain. http://doi.org/10.9753/icce.v33.waves.68.

Kubo, M., Barthel, V., 1992. Some Considerations How to Reduce the Motions of Ships Moored at an Open Berth. J. Japan Inst. Nav. 87, 47–58. http://doi.org/10.9749/jin.87.47.

Kubo, M., Sakakibara, S., 1999. A Study on Time Domain Analysis of Moored Ship Motion Considering Harbor Oscillations. In: Proc. 9th Int. Soc. Offshore Polar Eng. Conf. France, 574–581.
https://www.onepetro.org/conference-paper/ISOPE-I-99-309.

López, M., Iglesias, G., 2014. Long Wave Effects on a Vessel at Berth. J. Appl. Ocean Res. 47, 63–72.
http://doi.org/10.1016/j.apor.2014.03.008.

McKenna, H.A., Hearle, J.W.S., O'Hear, N., 2004. Handbook of Fibre Rope Technology. Cambridge: Woodhead Publishing.

MLIT (Ministry of Land, Infrastructure, Transport and Tourism), 2009. Technical standards and commentaries for port and harbour facilities in Japan. Translated and edited by The Overseas Coastal Area Development Institute of Japan, Tokyo. http://ocdi.or.jp/en/technical-st-en.

Nabijou, S., Hobbs, R.E., 1995. Frictional Performance of Wire and Fibre Ropes Bent over Sheaves. J. Strain Anal. Eng. 30 (1), 45–57. http://doi.org/10.1243/03093247V301045.

Ning, F., Li, X., Hear, N.O., Zhou, R., Shi, C., Ning, X., 2019. Thermal Failure Mechanism of Fiber Ropes When Bent over Sheaves. Text. Res. J. 89 (7), 1215–1223. http://doi.org/10.1177/0040517518767147.

OCIMF (Oil Companies International Marine Forum), 2018. Mooring Equipment Guidelines. 4th ed. London: Oil Companies International Marine Forum.

Overington, M.S., Leech, C.M., 1997. Modelling Heat Buildup in Large Polyester Ropes. Int. J. Offshore Polar Eng. 7 (01), 63–69. https://www.onepetro.org/journal-paper/ISOPE-97-07-1-063.

PIANC (World Association for Waterborne Transport Infrastructure), 1995. Criteria for movements of moored ships in harbor: A practical guide. Brussels: PIANC General Secretariat.

Ridge, I.M.L., Wang, P., Grabandt, O., O'Hear, N., 2015. Appraisal of Ropes for LNG Moorings. In: Proc. OIPEEC Conf. 5th Int. Stuttgart Rope days, Stuttgart, Germany. https://oipeec.org/products/appraisal-of-ropes-for-lng-moorings.

Sakakibara, S., Kubo, M., 2009. Initial Attack of Large-Scaled Tsunami on Ship Motions and Mooring Loads. J. Ocean Eng. 36 (2), 145–157. http://doi.org/10.1016/j.oceaneng.2008.09.010.

Sasa, K., Kubo, M., Shiraishi, S., Nagai, T., 2001. Basic research on frequency properties of long period waves at harbour facing to the Pacific Ocean. In: Proc. 11th Int. Soc. Offshore Polar Eng. Conf. Stavanger, Norway, 593–600. https://www.onepetro.org/conference-paper/ISOPE-I-01-322.

Sasa, K., 2017. Optimal Routing of Short-Distance Ferry from the Evaluation of Mooring Criteria. In: Proc. Int. Conf. Offshore Mech. Arct. Eng. OMAE, 6 (2), 1–8. http://doi.org/10.1115/OMAE201761077.

Sasa, K., Mitsui, M., Aoki, S., Tamura, M., 2018. Current Analysis of Ship Mooring and Emergency Safe System. J. Japan Soc. Civ. Eng. Ser. B2 (Coast. Eng.) 74 (2), 1399–1404. http://doi.org/10.2208/kaigan.74.I_1399. [in Japanese].

Sasa, K., Aoki, S., Fujita, T., Chen, C., 2019. New Evaluation for Mooring Problem from Cost-Benefit Effect. J. Japan Soc. Civ. Eng. Ser. B2 (Coast. Eng.) 75 (2), 1243–1248. http://doi.org/10.2208/kaigan.75.I_1243. [in Japanese].

Shiraishi, S., Kubo, M., Sakakibara, S., Sasa, K., 1999. Study on numerical simulation method to reproduce long-period ship motions. In: Proc. 9th Int. Soc. Offshore Polar Eng. Conf. France, 536–543. https://www.onepetro.org/conference-paper/ISOPE-I-99-304.

Shiraishi, S., 2009. Numerical simulation of ship motions moored to quay walls in long-period waves and proposal of allowable wave heights for cargo handling in a port. In: Proc. 19th Int. Soc. Offshore Polar Eng. Conf. Japan, 1109–1116. https://www.onepetro.org/conference-paper/ISOPE-I-09-232.

Sloan, F., Nye, R., Liggett, T., 2003. Improving Bend-over-Sheave Fatigue in Fiber Ropes. In: Proc. OCEANS 2003 IEEE/MTS, USA, 1054–1057. http://doi.org/10.1109/oceans.2003.178486.

TTI and Noble Denton, 1999. Deepwater Fibre Moorings: an Engineers' Design Guide. Ledbury.

Van der Molen, W., Monárdez, P., van Dongeren, A.P., 2006. Numerical Simulation of Long-Period Waves and Ship Motions in Tomakomai Port, Japan. Coast. Eng. J. 48 (1), 59–79. http://doi.org/10.1142/S0578563406001301.

Van der Molen, W., Scott, D., Taylor, D., Elliott, T., 2015. Improvement of Mooring Configurations in Geraldton Harbour. J. Mar. Sci. Eng. 4 (3). http://doi.org/10.3390/jmse4010003.

Van Essen, S., Van der Hout, A., Huijsmans, R., Waals, O., 2013. Evaluation of Directional Analysis Methods for Low-Frequency Waves to Predict LNGC Motion Response in Nearshore Areas. In: Proc. Int. Conf. Offshore Mech. Arct. Eng. OMAE 2013. https://doi.org/10.1115/OMAE2013-10235.

Villa-Caro, R., Carral, J.C., Fraguela, J.Á., López, M., Carral, L., 2018. A review of ship mooring systems. Brodogradnja 69 (1), 123–149. http://doi.org/10.21278/brod69108.

Yamamoto, K., Kubo, M., Asaki, K., Kanuma, Y., 2004. An Experimental Research on Internal Stress of Ropes Under Repeated Load. J. Japan Inst. Nav. 112, 353–359. http://doi.org/10.9749/jin.112.353. [in Japanese].

Yamamoto, K., Kubo, M., Asaki, K., 2006. Comparison between Numerical Calculation and Experimental Results of Temperature Rise on Rope under Repeated Load. J. Japan Inst. Nav. 116, 269–275. http://doi.org/10.9749/jin.116.269. [in Japanese].

Yamamoto, K. 2007. Basic research on preventing breakage of mooring ropes. PhD diss., Kobe University. [in Japanese].

Yoneyama, H., Minemura, K., Moriya, T., 2017. A study on calculation methods of allowable wave heights of a moored ship in remote island ports. J. Japan Soc. Civ. Eng. 73(2), 803–808. http://doi.org/10.2208/jscejoe.73.I_803. [in Japanese].

Chapter 4 Safety Evaluation of Anchored Ship under Rough seas

4.1 Background

Maritime cargo is estimated to reach approximately 15 billion tons by 2050 (Qinetiq et al., 2013), which indicates that maritime transportation will dominate the world of transportation in the future (Corbett et al., 2010; Ducruet, 2020). However, several factors, such as the optimal ship routing to ensure safety, environmental issues, and energy savings by the Energy Efficiency Design Index (EEDI) enforcement in 2012, could affect safe and efficient transportation. Many related studies have been conducted to minimize gas emission, fuel consumption, and voyage time by accurately estimating the loss of speed in rough seas, etc. (Plessas et al., 2018; Zhang et al., 2019; Du et al., 2021; Sasa et al., 2021). Lockdown measures adopted by various countries due to the corona virus (COVID-19) pandemic caused difficulties and complications for global trade regarding maritime transportation (UNCTAD, 2020). According to CNN (2021) and The New York Times (2021), many ships (around 100 ships) had to stay in offshore harbors for 7-10 days on average due to the increase in maritime transport and the decrease in the number of port workers, which lead to congestion in offshore anchorage. Furthermore, operational issues when ships stay in ports or offshore harbors were also affected. Between 1990-2000, many studies were conducted on moored ship motions to analyze mooring accidents such as the breakage of mooring lines, fenders, quay walls, and ship hulls, caused by long-period waves around 1–3 min (Van der Molen et al., 2006; Figuero et al., 2019). Although it is recommended to enforce mooring facilities in ports to reduce ship motions, very few practice it owing to financial concerns. Therefore, a weather forecasting service was introduced in some ports such as VLCC, LNG, and coal terminals as an alternative countermeasure. In these terminals, the berthing schedules are determined depending on the forecasting systems. The Ministry of Land, Infrastructure, Transport and Tourism, Japan (MLIT, 2009) recommended operation standards for significant wave heights of 0.3–0.5 m inside the harbor and 0.1–0.2 m for long-period waves. Berthing schedules are sometimes adjusted to avoid accidents based on the forecasting system and operational standards. Therefore, ships are ordered to wait at the offshore harbor if rough weather is forecasted (Sasa et al., 2018 and 2019; Lee et al., 2021). However, the safety of anchored ships under severe weather has not been considered. Ventikos et al. (2015) and EMSA (2020) reported that approximately 50-70% of ship accidents occur in port or coastal waters. Sugomori (2010) analyzed several accidents caused by anchoring operations and demonstrated the need for increased knowledge on anchoring

operations. However, the current optimal ship routing only focuses on the phase of the voyage in oceans. It makes the total evaluation of ship operations insufficient because safety evaluations such as moored or anchored ships are not considered.

From these backgrounds, this study is organized as follows. Section 4.2 presents the related studies and describes the methodology for safety evaluation. Section 4.3 presents the numerical simulation used to reproduce anchored ship motions and describes the algorithms for the risk of collision. Section 4.4 summarizes the results of onboard measurement against the 28,000-DWT class bulk carrier for approximately three years in global sea areas. The period of voyage, offshore anchoring, and stay inside the harbor was obtained from the measured data. It was noted that the ship was not on the voyage for approximately 40% of the operation time. Section 4.5 presents the simulation results of anchored ship motions for each case and compares them with the measured ship motions. The forecasting error should be considered to evaluate the emergency operation in the worst case scenario. Therefore, the simulation of anchored ship motion was conducted if the wave conditions were assumed as the underestimated results. Section 4.6 presents the construction of risk assessment for the anchored ship including stranding, damaging, and collision accidents in anchorage. In particular, the risk of collision was evaluated by introducing the relative risk factors with the AIS data. Finally, Section 4.7 presents the conclusions of this study and subjects for future research.

4.2 Methodology for Safety Evaluation of Anchored Ships

This section describes the methodology to conduct the safety evaluation for anchored ships with related studies. Section 4.2.1 presents the safety evaluation of anchored ship motions in winds and waves. Section 4.2.2 summarizes the current accuracy of weather forecasting for winds and waves. In Section 4.2.3, the risk of collisions is additionally introduced for safety evaluation of anchored ships. Based on these points, the methodologies are presented with the main merits of this study here.

4.2.1 Safety Evaluation of Anchored Ship Motions

Some studies have evaluated the anchored ship motions to simulate the dragging anchor, which occurs under strong winds during the offshore harbor refuge for typhoons (Inoue, 1981; Kikutani et al., 1983). However, these studies only considered wind forces. Zou et al. (2012) simulated

anchored ship motions considering wave forces besides wind forces; however, the dragging anchors under stormy conditions were not analyzed. Sasa and Incecik (2012) studied the anchored ship motions for a stranded accident offshore harbor facing the Pacific Ocean during the offshore harbor refuge from a big typhoon. The ship stranded after it had drifted into the coast with the dragging anchor of long distances. Additionally, the dynamic model of anchor chain forces and the lumped mass method were introduced to accurately evaluate the mooring forces. Wave forces are considered as the dominant factor in causing ships to be stranded, given that stranding occurs due to vertical motions, and the dragging anchor, other than wind forces, can occur due to long periods of drift forces in irregular sea. The anchored ship motions are compared in each combination of external forces, such as wind forces, linear and non-linear wave forces in time domain motion analysis. It was observed that stranding accidents can occur due to combined external forces among wind forces, and linear and non-linear wave forces. However, these studies are not widely applied to the safety analysis of ships in coastal sea areas, indicating that the emergency operation still depends on the intuition of ship masters (Sharpey-Schafer, 1954; Zhang and Zhao, 2013; Lu and Bai, 2015). As a result, the accuracy of weather forecasting and knowledge of anchored ship motions becomes inevitable in handling dangerous situations. Theoretical descriptions of anchored ship motions are shown in 4.3.1 and 4.3.2.

4.2.2 Current Accuracy of Weather Forecasting

Many studies have been conducted on weather forecasting at seas, which have been used to operate ships and ports (Chen et al., 2020; Lee et al., 2021). Weather forecasting is one of the most important tools in all ship operation situations and is the fundamental part of optimal ship routing. Despite the various developments in the weather forecasting technology, it is impossible to be perfectly accurate, that is, some errors still exist (Natskår et al., 2015; Girolamo et al., 2017). Chen and Wang (2020) demonstrated that forecasted results are sometimes significantly underestimated against the measured values, by 1.5–2 times. Considering underestimated weather conditions can be very dangerous for ships; it is crucial to understand its influence on ships quantitatively.

4.2.3 Safety Evaluation for Risk of Collision

Ship motions with dragging anchor are the key factor for evaluating safety for ships in coastal

areas. It is important to reproduce the following points, which are vertical ship motions when stranding in shallow waters, damaging structures under the seabed such as cables or pipes by the anchor motion, and collisions with other ships. In the field of maritime transportation, many studies have been conducted on ship domains to analyze the risk of collision (Fujii and Tanaka, 1971; Kearon, 1977; Coldwell, 1983; Pietrzykowski and Uriasz, 2009; Hansen et al., 2013; Wang and Chin, 2016). Im and Luong (2019) proposed Potential Risk Ship Domain (PRSD) to evaluate the potential risk of collision in real time within the Collision Assessment zone. Further, Luong et al. (2021) developed the Marine Traffic Hazard Index (MaTha Index) to represent the dynamic waterway risk. The MaTha Index shows the high-risk collision area of the waterway using the Harbour Traffic Hazard Map. Pietrzykowski and Wielgosz (2021) determined the impact of ship size and speed to ship domain area based on simulation tests. Various risk assessment models of autonomous ships in actual seas have been derived to avoid collision of ships (Tam and Bucknall, 2010; Chai et al., 2017; Liu and Shi, 2020). As mentioned, congestion of ships in the offshore anchorage should be considered given that most collisions occur in coastal areas, especially in the vicinity of anchorage (Yeo et al., 2007; Debnath and Chin, 2016). Burmeister et al. (2014) proposed a collision model for marine risk assessment in offshore anchorages. The model estimated the risk of collision based on the function of collision frequency and consequence loss.

In most related models, the ship domain have shown as the ellipse shape due to the effect of the forward speed of the ship. However, it is not appropriate to analyze the collision risk of anchored ships with the same ship domain, because the anchored ships have almost zero speed in case of no drift due to dragging anchors. Liu et al. (2020) proposed a model to identify the risk of collision in offshore anchorage using the Automatic Identification System (AIS) database to derive the collision risk index (CRI) between ships in offshore anchorages. To evaluate the index, parameters such as the Distance at Closest Point of Approach, DCPA, Time to Closest Point of Approach, TCPA, and the SDOI were considered the main risk factors. Theoretical descriptions for risk of collision are shown in 4.3.3.

Fig. 4.1 illustrates the flowchart of this study. It includes the safety evaluation of anchored ships in offshore harbors, as part of optimal ship routing. Main merits of this study are summarized as:

- Proposing a novel safety evaluation method for anchored ships, thereby enabling discussion on the multiple risk factors such as stranding in shallow waters, damaging with marine structures, and colliding with other ships.
- Predicting the unexpected situation for anchored ships in case of weather forecast failures,

which would enhance the safety of offshore anchorage.

- Proposing suitable methods to estimate the collision risk for the anchored ship, which could drift in all directions due to unexpected external forces.

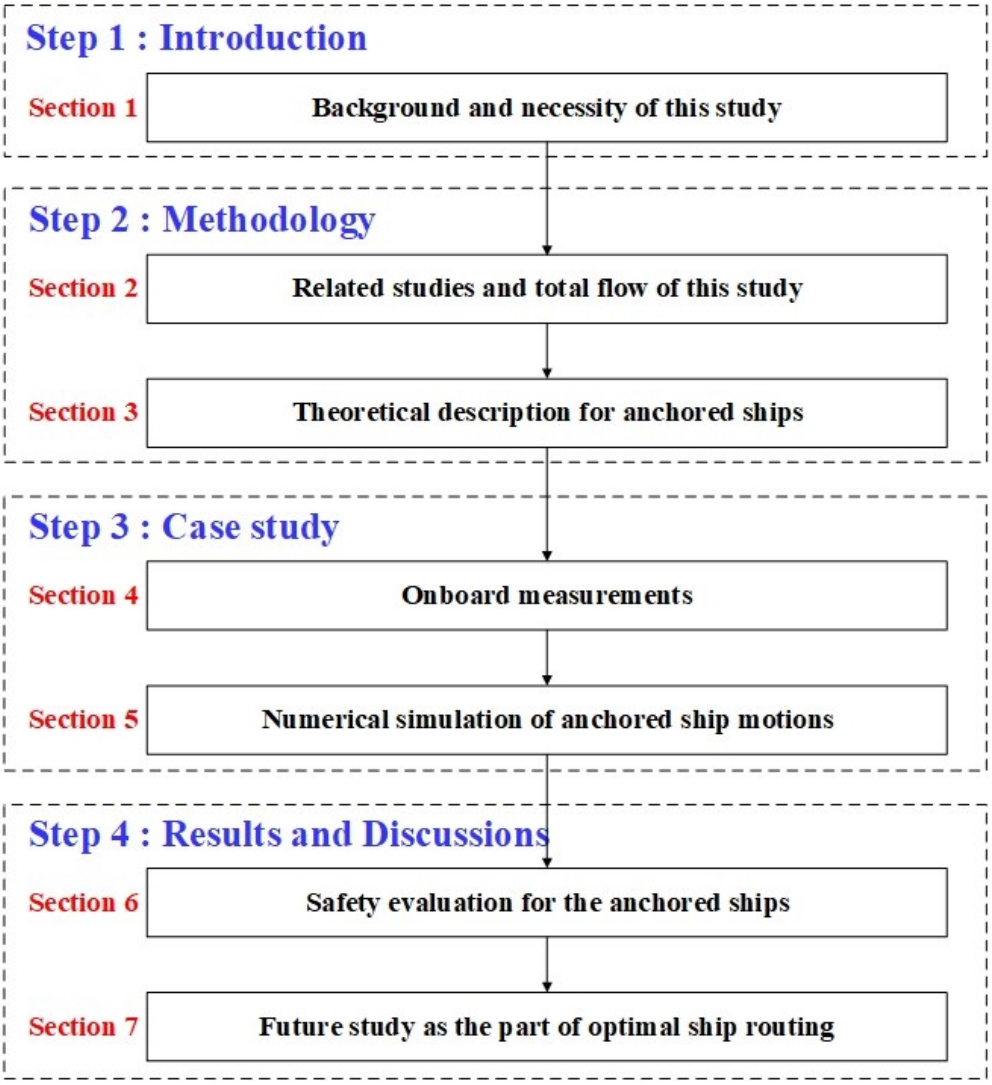

Fig. 4.1. Flowchart for safety evaluation of the anchored ship

4.3 Theoretical Description for Safety Evaluation of Anchored Ships

This section presents the theoretical descriptions for safety evaluation of anchored ships. First, the numerical simulation for the anchored ships is described in Section 4.3.1. Next, the lumped

mass methods is applied to calculate the anchor chain force in Section 4.3.2. Finally, in Section 4.3.3, the collision risk model is illustrated using the various risk factors.

4.3.1 Numerical Simulations for Anchored Ship Motions

Moored ship motions are usually analyzed as the time domain. It is already shown that the time domain model can accurately reproduce measured moored ship motions in the harbor (Kubo and Sakakibara, 1999; Shiraishi et al., 1999). Furthermore, the numerical simulation of anchored ship motions was performed for a ship with a dragging anchor to reproduce the stranded accident offshore harbor in Japan by considering the linear and non-linear wave exciting forces, as well as the dynamic chain force (Sasa and Incecik, 2012). The dragging anchor and strand accident were qualitatively computed if the non-linear wave and dynamic chain forces were considered. For verification, we compared the measured ship motions with the simulated results. Ship motions can be obtained as (Cummins, 1962):

$$\sum_{i=1}^{6}\left(M_{ij}+m_{ij}(\infty)\right)\ddot{X}_j(t)+\sum_{i=1}^{6}\int_{-\infty}^{t}L_{ij}(t-\tau)\dot{X}_j(\tau)d\tau+\sum_{i=1}^{6}\left(C_{ij}+K_{ij}\right)X_j(t)$$
$$=FWV(t)+FSD(t)+FWD(t)\ (i,j=1,2,\cdots,6)\quad , \tag{4.1}$$

where M is the mass matrix (including the moment of inertia) of the ship, $m(\infty)$ is the constant added mass, $L(t)$ is the memory effect function, C is the restoring force matrix, K is the mooring force matrix, and X is the displacement vector of ship motions. Subscripts i and j indicate the mode of ship motions. $FWV(t)$ and $FSD(t)$ are the linear and non-linear wave exciting forces, respectively, and $FWD(t)$ is the wind force. $L(t)$ and $m(\infty)$ can be expressed as:

$$L_{ij}(t)=\frac{2}{\pi}\int_0^{\infty}q_{ij}(\omega)\cos\omega t\,d\omega\ , \tag{4.2}$$

$$m_{ij}(\infty)=p_{ij}(\omega)+\frac{1}{\omega}\int_0^{\infty}L_{ij}(t)\sin\omega t\,dt\ , \tag{4.3}$$

where $p(\omega)$ and $q(\omega)$ are the added mass and damping coefficient at the angular frequency ω, respectively. Wave exciting forces were computed from the directional wave spectrum in each wave frequency and direction. The non-linear wave forces were obtained using the perturbation deployment method for each frequency of difference (Bowers, 1989). The wind forces were computed from the irregular wind history, which is the approximated Davenport spectrum. For the frequency analysis, the hydrodynamic and wave exciting forces were computed using the three-dimension Green function method (John, 1950).

4.3.2 Determining the Anchor Chain Force Using the Lumped Mass Method

The anchor chain force was simulated using the lumped mass method, a dynamic analysis model (Walton and Polachek, 1960; Nakajima et al., 1982) that can be applied to situations wherein the anchor chain is not a straight line, including slack condition. Fig. 4.2 shows the geometrical relationships of the forces around the j-th node of anchor chain.

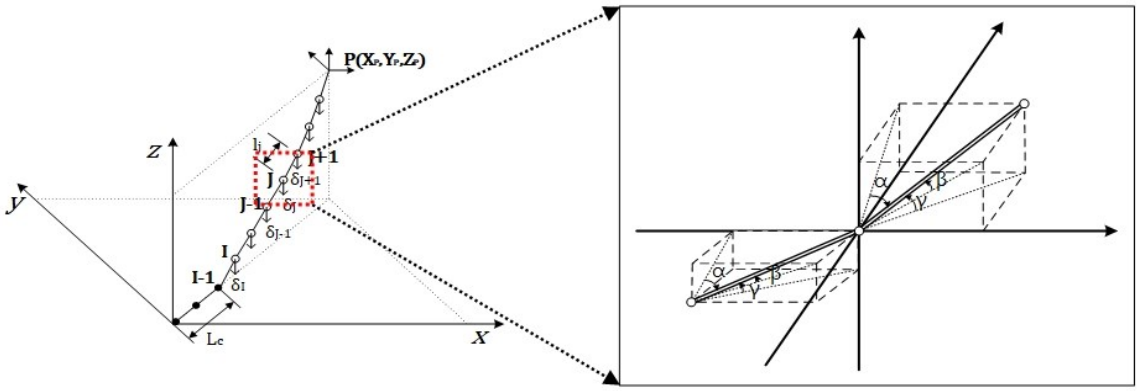

Fig. 4.2. Discrete representation of the anchor chain and its geometrical relationships

Equations pertaining to the motion around the j-th mass point can be expressed as:

$$FX_j = T_j \sin\alpha_j - T_{j-1}\sin\alpha_{j-1} + fx_j \ (j = 2{\sim}N+1) \ , \tag{4.4}$$

$$FY_j = T_j \sin\beta_j - T_{j-1}\sin\beta_{j-1} + fy_j \ (j = 2{\sim}N+1) \ , \tag{4.5}$$

$$FZ_j = T_j \sin\gamma_j - T_{j-1}\sin\gamma_{j-1} + fz_j - \delta_j \ (j = 2{\sim}N+1) \ , \tag{4.6}$$

where FX_j, FY_j, and FZ_j are the total forces in the *x*, *y*, and *z* directions at the *j*-th mass point, respectively, T_j is the tension at the *j*-th math point, and *α*, *β*, and *γ* are the angles between the *j*-th and *j*+1-th mass points. fx_j, fy_j, and fz_j are the drag forces in the *x*, *y*, and *z* directions at the *j*-th mass point, respectively, and δ_j is the weight in the water at the *j*-th mass point. The detail of numerical simulation can be referred to in Sasa and Incecik (2012). The dragging anchor occurs when the anchor chain forces exceed the holding power of the anchor, expressed as the equation of anchor motion:

$$(M_A + m_A)\ddot{X}(t) + D_A\dot{X}_A(t) = T_C(t) - T_{HP}(t) \ , \tag{4.7}$$

where T_C, T_{HP}, M_A, m_A, and D_A are the anchor chain force, holding power, mass, added mass, and frictional coefficient of the anchor, respectively. Here, m_A is defined from an empirical model (Ura and Toshim, 1980). The holding power of the anchor can be expressed as:

$$T_{HP}(t) = w_A\lambda_A + w_C\lambda_C L_C \ , \tag{4.8}$$

where w_A and w_C are the weights of the anchor and anchor chain per length, respectively. λ_A and λ_C are the drag coefficient of the anchor and anchor chain, respectively. The value of λ_A, which is 10.0 for mud and 7.0 for sand, depends on the seabed conditions. If the dragging distance exceeds 2 times the anchor chain length, λ_A decreases to 2.0.

4.3.3 Collision Risk Index for the Anchored Ship

Many studies have used the concept of the Closest Point of Approaching (CPA), which is the closest point between the underway ship and anchored ship, to calculate and analyze the risk of collision among ships. Fig. 4.3 illustrates the definition of CPA. The Distance at Closest Point of Approach (DCPA) indicates the closest distance between two ships, when the target ship arrived at the CPA in terms of spatial aspect. The Time to Closest Point of Approach (TCPA) indicates the time taken by a ship to reach the CPA, and represents the risk of collision in the temporal aspect. Related studies reported that the two factors account for nearly 80% of all factors that influence the risk of collision (Zhao et al., 2016; Liu et al., 2019). $DCPA$ and $TCPA$ can be calculated based on the relative distance and bearing between two ships, and the speed of underway ship as:

$$DCPA = Dist \times \sin C_{rbt} \quad , \tag{4.9}$$

$$TCPA = \frac{Dist}{v_t} \times \cos C_{rbt} \quad , \tag{4.10}$$

where $Dist$ and C_{rbt} are the relative distance and bearing between ships, respectively. v_t is the speed of the target ship. The relative distance and bearing can be estimated based on the position, bearing, and speed of the ship.

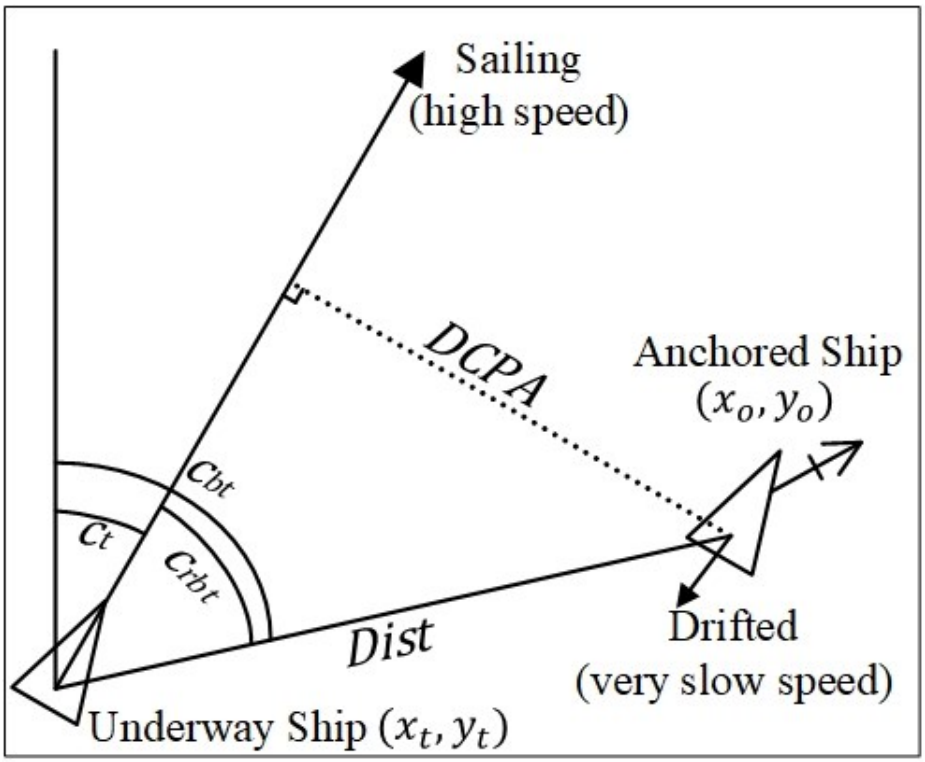

Fig. 4.3. Illustration of CPA between two ships

$DCPA$ and $TCPA$ can represent the risk of collision between two ships. However, the real-time distance and bearing were not sufficiently included from the concept of CPA. The ship domain has been widely used and developed to examine the collision risk for maritime traffic (Fujii and Tanaka, 1971; Kearon, 1977; Coldwell, 1983; Pietrzykowski and Uriasz, 2009; Hansen et al., 2013; Wang and Chin, 2016). Im and Luong (2019) compared the ship domains of several studies and proposed the PRSD model by calculating the Potential Collision Risk (PCR). However, the ship domains have been considered only for the underway ships, and the anchored ships with low speeds have not been considered. In this study, the ship domain of the underway ships with the forward speed was considered as an ellipse shape with a distance of 1.35 nm in the forward direction, and 0.64 nm in the port, starboard, and afterward directions; further, the ship domain for the anchored ship was considered as the circle shape with the distance of 0.64 nm, as shown in Fig 4.4.

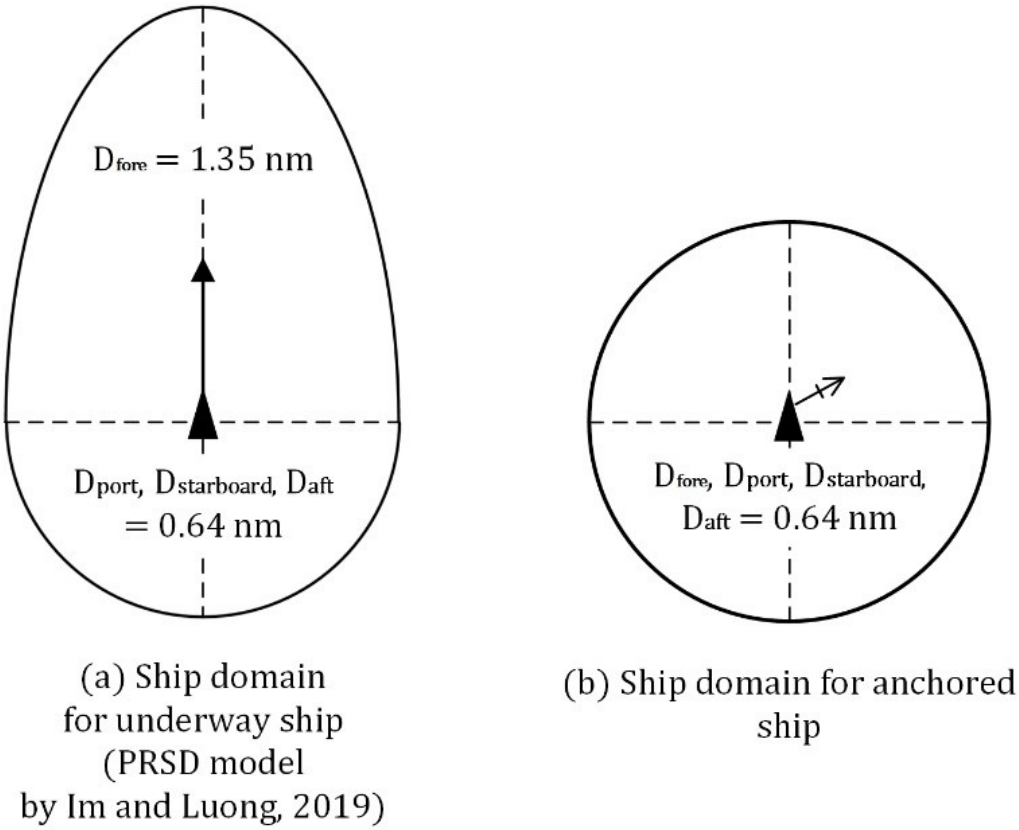

Fig. 4.4. Applying ship domain for underway ships and anchored ships

Im and Luong (2019) introduced the PCR index to reflect the potential collision risk as the combination of non-dimensional $DCPA$ and $TCPA$. The non-dimensional of $DCPA$ and $TCPA$ were obtained as follows.

$$DCPA' = \frac{Dist \times \sin C_{rbt}}{LOA} = \frac{DCPA}{LOA} \quad , \tag{4.11}$$

$$TCPA' = \frac{Dist \times \cos C_{rbt}}{LOA \times v_t} = \frac{TCPA}{LOA} \quad , \tag{4.12}$$

where LOA is the ship length overall. The risk diameter R based on the model of Kearon (1977) and the PCR index of Im and Luong (2019) were calculated as follows.

$$R = \sqrt{\lambda DCPA'^2 + TCPA'^2} \quad , \tag{4.13}$$

$$PCR = e^{-\frac{R^2}{2\sigma^2}} \quad , \tag{4.14}$$

where λ and σ are the lateral and longitudinal influence parameter. The value of PCR indicated the risk of collision in range 0 to 1, indicating that the risk of collision increased as this value increased.

It was possible to confirm the risk of collision by determining whether these ship domains overlapped or not (see Fig. 4.5). If the ship domains overlapped, there may be risk of collision. However, it was necessary to express the risk of collision as the quantitative values based on the overlaps.

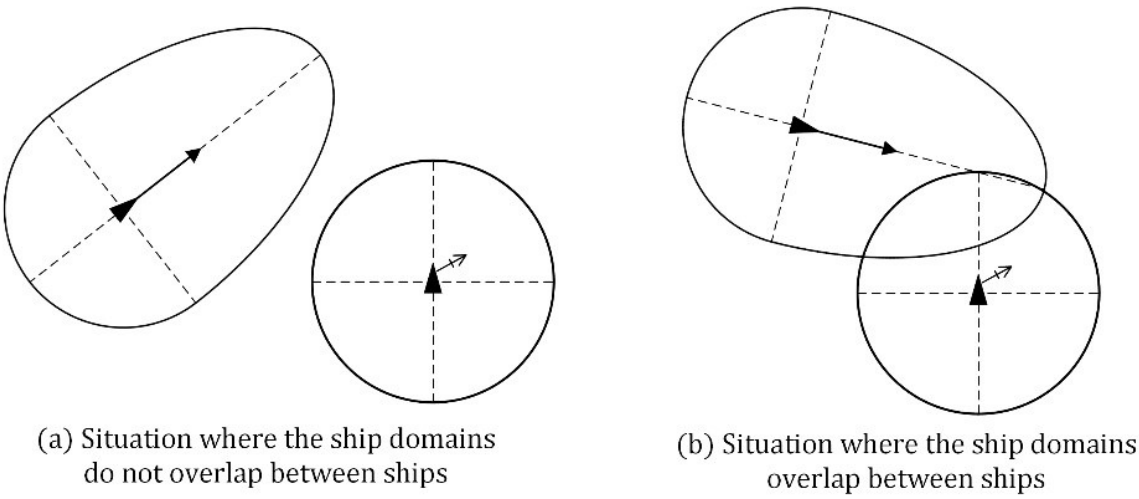

Fig. 4.5. Situation where two ship domains overlap

To include the relative distance and direction between ships, the SDOI, was introduced for the risk of collision (Liu et al., 2019). The value of $SDOI$ could be obtained by comparing the

relative distance of the ships with the safety domain. As the value of $SDOI$ decreased, the risk of collision increased considering the distance of the ship was smaller than that of the ship domain. $SDOI$ between two ships was given as:

$$SDOI = \frac{\sqrt{(x_o - x_t)^2 + (y_o - y_t)^2}}{R_o + R_t} \quad , \tag{4.15}$$

where R_o and R_t were the radius of the ship domains of the own and target ships, respectively. For the size of the ship domain, different ship domains were applied depending on whether the ship was an underway ship or an anchored ship (see Fig. 4.4).

It is necessary to quantitatively express the risk of collision using $DCPA$, $TCPA$, and $SDOI$ between ships. In previous studies, a negative exponential function was used to express the relationship between three collision factors and collision risk. The CRI between ships can be obtained as:

$$CRI_{DCPA} = \alpha_D \exp(\beta_D \times DCPA) \quad , \tag{4.16}$$

$$CRI_{TCPA} = \alpha_T \exp(\beta_T \times TCPA) \quad , \tag{4.17}$$

$$CRI_{SDOI} = \alpha_S \exp(\beta_S \times SDOI) \quad , \tag{4.18}$$

where CRI_{DCPA}, CRI_{TCPA}, and CRI_{SDOI} are the CRI of $DCPA$, $TCPA$, and $SDOI$, respectively. α_D, β_D, α_T, β_T, α_S, and β_S are the coefficients for the CRI of $DCPA$, $TCPA$, and $SDOI$ (Zhen et al., 2017). The total CRI of two ships can be identified by combining of collision risk of $DCPA$, $TCPA$, and $SDOI$ linearly, as follows:

$$CRI_{Total} = w_D CRI_{DCPA} + w_T CRI_{TCPA} + w_S CRI_{SDOI} \quad , \tag{4.19}$$

where w_D, w_T, and w_S are the weight coefficients of each factor. The sum of w_D, w_T, and w_S is 1 and can be preset depending on the traffic situation or the characteristics of the waterway.

4.4 Case Study: Onboard Measurements

In this section, the overview of the onboard measurement systems is presented, including the analysis of the total ratio of operation phase for the target ship in Section 4.4.1. The information on the three case studies is introduced which are staying in offshore anchorage under the rough seas, in Section 4.4.2.

4.4.1 Onboard Measurements

In this study, we conducted onboard measurements using the 28,000-DWT class bulk carrier, which transported general cargo through a tramper, irregular route. Table 4.1 summarizes the main dimensions of the bulk carrier. Various parameters pertaining to the performance of the ship operation were monitored by the onboard measurement system, which comprises the motion sensor and the nautical instrument, including the navigation and engine information. The main information of the nautical instrument is the voyage parameters (ship position, ship speed, ship heading, course, and rudder angle), weather data (wind direction and speed), and the engine performance data (engine revolutions, engine power, shaft thrust, and fuel consumption), recorded at 1 s intervals. The motion sensor comprises the inertial measurement unit (NAV440), which measures the rotation angles (roll, pitch, and yaw), rotation angular velocity, and the acceleration along the horizontal and vertical axes, recorded at 0.1 s intervals. This study mainly analyzed the ship position and heading for the anchored ship motions. While the onboard measurement has been continued from 2010 to 2016, the measured data was unavailable for 2011–2012 and 2014–2015 owing to mechanical troubles in the PC drives and electric units.

Table 4.1 Dimensions of the 28,000-DWT-class bulk carrier

Length between perpendiculars	160.4 m
Breadth	27.2 m
Draft (full loaded/ballasted)	9.82 m / 4.54 m

Several studies have demonstrated that ships encounter 10-15 rough sea conditions during onboard measurements, and the ship performance and weather conditions were analyzed from various aspects (Lu et al., 2017; Chen et al., 2021; Jing et al., 2021; Sasa et al., 2021). However, these studies only focused on the ship operation under voyage in oceans, and hence, the operational situation when the ship has not been on voyage is not known. The tramper, such as a bulk carrier, tends to stay offshore harbor longer than the liner, such as a container ship. The stay period can be roughly divided into the mooring inside the harbor and the offshore anchoring. While the safe operation of mooring inside the harbor has already been studied (Lee et al., 2021), only a few studies have evaluated offshore anchoring based on ship motions in waves. This study clarifies the ratio of operation periods such as voyage, anchoring, and mooring. Furthermore, to classify the operation, the ship was defined on voyage situation if the speed of the ship was over 1.0 knot. The rest of the time was defined as the stay period. It is necessary to divide into the anchoring and mooring, and the ship's heading is used for this division. If fixed, the ship is defined as mooring, and if varied, the ship is defined as anchoring. Additionally, the position of the ship was checked in port terminals or offshore anchorage. Fig. 4.6 shows the ratio of the operation period of the ship.

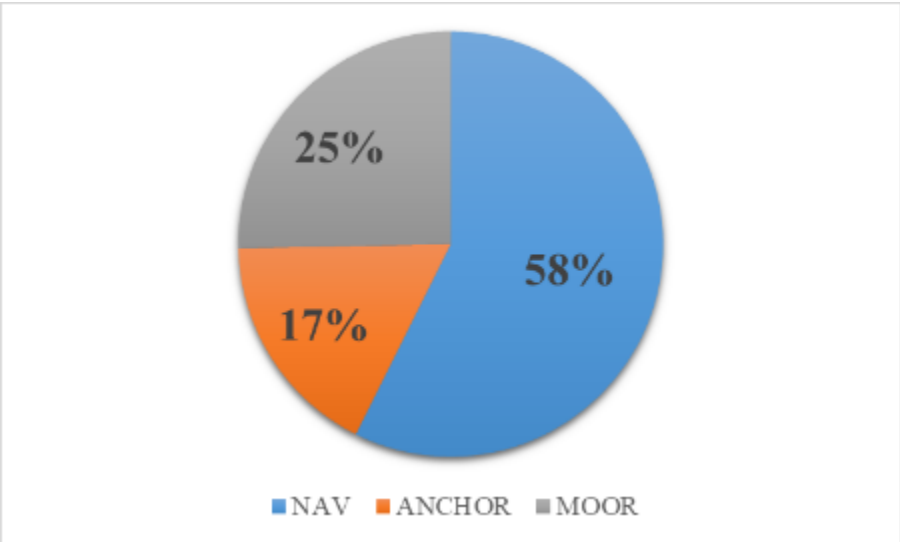

Fig. 4.6. Total ratio of the operation phase based on the total observation record

As a result, the actual ship status during the voyage was shown as 58% of the total period.

Therefore, to complete the optimal ship routing, the ship operation for the remaining 42% of anchoring and mooring conditions must be included. This study focuses on the anchored ship motions when the ship is affected by rough seas.

4.4.2 Observation Cases of Offshore Anchoring

During the observation period, the ship sailed and encountered rough seas worldwide, as shown in Fig. 4.7. The figure also shows the locations of anchorage for these cases. We discuss three cases on large anchored ship motions offshore harbor in rough sea conditions. The ship had been in offshore anchorage facing the open seas in each case. In Case 1, the ship anchored on the coast of Morocco in North Africa, facing the North Atlantic Ocean, and might have waited in offshore anchorage for 7 days before berthing. Although the reason for waiting is unknown, the sea conditions were supposedly rough at that time. When at the offshore harbor, the wind speed and wave height reached approximately 13 m/s and 3.5 m, respectively. In Case 2, the ship stayed in offshore anchorage of Shanghai Port for 2 days, facing the East China Sea. The wind speed had a peak value of approximately 15 m/s, and the significant wave height exceeded 3 m. It is known that larger horizontal motions were measured here, and the ship drifted for nearly 2,500 m. In Case 3, the ship had been anchoring offshore for 6 days on the southwestern coast of Australia, facing the Indian Ocean. During anchoring, the wind speed and wave height reached 18 m/s and 3.5 m, respectively. A low pressure was detected, considering the swirling of wind vector was visible in the distribution of winds, as shown in Section 4.5.1.

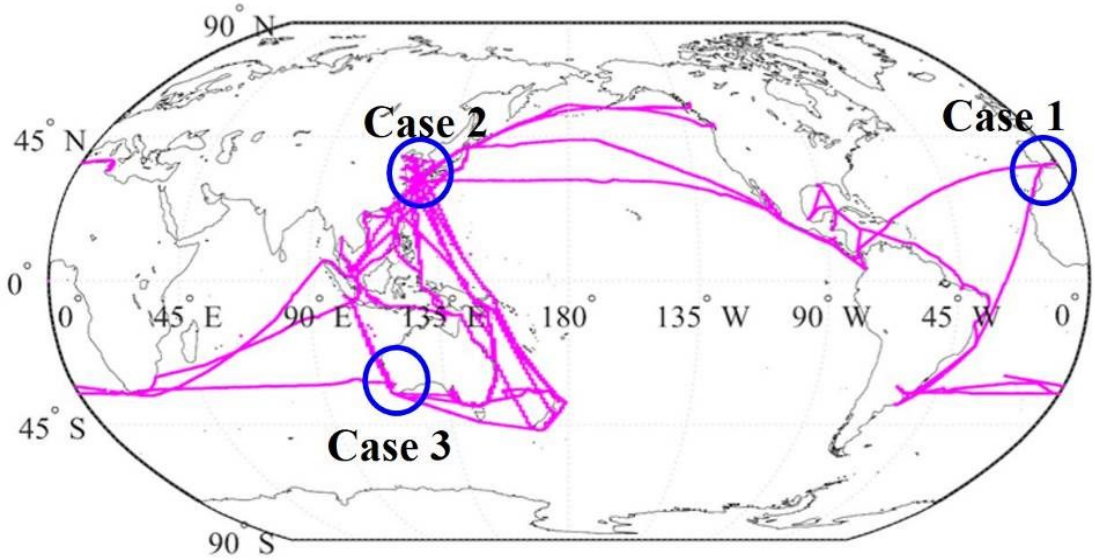

Fig. 4.7. Ship trajectory during the observation period, and the geographical location for each observation case

4.5. Case Study: Simulation of Anchored Ship Motions

This section discusses the three cases of anchored ship motions based on the measured and simulated results. First, the measured ship motions were reproduced based on the numerical simulations in the previous section to validate the accuracy. Furthermore, we confirm the reliability of the numerical simulations based on the comparison in each case. Second, the anchored ship motions were simulated assuming the wave height was underestimated. Failed forecasting results can sometimes result in very dangerous situations for ships (Sasa et al., 2014), which could still happen using the current technology of weather forecasting.

4.5.1 Weather Conditions of Case Studies

Many studies have used the WaveWATCH III (WW3 model; version 4.18) model as the third-generation phase-averaged wave model for the wave hindcasts simulation (Booij and Holthuijsen, 1987; Tolman, 1989 and 2014). Wind input was the most dominant factor in the wave simulation, and there were several kinds of wind input with various spatial and temporal resolutions. Two major databases, the National Centers for Environmental Prediction Final, NCEP-FNL, and the

European Center for Medium-range Weather Forecasts Interim Reanalysis, ERA-Interim, were used. Many studies have discussed the validity of wave simulation depending on the wind input sources. Stopa and Cheung (2014) showed that the ERA-Interim wind input generally underestimates the wind speed and wave height. Campos and Guedes Soares (2016) demonstrated that the ERA-Interim wind input resulted in certain underestimation under extreme conditions. Chen et al. (2020) compared the wave simulation results with different wind inputs based on the ship motion calculations. It was found that the NCEP-FNL showed better performance than ERA-Interim for ship routing. Therefore, in this study, the wave simulation was performed using the NCEP-FNL wind input to accurately replicate the rough waves. The WaveWATCH III is a directional spectrum model, and the directional interval is defined as 10°, which covers 36 directions. The range of wave frequencies is set from 0.0345–1.17 Hz and defined by a logarithmic frequency factor of 1.1 for 38 steps. Additionally, to initiate the simulation, a spin-up simulation was performed starting from 1 month ago till the start time in each case. Directional wave spectrum was obtained by solving the equation of motions for defined grids. Distribution of the significant wave height, wave direction, and wave period can be determined from the directional spectrum in each grid. Figs. 4.8–4.10 show the distribution of wave height in each case, where the ship position is indicated by the red circle. The red and black arrows represent the wind and wave directions, respectively.

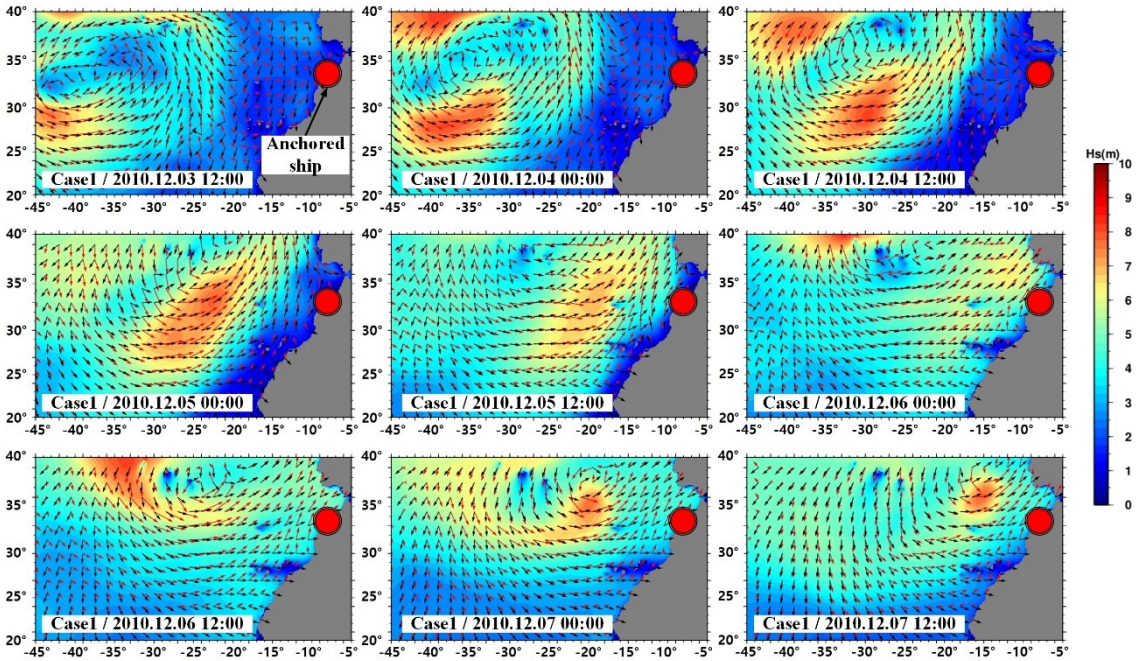

Fig. 4.8. Case 1: Variations in the weather conditions near Morocco (December 03–07, 2010)

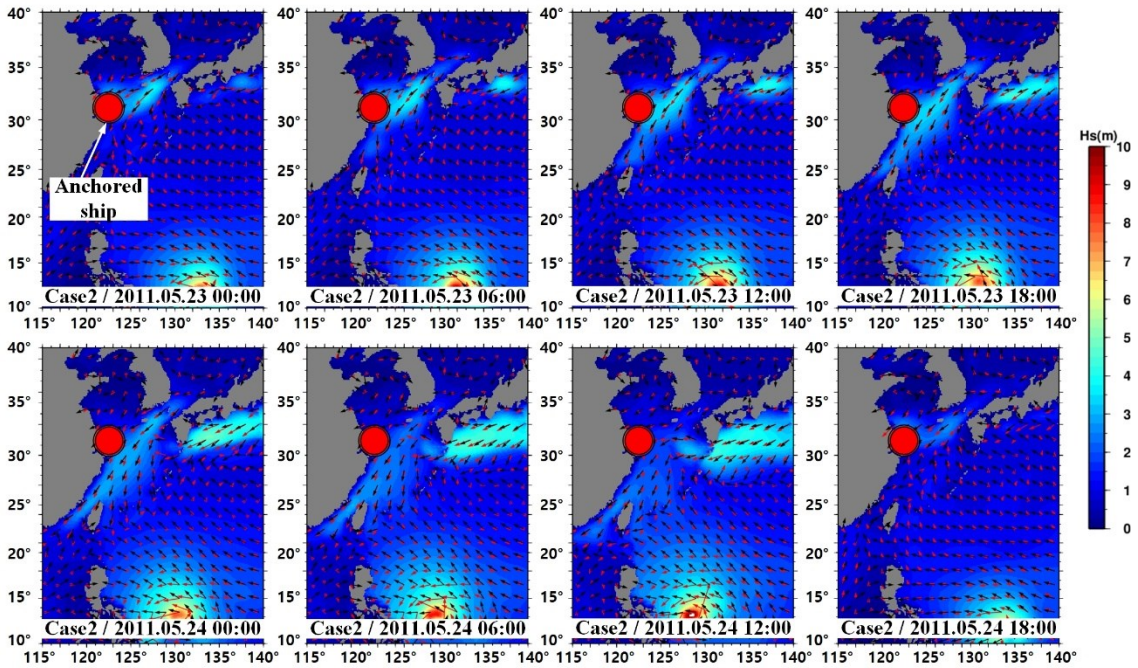

Fig. 4.9. Case 2: Variations in the weather conditions near China (May 23–24, 2011)

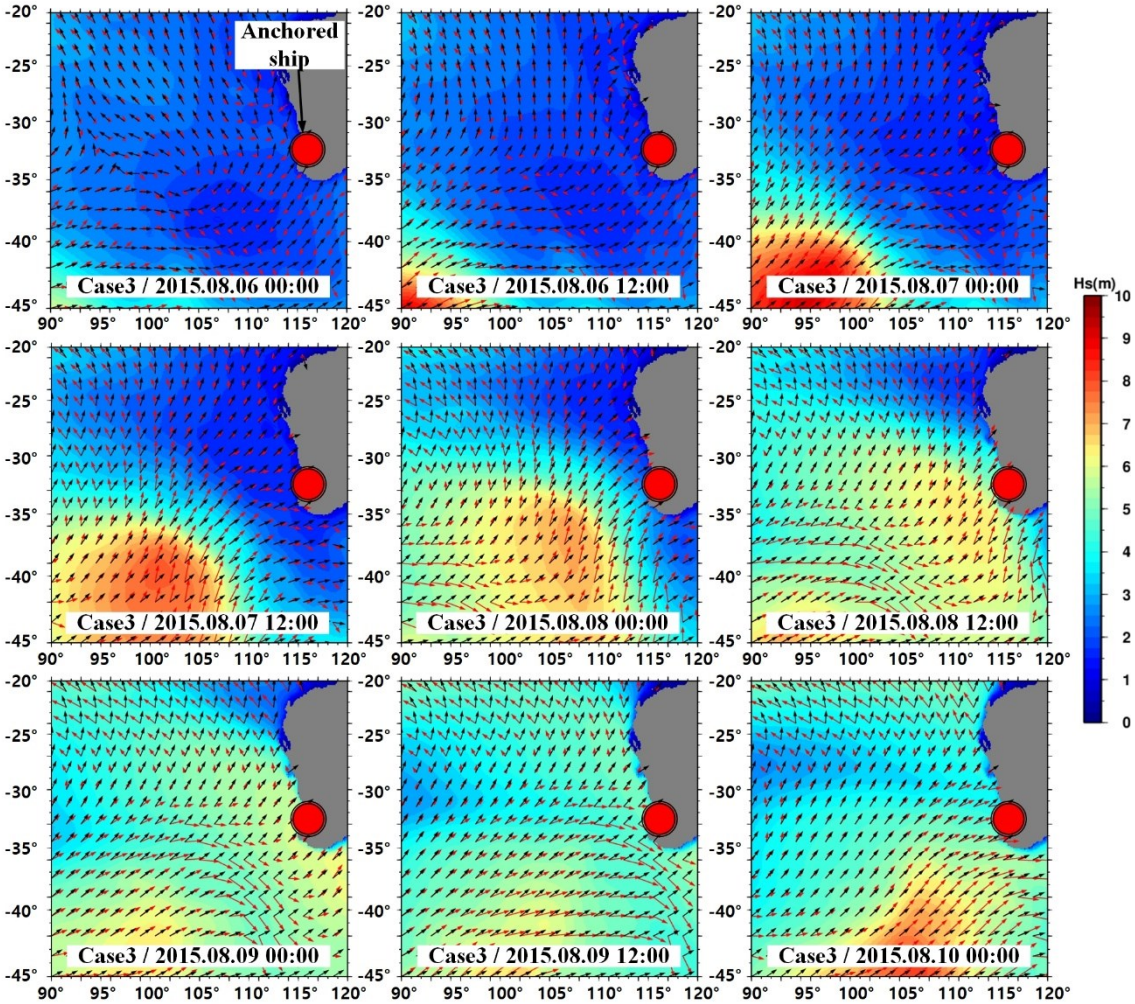

Fig. 4.10. Case 3: Variations in the weather conditions near Australia (August 06–10, 2015)

The above figures show the existence of strong winds and rough waves in each case. In Case 1, strong winds and waves were observed up to anchorage on the Moroccan coastal area, influenced by a low pressure located approximately 2,000 km west from the anchorage, as shown in Fig. 4.8. The main wave and wind directions were estimated as Southwest (240-270°) and from South to Southwest (180-240°), respectively, at the maximum wind speed of 12 m/s. Under the weather conditions, the anchored ship was dragged to the northeast.

In Case 2, higher waves exceeding 10 m were observed near the Philippine coast, where a

typhoon was located, as shown in Fig. 4.9. Another high wave was observed offshore the Chinese coast. The wave was generated due to a rainy front from China to Japan instead of the typhoon far from China. The rough sea could threaten the safety of all ships near Shanghai Port, including the anchored ship. Considering the main directions of the waves and winds were almost the same, Northeast (40-60°), the anchored ship might be dragged to the southwest.

In Case 3, higher waves propagated as swells from the Antarctic, whereas the main wave direction was from Southwest to West (240-270°), as shown in Fig. 4.10. Additionally, the main wind direction was from the Southwest (approximately 240°) at the maximum wind speed of 10 m/s. The wave simulation results showed that the anchored ship may have encountered higher swells and winds, resulting in violent ship motions. Figs. 4.11–4.13 compares all three cases for variations in the significant wave height, main wave direction, wind speed, and the wind direction near anchor ship positions.

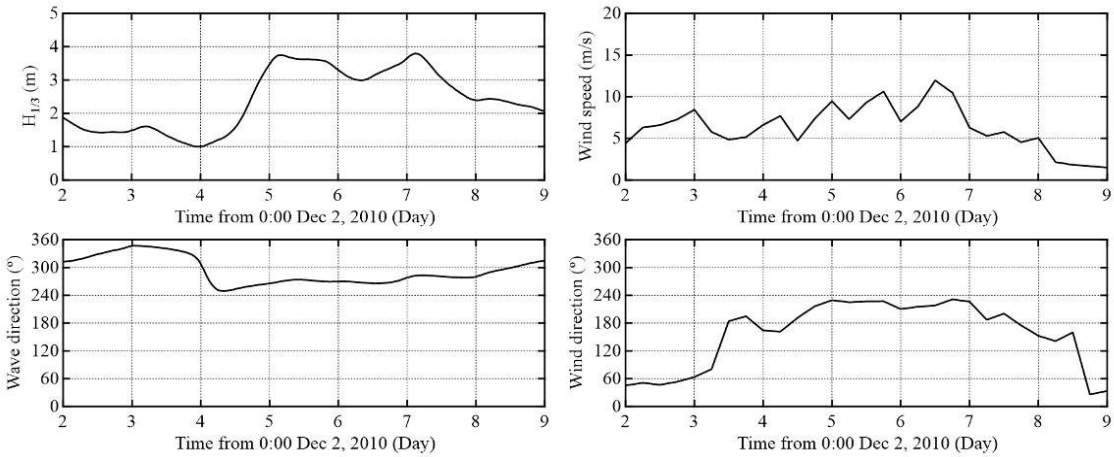

Fig. 4.11. Case 1: Variation in the weather parameter (December 03–09, 2010)

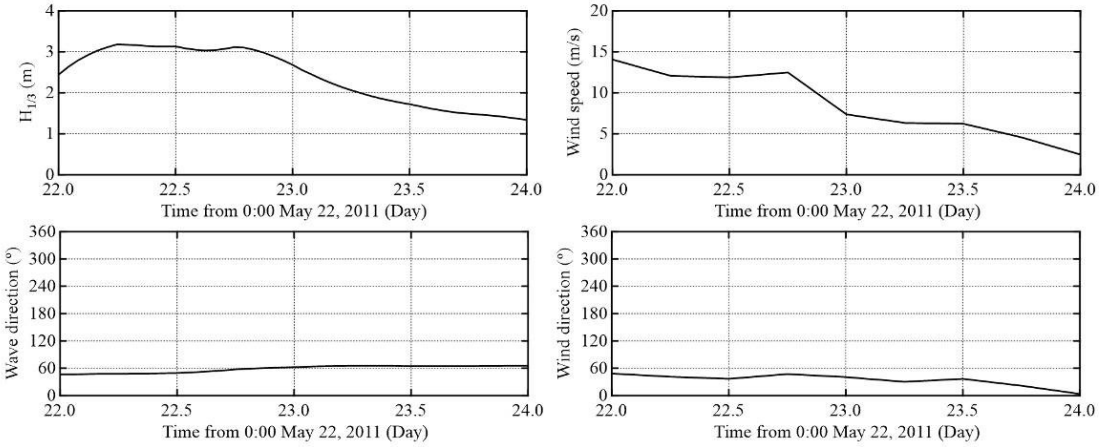

Fig. 4.12. Case 2: Variation in the weather parameter (May 23–24, 2011)

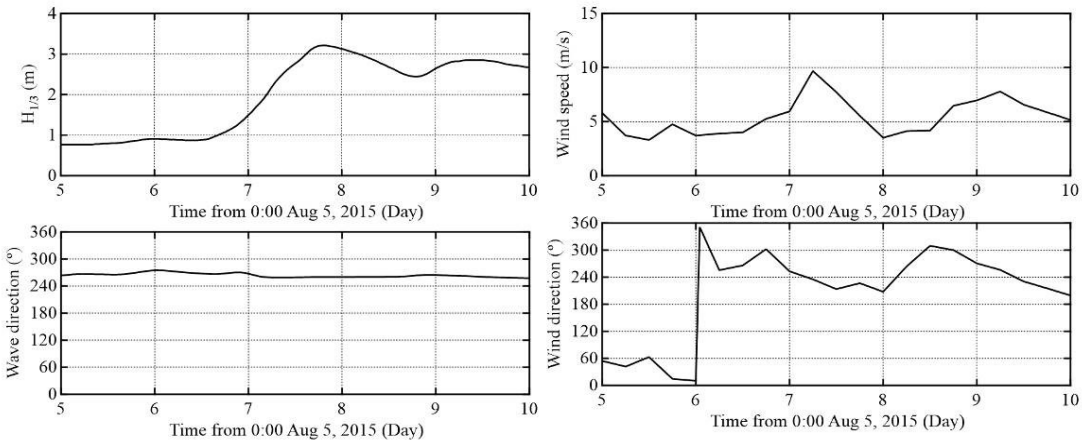

Fig. 4.13. Case 3: Variation in the weather parameter (August 06–10, 2015)

4.5.2 Validation of Anchored Ship Motions

We computed the anchored ship motions for the three measured cases to validate the accuracy of the numerical simulations described in Section 4.3. Environmental conditions of wind waves were numerically simulated using the WaveWATCH III with NCEP-FNL database. Then, anchored ship motions were conducted based on these environmental conditions. The main dimensions of the ship and the anchoring situation are shown in Sections 4.4.1 and 4.4.2, respectively. The anchor type used for simulation was AC-14, with a weight of 5.51 tons and anchor chain diameter of 66 mm with the weight per unit length of 0.1045 tons. Table 4.2

summarizes the simulation period, location, loading conditions of the ship, seabed materials, and the water depth.

Table 4.2 Loading conditions, seabed material, water depth, and simulation period

No.	Simulation period	Location	Loading condition	Seabed material	Water depth
Case 1	From 12:00 Dec 3 to 04:00 Dec 6, 2010	Jorf Lasfar,Morocco	Ballasted	Gravel and sand	40 m
Case 2	From 7:00 May 23 to 04:00 May 24, 2011	Shanghai, China	Fully loaded	Mud and sand	29 m
Case 3	From 12:00 Aug 6 to 14:00 Aug 10, 2015	Bunbury, Australia	Ballasted	Sand	23 m

The loading condition was ballasted in Cases 1 and 3 and fully loaded in Case 2. The left-hand side figures in Fig. 4.14 show the simulated results of the ship track on the gravity point, and are compared with the measured results. The right-hand side figures show the analyzed results of the drifted distance with horizontal ship motions from the initial ship position.

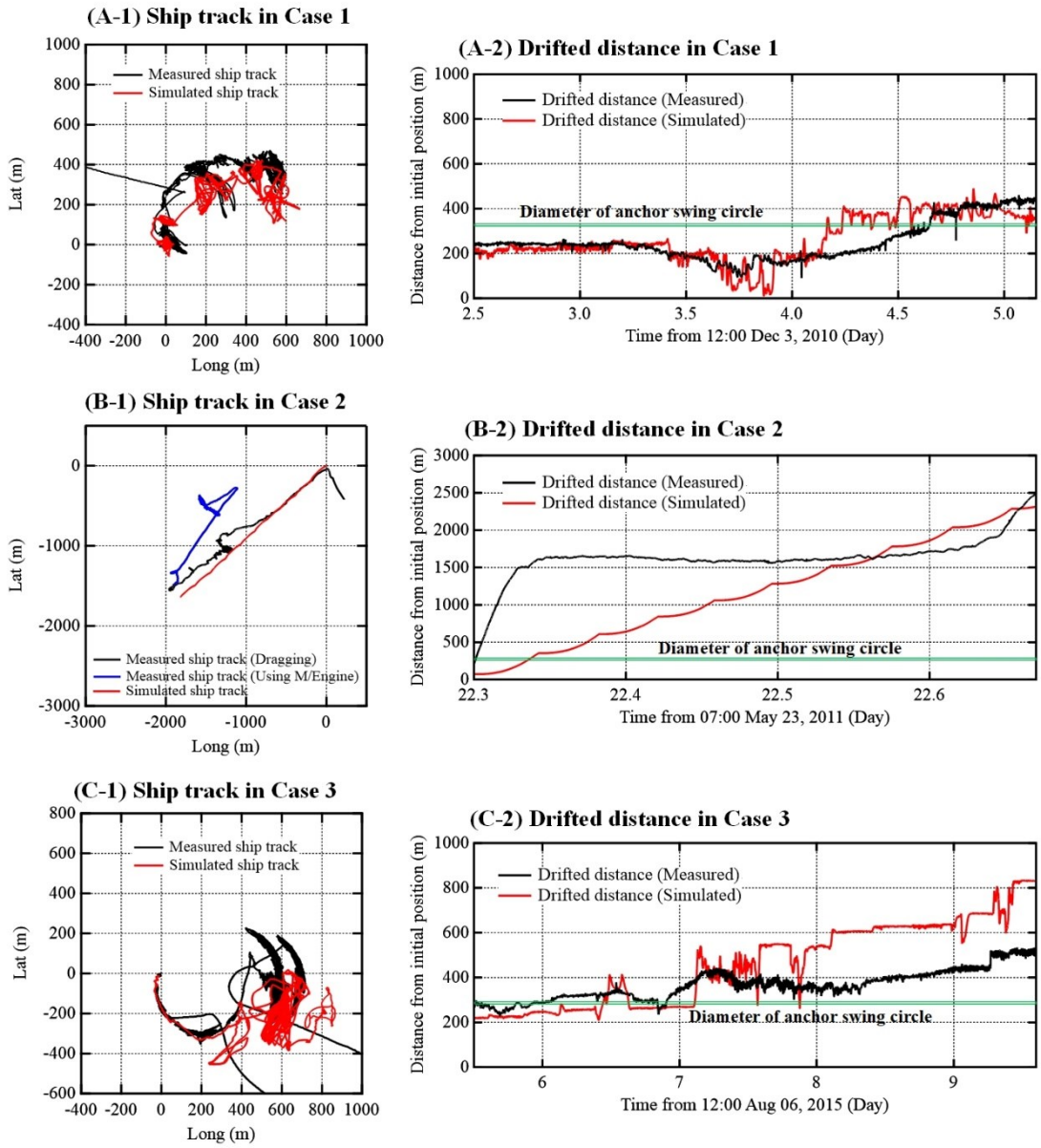

Fig. 4.14. Comparison of the ship track and the drifted distance from the initial position between simulation (Red) and measurement (Black, blue)

The simulated and measured ship tracks are indicated by the red, black, and blue lines, respectively, in the left-hand side figures in Fig. 4.14. The origin of ship tracks is defined as the initial position of the anchored ship for each case. The simulated and measured drifted distances from the initial ship position are indicated in red and black lines, respectively, in the right-hand figures. Herein, we can observe that the dragging anchor occurs by comparing the drifted distance

and the anchor swing circle. The diameter of the anchor swing circle is similar to the length of the anchor chain (Gao and Makino, 2017), which has been recommended based on the formula (Length of anchor chain = 4 × water depth + 145 m) for stormy weather (MAIA, 2006). The anchor swing circles are indicated for each case by green lines in the right-hand side figures. We can say that the ship drags her anchor when the drifted distance is greater than the anchor swing circle.

Case 1 shows that the ship drifts approximately 200 m in the initial 2 days, indicating that the ship does not drag her anchor given the drifted distance is less than 305 m of the anchor swing circle (= 4 × 40 + 145). On the last day (5 December 2010), the ship drags her anchor, indicating that the drifted distance was over 400 m. The measured ship track showed that the ship continuously pushed towards the northeast, which coincides with the simulated ship track, as shown in Fig. 4.14 (A-1). Furthermore, a good agreement was observed between the simulation and measurement results, with final drifted distances of approximately 400 m and 420 m, respectively, as shown in Fig. 4.14 (A-2).

Unlike the other cases, the anchor swing circle was not visible at all in Case 2, and the ship only drifted for approximately 2,500 m. Therefore, from the analyzed result of measured data, we can assume that the dragging anchor occurred considering the ship did not use the main engine at that time. As the ship drifted near the entrance of fairway, it used the main engine to move back to the original anchoring position, as indicated by the blue line in Fig. 4.14 (B-1). Before the ship uses the main engine, the simulated ship track follows the measured ship track, which is drifted to the southwest. The simulated and measured total distances from the origin were 2,300 m and 2,500 m, respectively, as shown in Fig. 4.14 (B-2). However, some major differences were observed between the simulated and measured results. According to the measured data, the dragging anchor occurred dominantly in the initial 1 h. From the total distance of 2,500 m, the main dragging of 1,700 m was observed in the first 1 h, whereas the remaining 800 m was observed in the last one hour. In contrast, the drifted distance of the simulated results showed that the ship continued to drift for 2,500 m. Although the tendency of dragging between the simulation and measurement results was different, the direction and distance of the dragging situation can be reproduced using the simulation model.

During the initial days of Case 3, the measured ship track followed the range of the anchor swing circle, as shown in Fig. 4.14 (C-1). Furthermore, the drifted distance from the anchor circle coincided with the diameter of the anchor swing circle at that time as shown in Fig. 4.14 (C-2).

On 08 August 2015, the drifted distance was greater than the diameter of the anchor swing circle, indicating that dragging anchor has occurred. At that time, high waves exceeding 3 m propagated along with the ship position, as shown in Figs. 4.10 and 4.13. It is obvious that the large horizontal ship motions were influenced by the strong waves. On comparing the measured and simulated ship tracks for Case 3, it was found that the simulation results were overestimated, which was approximately 800 m and 550 m of the drifted distance in simulation and measurement, respectively.

The simulation model in this study showed errors of approximately 50 m, 200 m, and 250 m in the drifted distance in Cases 1, 2, and 3, respectively, which can be attributed to errors between the simulations and measurements. One of the main reasons is the uncertainty of the wave simulations, which could not accurately replicate the weather condition. Owing to this, errors may have occurred in the anchored ship motions. Although the simulation model of anchored ship motions showed differences, the anchored ship motions were reproduced well by this model and coincided with the direction and tendency of the measured ship tracks. Especially, the model was able to reconstruct the presence of the dragging anchor, and accurately detect the time and direction of the dragging anchor.

4.5.3 Comparative simulation of the anchored ship motions in case of weather forecasting failures

Several studies on the weather forecast have demonstrated the errors and uncertainties of weather forecasting systems (Girolamo et al., 2017; Chen and Wang, 2020). The uncertainties of weather forecasting can endanger marine operations considering the operations are planned and conducted based on the weather forecasting information to minimize the risk under rough seas. (Natskår et al., 2015). Therefore, it is essential to recognize the uncertainties of weather forecasts for the safety analysis of the ship operation pertaining to optimal ship routing.

To investigate the differences based on the weather forecasting failures, it is necessary to conduct further simulations for the anchored ship motions, with 2–3 times the wave height for more severe weather. Fig. 4.15 shows the variations in the actual waves and waves that are 2–3 times higher than the significant wave height for each case. “U-1”, “U-2”, and “U-3” represent the significant wave heights for the actual wave condition, 2–3 times of the underestimated wave conditions, indicated by black, blue, and red lines, respectively. For these simulations, the wave

forces were only changed based on the significant wave height. The other weather conditions, such as the wave direction, wind speed, and direction were not changed.

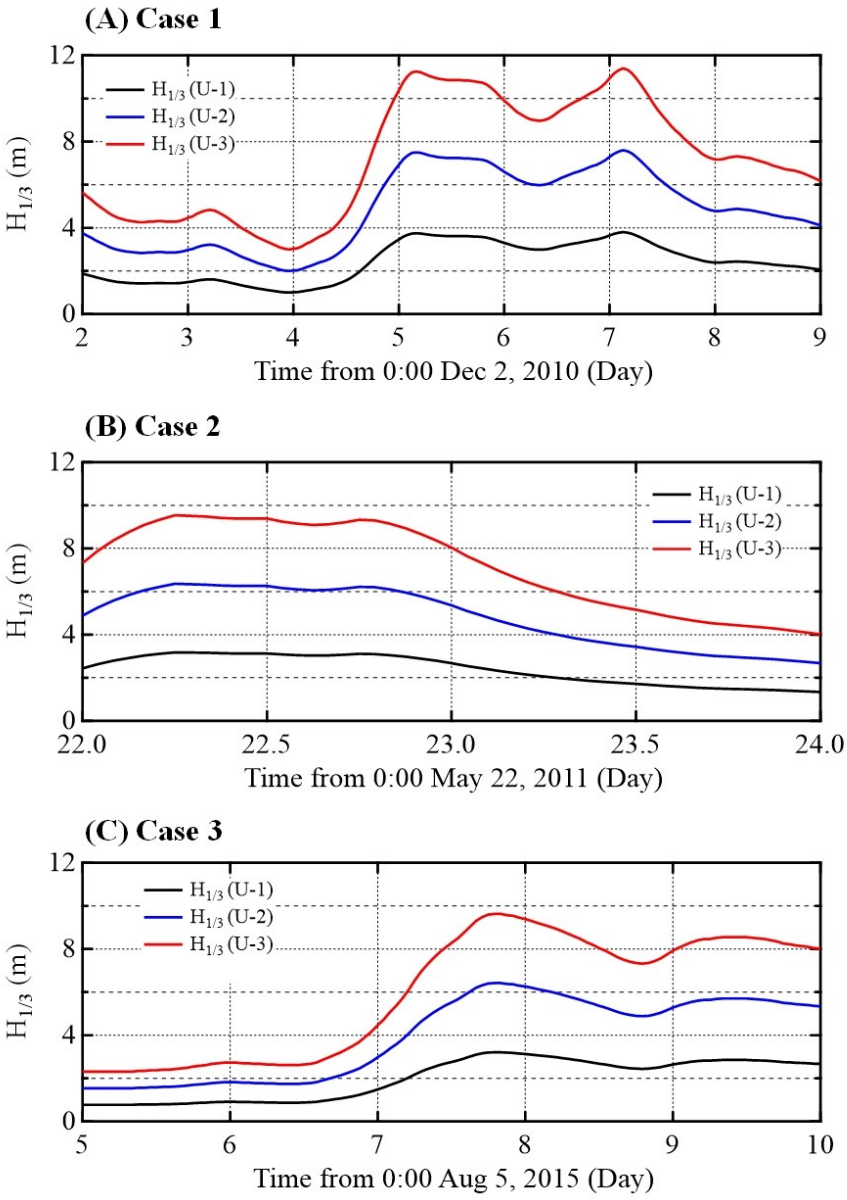

Fig. 4.15. Variations in the significant wave height of each case

Fig. 4.16 shows the simulated results of the ship track on the gravity point under different wave conditions. Furthermore, the analyzed results of the drifted distance with horizontal ship motions from the initial ship position are shown in the right-hand side figures of Fig. 4.16. The simulated

results under U-1, U-2, and U-3 conditions are indicated by black, red, and blue lines, respectively. The origin of ship tracks was defined as the initial position of the anchored ship for each case.

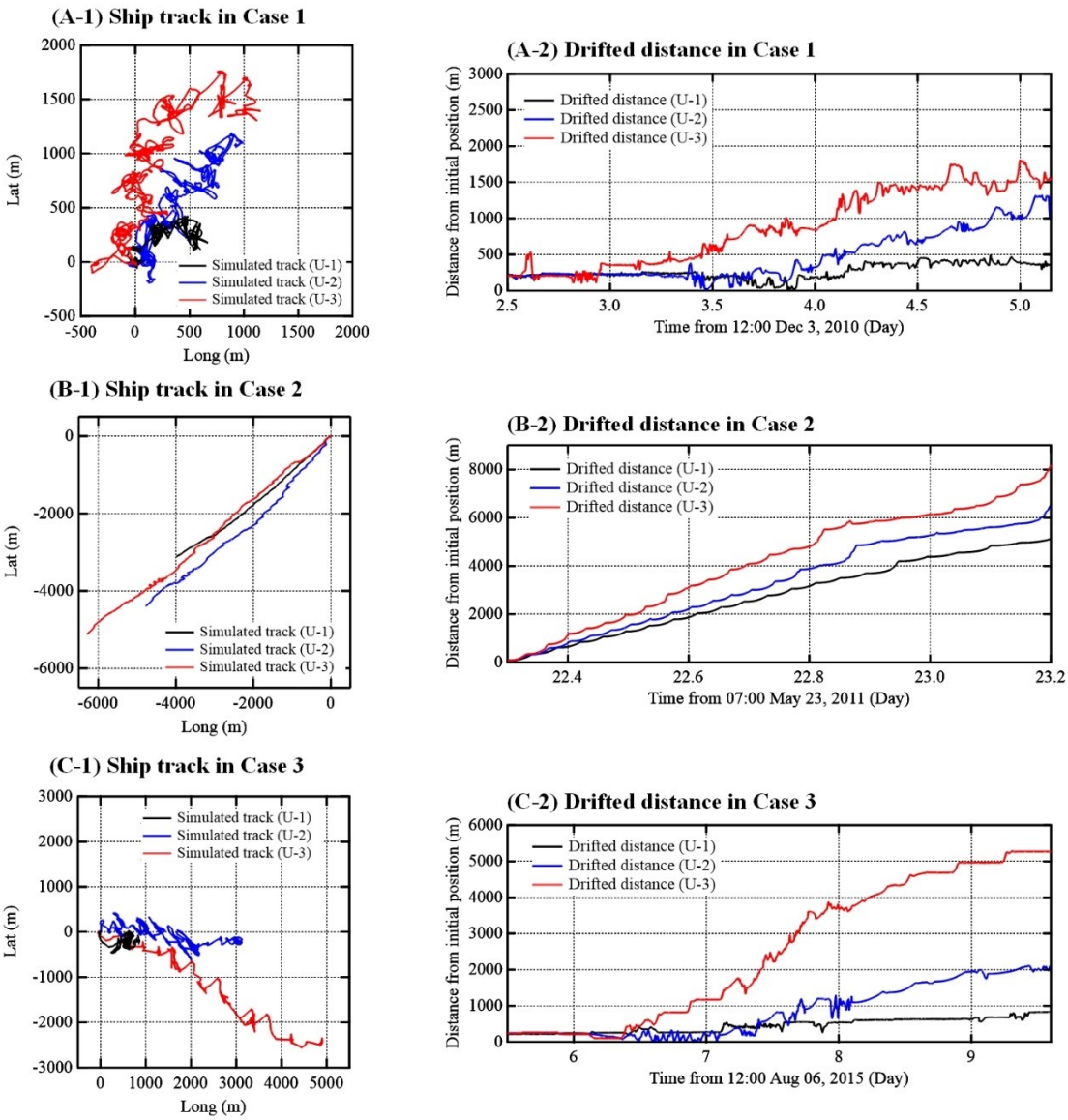

Fig. 4.16. Comparison of the simulated ship tracks and the drifted distances from the initial position under different wave conditions

In Case 1, the drifted distance from the initial position was less than 500 m under U-1 condition. Larger horizontal ship motions were observed under the more severe waves. The distance reached

1300 m and 1800 m under U-2 and U-3 conditions, respectively, indicating that the wave height significantly influenced the anchored ship motions. The main wave direction was from the southwest (240–270°), and hence, contributed to the horizontal ship motions in the northeast direction.

The measured data of Case 2 showed that the ship used the main engine after drifting for approximately 2,500 m. Herein, the simulations were conducted assuming the ship was continuously exposed to rough seas without using the main engine. The ship drifted for approximately 5,000 m under U-1 condition, which increased to 6,200 m and 8,000 m under U-2 and U-3 conditions, respectively. If the ship approached the fairway, it might encounter a dangerous situation.

In Case 3, the ship drifted for approximately 800 m under U-1 condition, which increased to 2,000 m and 5,000 m as the height increased under U-2 and U-3 conditions, respectively. It is obvious that the ship motions were not proportional to the wave heights, indicating that the high waves implicated large horizontal ship motions although the anchored ship motions were irregular, non-linear to the wave height. This point needs to be investigated further in future studies.

4.6 Results and Discussions

In this section, the potential risk of the anchored ship was newly evaluated for the entire safety of offshore anchorage. Although anchored ships are usually defined as fixed and immobile structures, the ship can drift for more than a nautical mile in rough seas. Therefore, to construct the risk assessment for the anchored ships, it is necessary to identify the risk in anchorage. Furthermore, the potential risk factors for anchored ships should be identified and analyzed depending on the accident reports and previous studies (Sugomori, 2010; Sasa and Incecik, 2012; Debnath and Chin, 2016; Gao and Makino, 2017). While previous studies only concentrated on stranding, this study presents the novel risk assessment method for anchored ships while including various parameters such as shallow depth, marine structures, and traffic situations, as shown in Fig. 4.17.

The variables of potential risk can be verified by analyzing the data using the navigational harbor chart for each case in Section 4.6.1. Furthermore, the historical AIS data, which can sufficiently explain the marine traffic situations, was used to further investigate the risk of collision in Section 4.6.2.

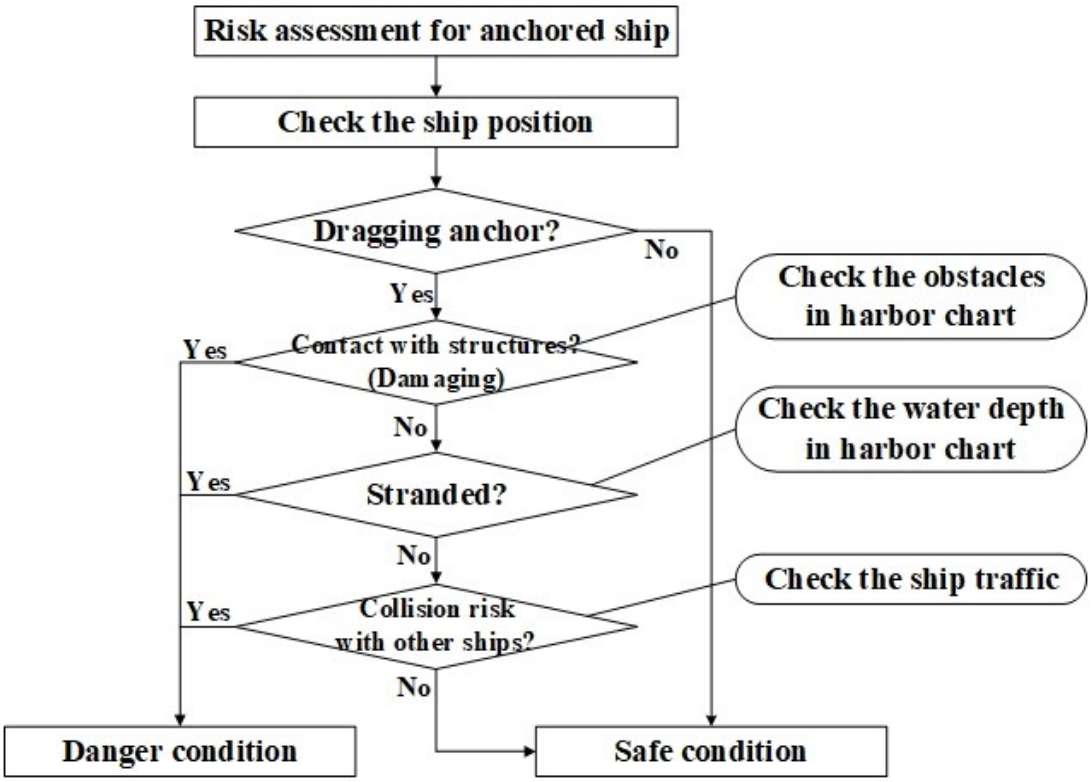

Fig. 4.17. Flowchart of the novel risk assessment method for anchored ships

4.6.1 Safety Evaluation of the Anchored Ship by the Harbor Chart

It is crucial to obtain fundamental information such as water depths and obstacles to identify the accident of damaging marine structures and stranding to shallow water. The fundamental information can be obtained from the harbor charts, as shown in Fig. 4.18.

Damaging accidents usually occur by contact with the dragged anchors to marine structures installed on the seabed, such as pipelines or cables. Initial anchor positions and drifted ranges from the simulated results are marked for each case in Fig. 4.18. The black, blue, and red circles indicate the range of simulated ship tracks under U-1, U-2, and U-3 conditions, respectively. Fig. 4.18 also shows that there are no marine structures around the ship trajectories in all three cases, indicating the relatively low risks of damage to marine structures by the dragging anchor.

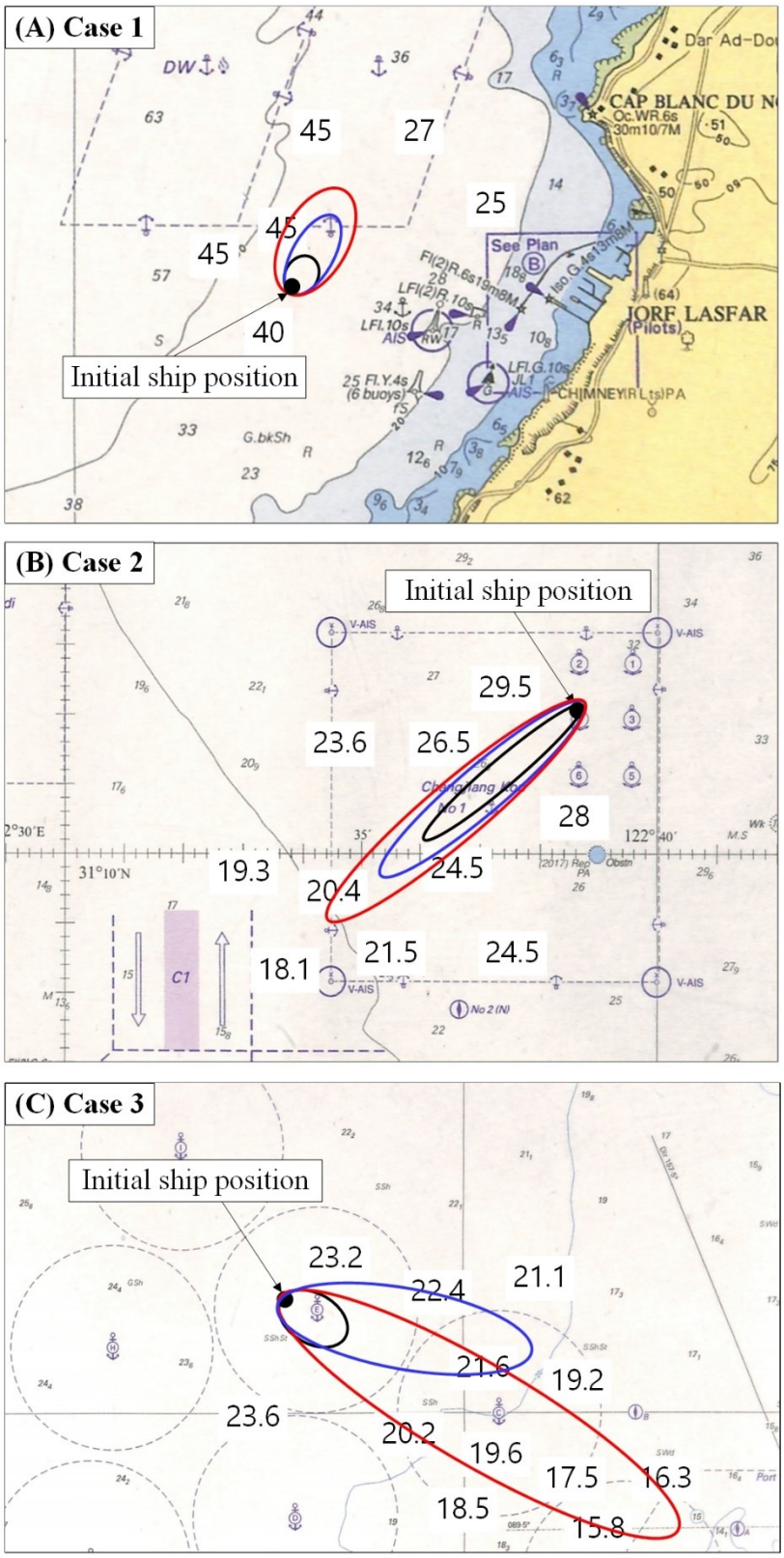

Fig. 4.18. Harbor chart with the drifted range of the simulated ship tracks for each case

Standing accidents occur owing to the relation between the Under Keel Clearance (UKC) and the vertical displacement due to heave, pitch, and roll motions. The UKC is decided based on the relation between draft and water depth. It is obvious that the minimum water depths are approximately 40 m, 20 m, and 15 m at the farthest drifted position in Cases 1, 2, and 3, respectively, as shown in Fig. 4.18. To evaluate the stranding accident, the UKC is calculated as (Sasa and Incecik, 2012):

$$UKC(t) = W_M - D - \left(\frac{L}{2} - MG\right)\sin X_4(t) - \frac{B}{2}\sin X_5(t) - X_3(t) \quad , \tag{4.20}$$

where W_D is the minimum water depth, D, L and B are the draft, length, breadth of the ship, respectively. MG is the distance between the gravity point and midship. $X_3(t)$, $X_4(t)$, and $X_5(t)$ are the vertical ship motions of heave, pitch, and roll, respectively. Fig. 4.19 shows the calculated results of UKC.

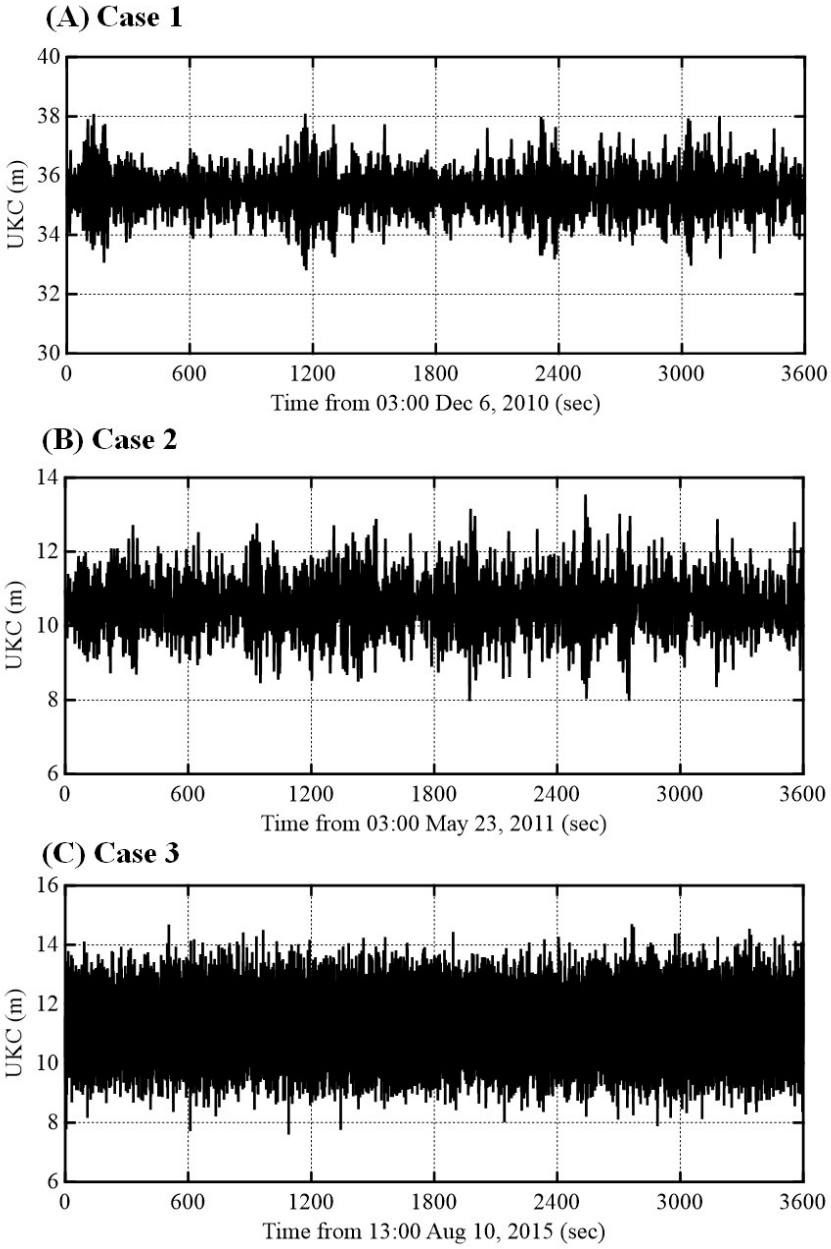

Fig. 4.19. Calculated under-keel clearance at the minimum water depths for each case

The stranding risk is determined by the UKC. If the UKC value reaches 0, the ship might be stranded by the shallow water. As shown in Fig. 19, the minimum UKC has adequate margins of approximately 32 m, 8 m, and 8 m from the seafloors in Cases 1, 2, and 3, respectively, which indicates that there are relatively low risks of stranding. Although the ship drifts more than a

nautical mile, it is obvious that the ship might not be in danger of stranding or damage based on the chart information and UKC calculations.

4.6.2 Safety Evaluation of the Anchored Ship Using AIS Data

To further investigate the collision risk of the anchored ship, it is essential to figure out the marine traffic characteristics with the historical AIS data. Although historical AIS data is purchased from the exactEarth Ltd., the amount of dynamic information (position, speed, heading, etc.) is less in Cases 1 (2010) and 2 (2011), making the analysis very difficult. Therefore, only the risk of collision for Case 3 (2015) was evaluated.

The AIS data for Case 3 was analyzed for 3 days from August 7 to 9, 2015, when the rough sea condition prevailed. The safety of the anchored ship was evaluated in the area between 115.50° E to 115.67° E longitude and 33.20° S to 33.32° S latitude. Approximately 13 ships enter or depart the harbor, as shown in Fig. 4.20.

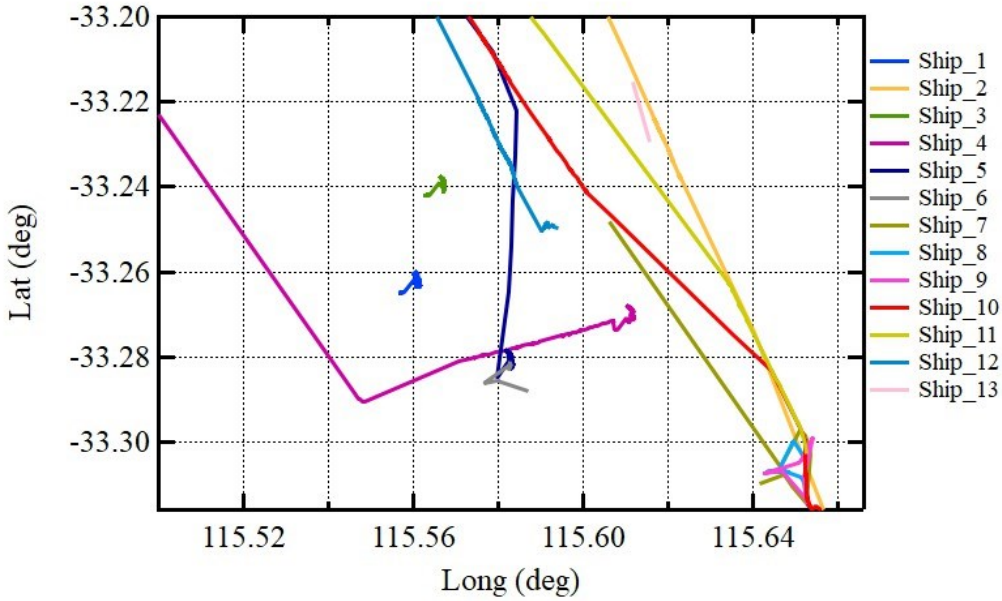

Fig. 4.20. Historical AIS data for all ships in Case 3 during 07-09 Aug, 2015

In Case 3, 3 ships approached the anchored ship within the distance of 2,500 m, which can cause a higher risk of collision. Trajectories of the 3 ships varied for 3 days, as shown in Fig. 4.21. “Own ship” represents the bulk carrier that was measured and simulated in the previous section. “Ships (A), (B), and (C)” represent the ships approaching the “Own ship”. Ship (C) drops its anchor after passing the own ship at the distance of 1,425 m and stays for nearly 3 days with little movement. On August 9, ships (A) and (B) approached the own ship at distances of 2,275 m and 1,310 m, respectively. Ship (A) entered the harbor after passing there. Particularly, high collision risk was expected with ship (B), considering ship (B) stayed with an anchor within a nautical mile from the Own ship. Although anchored ships are usually defined as the stationary subjects (Debnath and Chin, 2016; Liu et al., 2020), it is necessary to consider the drifting speed owing to the dragging anchor.

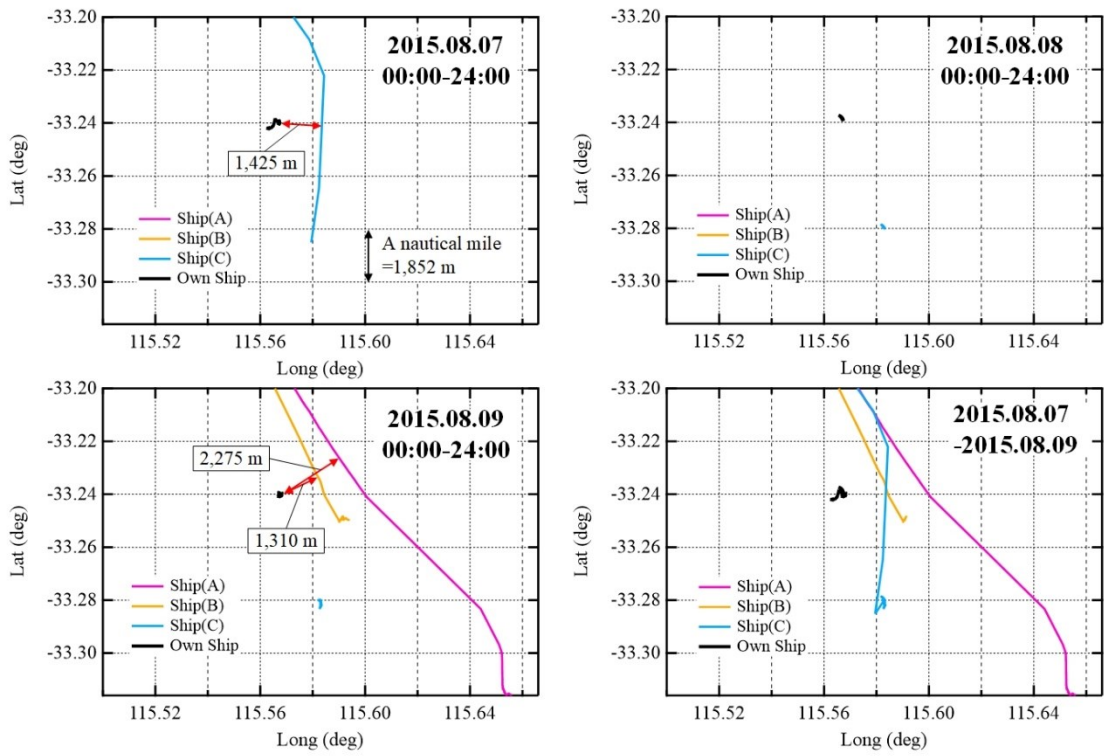

Fig. 4.21. Relationship with between the own ship and the closest three ships

4.6.3 Result of Collision Risk for the Anchored Ship

The risk of collision was estimated from the simulated results of anchored ship motions. When the weather forecast was underestimated, as shown in Section 4.5.3, the drifted distance increased from 800 m under U-1 condition to 5,200 m under U-3 condition. Fig. 4.22 shows the variations in the PCR and CRI of each ship (Ships [A], [B], and [C]) under different wave conditions (U-1, U-2, and U-3 conditions).

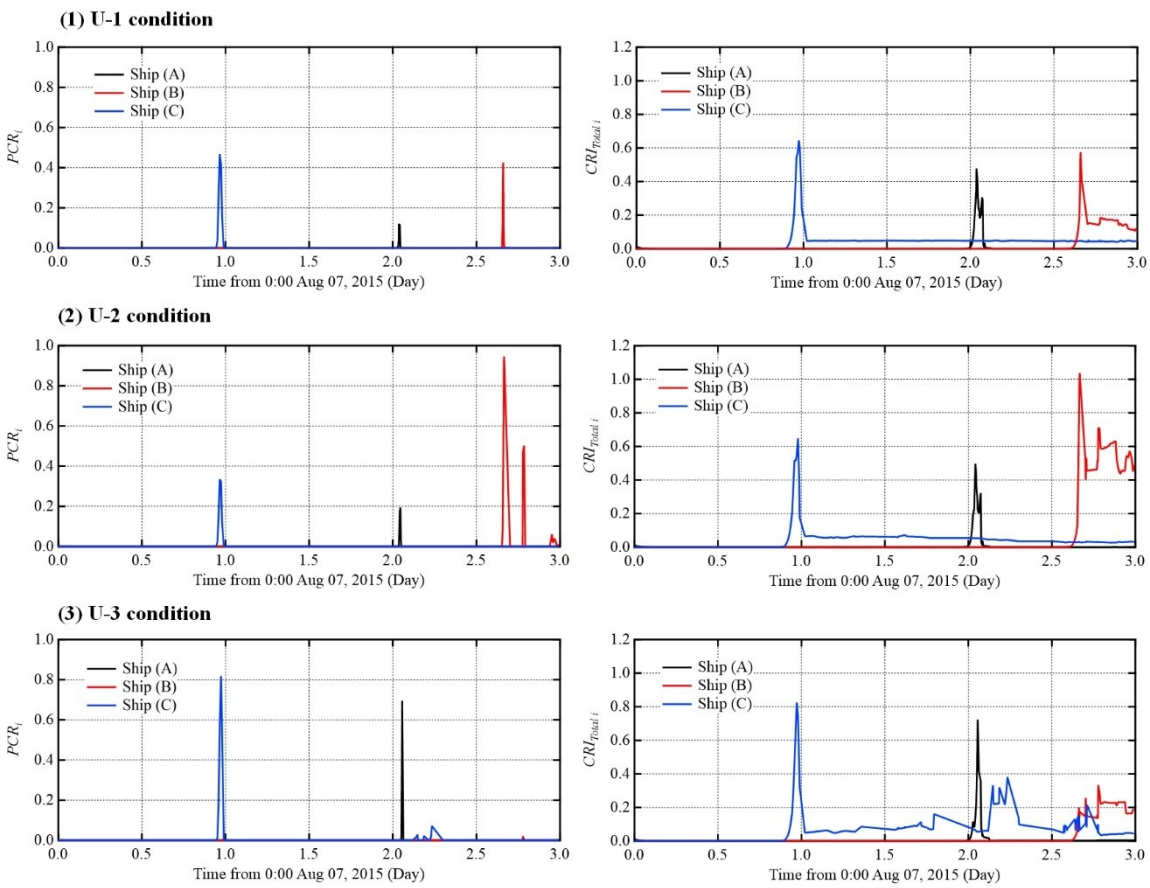

Fig. 4.22. Results of the total CRI for each ship

The collision risk with ship (C) increased to approximately 1.0 day when it passed the anchored ship at a distance of 1,425 m (0.77 nm). Then, ship (C) dropped the anchor near the own ship (the anchored ship), and the value of PCR and CRI was less than 0.2 after the peak value at approximately 1.0 day. Furthermore, ship (A) passed the own ship at a distance of 2,275 m (1.23

nm) on around 2.1 day. Ship (A) did not stay near the own ship, indicating that the value of PCR and CRI only increased around 2.1 days, and was almost zero for the rest of period. Ship (B) passed the own ship at a distance of 1,310 m (0.71 nm) at around 2.7 days. The collision risk of ship (B) was expected to be higher, especially for the underestimated cases (U2 and U3 conditions), considering the own ship (anchored ship) had drifted for 2,000 m to 5,200 m (1.08 nm to 2.81 nm) owing to the dragging anchor towards ship (B). This increased the value of PCR (from 0.4 to 0.9) and CRI (from 0.6 to 1.1) of ship (B) under U-2 condition. However, the value of PCR decreased to zero and the value of CRI decreased to 0.3 under U-3 condition, irrespective of whether the wave height was three times underestimated. As Fig. 4.16 (C-1) shows, the drifted distance under U-3 condition was approximately 5,200 m (2.81 nm). Therefore, the own ship (anchored ship) had already passed the area before ship (B) arrived at the anchorage. Fig. 4.23 shows the comparison of the maximum values of PCR and CRI.

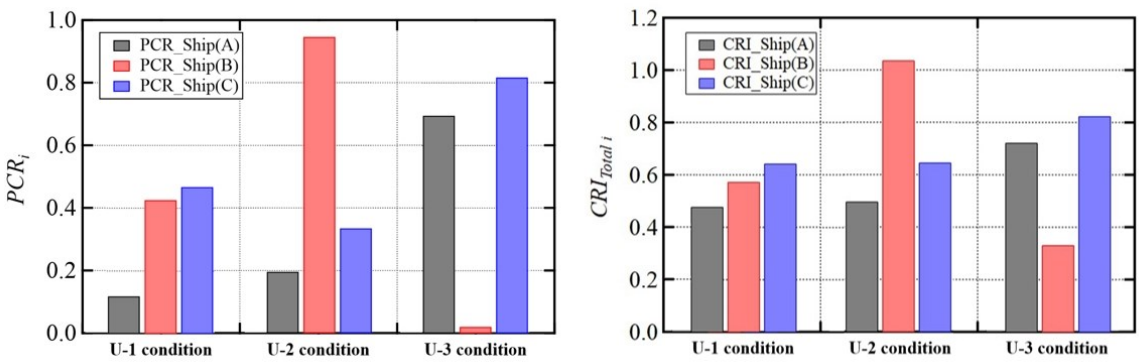

Fig. 4.23. Comparing each ship's maximum PCR and CRI values

The results of PCR and CRI showed that the risk of collisions increased as the weather worsened, with a few exceptions. The collision risk with ships (A) and (C) increased as the weather conditions worsened, especially in U-3 condition (three times the wave heights). This indicated that the drift due to dragging anchor could increase the risk of collision, even in the anchoring situation. However, there was a difference in the results of collision risk with ship (B) in U-3 condition. The value of PCR with ship (B) was almost 0.0, while the value of CRI was approximately 0.3, showing the risk of collision. As mentioned, the own ship had already passed the route of ship (B) in U-3 condition, which reduced the risk of collision in terms of DCPA and TCPA. The calculation of PCR could not reflect the relative distance between ships because it

was based on DCPA and TCPA. Since the anchored ship could drift in all directions due to unexpected external forces, the CRI method including the relative distance and bearing was more reliable than the PCR method in case of offshore anchorage.

Results of collision risk showed that anchored ship motions were inevitable for accurately evaluating the collision risk in offshore anchorage. However, there are very few studies on the collision risk considering anchored ship motions. Furthermore, the safety evaluation of offshore harbor is essential, besides the safety in voyage and harbors, as part of the optimal ship routing.

4.7 Summary

Optimal ship routing is the key foundation to the safety of ship operations, including sailing in the ocean, mooring inside the port, and anchoring outside the harbor. However, very few studies have considered the anchoring status in optimal ship routing. Furthermore, it is necessary to develop safety measures for anchored ships in underestimated weather conditions, given that anchored ships have been exposed to accident risks such as stranding, and collision with other ships under rough seas. Stranding can be evaluated by the UKC based on the water depth, the draft of the ship, and the vertical ship motions. Furthermore, the risk of collision should be considered simultaneously. The anchored ship should be treated as a movable object with a dragging anchor. In this study, we simulated anchored ship motions to validate the results with the onboard measurement results. Furthermore, additional simulations were conducted under underestimated wave conditions. The risk of collision was evaluated using the AIS data and anchored ship motions. The main conclusions of this are as follows.

(1) For the simulation of anchored ship motions, the directional wave spectrum can be given as the computation of the WW III model with NCEP-FNL wind source. The anchored ship motions can be reproduced using the directional wave spectrum and showed good agreement with the onboard measurement results. It quantitatively shows how the anchored ship motions and drifted distance increase with underestimated wave conditions.

(2) A novel risk assessment for anchored ships were constructed, which included the risk of stranding in shallow waters, damaging structures on the seabed, and the risk of collision with neighboring ships. The stranding was evaluated based on the relation between the estimated UKC owing to the vertical motions and water depth. The damaging accidents were evaluated based on the existence of obstacles near the simulated ship position.

(3) The index for the risk of collision was evaluated based the factors such as the DCPA, TCPA, and SDOI. It was observed that the drifting of the ship strongly influenced the risk of collision. The risk of collision increased simultaneously if the drifted distance increased as the underestimated wave condition worsened. However, the risk of collision decreased for one of the ships near the anchored ship, even if the underestimated wave height was 3 times higher. This indicated that the risk of collision depends on the relationship between time-varying anchored ship motions and the surrounding traffic situation.

(4) Anchored ships should be treated as drifting object when ships drift over the swing circle of anchoring. This should be considered in future studies on collision risk. Furthermore, it is necessary to apply the methodology of this study to other ship types and sea areas to develop optimal ship routing.

However, the proposed risk assessment still had some limitations. Here, the potential risk for the anchored ships was individually evaluated with the three aspects (i.e., stranding, damaging, and colliding). It was necessary to express the total risk index to evaluate the offshore anchorage. Furthermore, the safety evaluation was conducted with the one target ship, applying to the three anchorages. Therefore, it is necessary to include the various type and size of ships and port terminals to standardize the risk level in the future study.

References

Booij, N. and Holthuijsen, L. H., 1987. Propagation of ocean waves in discrete spectral wave models. *Journal of Computational Physics*. Vol. 68, No. 2, pp. 307–326.

https://doi.org/10.1016/0021-9991(87)90060-X.

Bowers, E. C., 1989. The mathematical formulation of non-linear wave forces on ships. *Report no. SR193. Hydraulic Research Limited*, Wallingford, p. 48

Burmeister, H. C., Walther, L., Jahn, C., Toter, S. and Froese, J., 2014. Assessing the fr equency and material consequences of collisions with vessels lying at an anchorage i n line with IALA IWrap MkII. *TransNav, the International Journal on Marine Navig ation and Safety of Sea Transportation*. Vol. 8, No. 1, pp. 61–68. https://doi.org/10.1 2716/1001.08.01.07.

Campos, R. M. and Guedes Soares, C., 2016. Comparison of HIPOCAS and ERA wind and wave reanalyses in the North Atlantic Ocean. *Ocean Engineering*. Vol. 112, pp. 320–334. https://doi.org/10.1016/j.oceaneng.2015.12.028.

Chai, T., Weng, J. and Xiong, D., 2017. Development of a quantitative risk assessment model for ship collisions in fairways. *Safety Science*. Vol. 91, pp. 71–83.

https://doi.org/10.1016/j.ssci.2016.07.018.

Chen, C., Sasa, K., Ohsawa, T., Kashiwagi, M., Prpić-Oršić, J. and Mizojiri, T., 2020. Comparative assessment of NCEP and ECMWF global datasets and numerical approaches on rough sea ship navigation based on numerical simulation and shipboard measurements. *Applied Ocean Research*. Vol. 101, 102219. https://doi.org/10.1016/j.apor.2020.102219.

Chen, C., Sasa, K., Prpić-Oršić, J. and Mizojiri, T., 2021. Statistical analysis of waves' effects on ship navigation using high-resolution numerical wave simulation and shipboard measurements. *Ocean Engineering*. Vol. 229, 108757.

https://doi.org/10.1016/j.oceaneng.2021.108757.

Chen, S. T. and Wang, Y. W., 2020. Improving coastal ocean wave height forecasting d uring typhoons by using local meteorological and neighboring wave data in support vector regression models. *Journal of Marine Science and Engineering*. Vol. 8, No. 3, 149. https://doi.org/10.3390/jmse8030149.

CNN. 2021. Everything you're waiting for is in these containers.

https://edition.cnn.com/2021/10/20/business/la-long-beach-port-congestion-problem-national-impact/index.html. (accessed on 03 Feb 2022).

Coldwell, T. G., 1983. Marine traffic behaviour in restricted waters. *Journal of Navigation*. Vol. 36, No. 3, pp. 430–444. https://doi.org/10.1017/S0373463300039783.

Corbett, J. J., Winebrake, J., Endresen, O., Eide, M., Dalsøren, S., Isaksen, I. S. and Sø rgård, E., 2010. International Maritime Shipping: The impact of globalisation on activ

ity levels, in Globalisation, Transport and the Environment, *OECD Publishing*, Paris, pp.55-80. https://doi.org/10.1787/9789264072916-5-en.

Cummins, W. E., 1962. The impulse response function and ship motions. *Schiffstechnik*, *Bd.* 9, *Heft* 47, pp.101-109.

Debnath, A. and Chin, H., 2016. Modelling collision potentials in port anchorages: Appl ication of the Navigational Traffic Conflict Technique (NTCT). *Journal of Navigation*. Vol. 69, No. 1, pp. 183–196. https://doi.org/10.1017/S0373463315000521.

Du, W., Li, Y., Zhang, G., Wang, C., Chen, P. and Qiao, J., 2021. Estimation of ship routes considering weather and constraints. *Ocean Engineering*. Vol. 228, 108695.

https://doi.org/10.1016/j.oceaneng.2021.108695.

Ducruet, C., 2020. The geography of maritime networks: a critical review, *Journal of Tr ansport Geography*. Vol. 88, 102804. https://doi.org/10.1016/j.jtrangeo.2020.102824.

EMSA (European Maritime Safety Agency), 2020. Annual Overview of Marine Casualtie s and Incidents, Lisbon, Portugal, 147p. https://www.emsa.europa.eu/newsroom/latest-ne ws/item/4266-annual-overview-of-marine-casualties-and-incidents-2020.html.

Figuero, A., Sande, J., Peña, E., Alvarellos, A., Rabuñal, J. R. and Maciñeira, E., 2019. Operational thresholds of moored ships at the oil terminal of inner port of A Coruña (Spain), *Ocean Engineering*. Vol. 172, pp. 599–613.

https://doi.org/10.1016/j.oceaneng.2018.12.031.

Fujii, J. and Tanaka, K., 1971. Traffic capacity. *Journal of Navigation*, Vol. 24, No. 4, pp.543-552. https://doi.org/10.1017/S0373463300022384.

Gao, X. and Makino, H., 2017. Analysis of anchoring ships around coastal industrial complex in a natural disaster. *Journal of Loss Prevention in the Process Industries*. Vol. 50, Part B, pp. 355–363. https://doi.org/10.1016/j.jlp.2016.12.003.

Girolamo, P. D., Risio, M. D., Beltrami, G. M., Bellotti, G. and Pasquali, D., 2017. Th e use of wave forecasts for maritime activities safety assessment. *Applied Ocean Res earch*. Vol. 62, pp. 18–26. https://doi.org/10.1016/j.apor.2016.11.006.

Hansen, M., Jensen, T., Lehn-Schioler, T., Melchild, K., Rasmussen, F. and Ennemark, F., 2013. Empirical ship domain based on AIS data. *Journal of Navigation*. Vol. 66, pp. 931–940. https://doi.org/10.1017/S0373463313000489.

Im, N. and Luong T. N., 2019. Potential risk ship domain as a danger criterion for real-time ship collision risk evaluation. *Ocean Engineering*. Vol. 194, 106610.

https://doi.org/10.1016/j.oceaneng.2019.106610.

Inoue, K., 1981. An investigation on reducing cable tension caused by swing motion of ship moored at single anchor in wind-I: On the factors affecting the magnitude of cable tension. *The Journal of Japan Institute of Navigation*. Vol. 65, pp. 1–12.

https://doi.org/10.9749/jin.65.1. (In Japanese).

Jing, Q., Sasa, K., Chen, C., Yin, Y., Yasukawa, H. and Terada, D., 2021. Analysis of ship maneuvering difficulties under severe weather based on onboard measurements and realistic simulation of ocean environment. *Ocean engineering*. Vol. 221, 108524.

https://doi.org/10.1016/j.oceaneng.2020.108524.

John, F., 1950. On the motion of floating bodies II. *Communications on Pure and Applied Mathematics*. Vol. 3, No. 1, pp. 45–101. http://doi.org/10.1002/cpa.3160030106.

Kearon, J., 1977. Computer programs for collision avoidance and traffic keeping, *Conference on Mathematical Aspects on Marine Traffic*, London, United Kingdom, pp.229-242.

Kikutani, H., Tsuruta, S., Fukutani, T., 1983. Experimental and analytical study on the dynamic tension of mooring chain. *The Journal of Japan Institute of Navigation.* Vol. 69, pp. 17–23. https://doi.org/10.9749/jin.69.17. (In Japanese).

Kubo, M., Sakakibara, S., 1999. A Study on time domain analysis of moored ship motion considering harbor oscillations. *Proceedings of the 9th International Offshore and Polar Engineering Conference*, France, pp.574-581.

https://www.onepetro.org/conference-paper/ISOPE-I-99-309.

Liu, D. and Shi, G., 2020. Ship collision risk assessment based on collision detection al gorithm. *IEEE Access*. Vol. 8, pp. 161969–161980. https://doi.org/10.1109/ACCESS.2020.3013957.

Liu, Z., Wu, Z. and Zheng, Z., 2019. A novel framework for regional collision risk ide ntification based on AIS data. *Applied Ocean Research.* Vol. 89, pp. 261–272.

https://doi.org/10.1016/j.apor.2019.05.020.

Liu, Z., Wu, Z. and Zheng, Z., 2020. A novel model for identifying the vessel collision risk of anchorage. *Applied Ocean Research*. Vol. 98, 102130.

https://doi.org/10.1016/j.apor.2020.102130.

Lee, S. W., Sasa, K., Aoki, S., Yamamoto, K. and Chen C., 2021. New evaluation of ship mooring with friction effects on mooring rope and cost-benefit estimation to improve port safety. *International Journal of Naval Architecture and Ocean Engineering*. Vol. 13, pp. 306–320. https://doi.org/10.1016/j.ijnaoe.2021.04.002.

Lu, L. F., Sasa, K., Sasaki, W., Terada, D., Kano, T. and Mizojiri, T., 2017. Rough wave simulation and validation using onboard ship motion data in the southern hemisphere to enhance ship weather routing. *Ocean Engineering*. Vol. 144, pp. 61–77.

https://doi.org/10.1016/j.oceaneng.2017.08.037.

Lu, Y. and Bai, C., 2015. Dragging anchor event and theoretical verification of single m ooring ship. *Proceedings of the 9th International Conference on Frontier of Compute r Science and Technology, FCST 2015*, pp. 209–213.

https://doi.org/10.1109/FCST.2015.16.

Luong, T. N., Hwang, S. and Im, N., 2021. Harbour Traffic Hazard Map for real-time a ssessing waterway risk using Marine Traffic Hazard Index. *Ocean Engineering*. Vol. 239, 109884. https://doi.org/10.1016/j.oceaneng.2021.109884.

MAIA (Marine Accident Inquiry Agency), 2006. Collection of Maritime Disaster Typhoo n and Maritime Disaster, 131p.

http://www.mlit.go.jp/jtsb/kai/bunseki/bunsekikohosiryo/no6_taihu/taihutokainantop.htm. (In Japanese).

MLIT (Ministry of Land, Infrastructure, Transport and Tourism), 2009. Technical standar ds and commentaries for port and harbour facilities in Japan. Translated and edited b y The Overseas Coastal Area Development Institute of Japan, Tokyo, 981p.

http://ocdi.or.jp/en/technical-st-en.

Nakajima, T., Motora, S. and Fujino, M., 1982. On the dynamic analysis of multi-comp onent mooring lines. *Proceedings of the Annual Offshore Technology Conference*. pp. 105–110. https://doi.org/10.4043/4309-MS.

Natskår, A., Moan, T. and Alvær, P., 2015. Uncertainty in forecasted environmental cond itions for reliability analyses of marine operations. *Ocean Engineering*. Vol. 108, pp. 636–647. https://doi.org/10.1016/j.oceaneng.2015.08.034.

Pietrzykowski, Z. and Uriasz, J., 2009. The ship domain – A criterion of navigational s afety assessment in an open sea area. *Journal of Navigation*. Vol.62, pp. 93–108.

https://doi.org/10.1017/S0373463308005018.

Pietrzykowski, Z. and Wielgosz, M., 2021. Effective ship domain – Impact of ship size and speed. *Ocean Engineering*. Vol. 219, 108423.

https://doi.org/10.1016/j.oceaneng.2020.108423.

Plessas, T., Kanellopoulou, A., Zaraphonitis, G., Papanikolaou, A. and Shigunov, V., 2018. Exploration of design space and optimisation of RoPax vessels and containerships in view of EEDI and safe operation in adverse sea conditions. *Ocean Engineering*. Vol. 162, pp. 1–20.

https://doi.org/10.1016/j.oceaneng.2018.05.022.

Qinetiq, Lloyd's Register, and Univ. of Strathclyde, 2013. Global marine trends 2030. pp. 1–144.

Sasa, K. and Incecik, A., 2012. Numerical simulation of anchored ship motions due to wave and wind forces for enhanced safety in offshore harbor refuge. *Ocean Engineer ing*. Vol. 44, pp. 68–78. https://doi.org/10.1016/j.oceaneng.2011.11.006.

Sasa, K., Chen, C., Shiotani, S., Ohsawa, T., and Terada, D., 2014. Numerical analysis of failed forecasts of waves under low pressures from viewpoint of ship operation, *Proceedings of the 33rd International Conference on Ocean, Offshore and Arctic Engineering*, *OMAE2014*, pp. 1–8. https://doi.org/10.1115/OMAE2014-23876.

Sasa, K., Mitsui, M., Aoki, S. and Tamura, M., 2018. Current analysis of ship mooring and emergency safe system. *Journal of Japan Society of Civil Engineers, Ser. B2 (Coastal*

Engineering). Vol.74, No.2, pp.1399-1404. http://doi.org/10.2208/kaigan.74.I_1399. (In Japanese).

Sasa, K., Aoki, S., Fujita, T. and Chen, C., 2019. New evaluation for mooring problem from cost-benefit effect. *Journal of Japan Society of Civil Engineers, Ser. B2 (Coastal Engineering)*. Vol. 75, No. 2, pp. 1243–1248. http://doi.org/10.2208/kaigan.75.I_1243. (In Japanese).

Sasa, K., Chen, C., Fujimatsu, T., Shoji, R. and Maki, A., 2021. Speed loss analysis and rough wave avoidance algorithms for optimal ship routing simulation of 28,000-DWT bulk carrier. *Ocean Engineering*. Vol. 228, 108800. https://doi.org/10.1016/j.oceaneng.2021.108800.

Sharpey-Schafer, J. M., 1954. Anchor Dragging. *Journal of Navigation*. Vol. 7, No. 3, p p. 290–300. https://doi.org/10.1017/S0373463300020968.

Shiraishi, S., Kubo, M., Sakakibara, S. and Sasa, K., 1999. Study on numerical simulation method to reproduce long-period ship motions. *Proceedings of the 9th International Offshore and Polar Engineering Conference*, France, pp. 536–543. https://www.onepetro.org/conference-paper/ISOPE-I-99-304.

Stopa, J. E. and Cheung, K. F., 2014. Intercomparison of wind and wave data from the ECMWF Reanalysis Interim and the NCEP Climate Forecast System Reanalysis. *Ocean Modelling*. Vol. 75, pp. 65–83. https://doi.org/10.1016/j.ocemod.2013.12.006.

Sugomori, M., 2010. An empirical study on the need for anchor operation education and training. *World Maritime University Dissertations*. 418, http://commons.wmu.se/all_dissertations/418.

Tam, C. and Bucknall, R., 2010. Collision risk assessment for ships. *Journal of Marine Science and Technology*. Vol. 15, No. 3, pp. 257–270. https://doi.org/10.1007/s00773-010-0089-7.

The New York Times. 2021. 'I've Never Seen Anything Like This': Chaos Strikes Global Shipping. https://www.nytimes.com/2021/03/06/business/global-shipping.html. (accessed on 03 Feb 2022).

Tolman. H. L., 1989. The numerical model WAVEWATCH: a third-generation model for hindcasting of wind waves on tides in shelf seas. Faculty of Civil Engineering, Delft University of Technology.

Tolman. H. L., 2014. User manual and system documentation of WAVEWATCH III, Version 4.18, p. 282, *National Oceanic and Atmospheric Administration/National Weather Service/National Centers for Environmental Prediction (NOAA/NWS/NCEP)*. Technical Note.

UNCTAD (United Nations Conference on Trade and Development), 2020. Review of maritime transport. New York; Geneva, 146p. https://doi.org/10.18356/9789210052719.

Ura, T. and Toshim, T, 1980. A basic study on the transient behaviors of moored structures on the sea. *Journal of the Society of Naval Architects of Japan*. Vol. 148, pp. 121–127.

https://doi.org/10.2534/jjasnaoe1968.1980.148_121. (in Japanese).

Van der Molen, W., Monardez, P. and van Dongeren, A. P., 2006. Numerical simulation of long-

period waves and ship motions in Tomakomai port, Japan. *Coastal Engineering Journal*. Vol. 48, pp. 59–79. https://doi.org/10.1142/S0578563406001301.

Ventikos, N. P., Koimtzoglou, A. and Louzis, K., 2015. Statistics for marine accidents in adverse weather conditions. Maritime Technology and Engineering – Guedes Soares & Santos (Eds). Taylor & Francis Group, London. pp. 243–251.

https://doi.org/10.1201/b17494

Walton, T. S. and Polachek, H., 1960. Calculation of transient motions of submerged ca bles. *Journal of Mathematics of Computation*. Vol.14, No.69, pp.27–46.

https://doi.org/10.2307/2002982.

Wang, Y. and Chin, H., 2016. An empirically-calibrated ship domain as a safety criterio n for navigation in confined waters. *Journal of Navigation*. Vol. 69, pp. 257–276.

https://doi.org/10.1017/S0373463315000533.

Yeo, G. T., Roe, M. and Soak, S. M., 2007. Evaluation of the marine traffic congestion of north harbor in Busan port. *Journal of Waterway, Port, Coastal, and Ocean Engin eering*. Vol.133, No.2, pp.87-93. https://doi.org/10.1061/(asce)0733-950x(2007)133:2(87).

Zhang, C., Zhang, D., Zhang, M. and Mao, W., 2019. Data-driven ship energy efficiency analysis and optimization model for route planning in ice-covered Arctic waters. *Ocean Engineering*. Vol.186, 106071. https://doi.org/10.1016/j.oceaneng.2019.05.053.

Zhang, P. and Zhao, J., 2013. The obligations of an anchored vessel to avoid collision at sea. *Journal of Navigation*. Vol. 66, No. 3, pp. 473–477.

https://doi.org/10.1017/S0373463313000088.

Zhao, Y., Li, W. and Shi, P., 2016. A real-time collision avoidance learning system for Unmanned Surface Vessels. *Neurocomputing*. Vol. 182, pp. 255–266.

https://doi.org/10.1016/j.neucom.2015.12.028.

Zhen, R., Riveiro, M. and Jin, Y., 2017. A novel analytic framework of real-time multi-vessel collision risk assessment for maritime traffic surveillance. *Ocean Engineering*. Vol. 145, pp. 492–501. https://doi.org/10.1016/j.oceaneng.2017.09.015.

Zou, Y., Shen, C. and Xi, X., 2012, Numerical simulations on the motions of anchored capesize ships. *Journal of Navigation*. Vol. 65, No. 1, pp. 145–158.

https://doi.org/10.1017/S0373463311000580.

Chapter 5 Further Consideration on Ship Safety on Coastal Area

In this study, the ship operation on coastal area was analyzed such as the berthing, mooring, and anchoring to improve the ship safety and reduce the risk of accidents. This study has the meaning by suggesting the novel methods of safety evaluation for the each ship operation. However, there are limitations to be solved for the best solutions.

5.1 The Limitation of this Study for the Berthing Operation

(1) The berthing velocity data analyzed in this study were measured only at one tanker terminal. The range of berthing velocity could vary depending on the characteristics of the port and the type of target vessel. Therefore, the analysis results in this study can be applied to the only port terminal, which is conducted for the measurement, but it is difficult to apply to the other port terminal with different characteristics.

(2) It is impossible to evaluate the entire process of the berthing operation based on the berthing velocity alone. Although the berthing velocity is the most important factor in berthing safety, evaluation of the berthing angle and the area touching the fender should be made at the same time.

(3) In this study, there was no comparison between the kinetic energy generated from the berthing velocity and the absorbed energy due to the deformation of the fender. It is necessary to consider the damage of the fender, which is a direct problem due to excessive berthing velocity.

(4) There was insufficient consideration of side effects and economic losses that could be caused by the proposed berthing speed in this study. The appropriate berthing velocity was proposed as a statistical approach to the actually measurements. However, when these results are applied to an actual port terminal, the calculation of additional economic losses or gains should be considered.

5.2 The Limitation of this Study for the Mooring Operation

(1) There was no actual measurement for the moored ships under rough seas. It is necessary to

verify the simulation model for the moored ship. In particular, the simulation model for the mooring rope is necessary to compared with the actual measurements in port to get the reliability for this study.

(2) The additional comparison is necessary under the various conditions to compare and evaluate the characteristics of the mooring ropes. Due to the nature and location of moored ships, the mooring rope could be easily exposed to seawater. Therefore, it is necessary to consider the different condition for the mooring rope in wet conditions or dry conditions.

(3) This study was conducted on port terminal exposed to open sea and affected by long-period waves. It is necessary to compare and evaluate various ports with various characteristics through simulations. In addition, it is necessary to add consideration to the actual investigation into the port where the mooring accident occurred and the cause of the accident.

(4) The economic feasibility was evaluated by cost-benefit performance. However, the results of this economic evaluation may vary greatly depending on the development of weather forecasting. It is necessary to additionally examine the consideration of ways to strengthen mooring safety in various aspects.

5.3 The Limitation of this Study for the Anchoring Operation

(1) It was not sufficient to simulate the dragging anchor under the rough sea condition. Dragging anchor could occur when the anchor chain force is stronger than the anchor holding force. However, these forces could be different depending on various factors such as the water depth, the seabed conditions, and the shape of the anchor, etc. It can contribute to reducing the risk of accident, if there are considerations on ways to reduce dragging anchors.

(2) It is necessary to consider the additional potential risk of anchor ships. There were other accident for the anchored ships, such as the anchor loss for various reasons. It is necessary to identify the main cause of the accidents through numerical analysis and safety evaluation of anchor loss.

(3) It is necessary to evaluate the safety of anchorages of various port terminals. Although anchorages with various characteristics exist around the world, a specific safety evaluation for the anchorage has not been carried out yet. In particular, in order to identify the cause of

accidents for the offshore anchorage where accidents occur frequently, it is necessary to conduct the safety evaluation for the offshore area.

(4) It is necessary to conduct the additional research on the model of collision risk for the anchored ships. In the previous studies for the collision risk models, anchored ships were treated as fixed targets. It means that the anchored ships could not affect to the risk of collision, which is differently considered with the underway ships. However, in this study, anchored ships showed large ship motions under the rough seas, which can affect the maritime traffic increasing the collision risk. To make further consideration for the collision risk on coastal area, it is necessary to conduct to make the collision risk model near the port terminal including the anchored ships and moored ships.

Chapter 6 Conclusions

There is an urgent need for the guidelines of the safety of ship operation on coastal area. Unlike ships sailing in the ocean, the ship operations in coastal water could be in various forms such as mooring, anchoring, and berthing. In addition, all operation in the coast must be ensured to enable the safe completion of the voyage of the vessel. However, since several parties, such as shipping companies, cargo owners, port operators, and local governments are politically involved, it is difficult to solve operational problems near the port area. Therefore, more objective data and research results are needed to strengthen the safety of ship operations here.

Based on the research work discussed in this thesis, the following conclusions can be drawn:

In Chapter 2, it was performed with the statistical approach to analyze the berthing energy and berthing velocity generated during the berthing process. The berthing energy has a large effect on the berthing velocity. Such berthing velocity should be appropriately managed and supervised to prevent berthing accidents, but the research results that were actually confirmed and measured are insufficient.

(1) It was analyzed to be closer to the Weibull distribution than the lognormal distribution. Since most of the existing research results are based on the assumption that the berthing velocity follows the lognormal distribution, further studies on the assumption that it follows the Weibull distribution are needed.

(2) Also, it is necessary to revise the berth design velocity of many ports by introducing the berthing velocity in the concept of probability of exceedance following the Weibull distribution. Further studies are needed on the actual data measured on different types of vessels and other quays.

(3) It is necessary to develop a new curve to replace Brolsma's curve by deriving the relationship between berthing velocity and size of vessels (DWT) by the confidence interval.

In Chapter 3, new evaluation methods were proposed to reduce the risk of a moored ship. The safety of a moored ship is essential to maintain safety in the port (harbor tranquility). Many port

terminals facing open seas suffer from mooring problems and are exposed to mooring accidents. Therefore, it is necessary to develop more practical safety evaluation methods. In this study, new evaluation methods were proposed for the safety of moored ship operations. Unlike other studies that focused only on the tension of the mooring rope, in this study, several factors, such as friction and bending fatigue, were considered. The method suggested in this study is more effective and accurate because it encapsulates the rope-breaking mechanism. In addition, using the suggested method, optimal mooring methods were verified in terms of safety and economic efficiency. The summary of this study is as follows.

(1) With these evaluation methods, the simulation was conducted with modified mooring methods: (A) revised mooring arrangement with PP rope, (B) current mooring arrangement with HMPE rope, and (C) revised mooring arrangement with HMPE rope. By comparing these three mooring methods with the present method, we evaluated them in terms of safety and cost benefits.

(2) From the viewpoint of safety, the simulation results were compared with the safety criteria on an hourly basis. If the simulation result exceeded the criteria, this hour was defined as a dangerous hour. Therefore, the optimal mooring method from the safety point of view is the method of maintaining the lowest dangerous mooring hours. As a result, Method (C) shows the lowest number of dangerous hours. Therefore, Method (C) is the optimal mooring method for safety aspects, which is a balanced mooring arrangement with HMPE rope.

(3) To confirm economic efficiency, the FSTP was introduced. The FSTP was de-fined as total costs including investment, maintenance, and demurrage. With the FSTP, it was possible to calculate the amount of total costs as time passed. The suggested mooring methods require investment costs. Therefore, the main purpose of the FSTP is to verify that it is economically efficient enough to recover the initial investment cost. If the economic efficiency is sufficient, the FSTP ac-cumulates over time. However, Methods (A) and (B) showed negative effects, which meant that economic efficiency was not sufficient. Method (C) showed the economic benefits among the three suggested mooring methods.

(4) As a result of checking with the proposed evaluation methods in terms of economic and safety, Method (C), a balanced mooring arrangement with HMPE rope, was verified to be the optimal mooring method. Moreover, Methods (A) and (B) showed worse efficiency than the present method in terms of safety and economic efficiency.

(5) The novel mooring safety evaluation methods and the verification of the optimal mooring methods in this study are expected to help port terminals experiencing mooring problems in terms of economic and safety. However, it is necessary to verify these through actual measurements in further research. Moreover, a further analysis of the mooring safety must be conducted for different port regions, weather conditions, ship types, etc.

In Chapter 4, novel safety evaluation for the anchored ship was proposed to reduce the risk of an anchored ship as the part of optimal ship routing. To develop safety measures for anchored ships in underestimated weather conditions, it was analyzed that anchored ships have been exposed to accident risks such as stranding, and collision with other ships under rough seas. Stranding can be evaluated by the UKC based on the water depth, the draft of the ship, and the vertical ship motions. Furthermore, the risk of collision should be considered simultaneously. The anchored ship should be treated as a movable object with a dragging anchor. In this study, we simulated anchored ship motions to validate the results with the onboard measurement results. Furthermore, additional simulations were conducted under underestimated wave conditions. The risk of collision was evaluated using the AIS data and anchored ship motions. The main conclusions of this are as follows.

(1) For the simulation of anchored ship motions, the directional wave spectrum can be given as the computation of the WW III model with NCEP-FNL wind source. The anchored ship motions can be reproduced using the directional wave spectrum and showed good agreement with the onboard measurement results. It quantitatively shows how the anchored ship motions and drifted distance increase with underestimated wave conditions.

(2) A novel risk assessment for anchored ships were constructed, which included the risk of stranding in shallow waters, damaging structures on the seabed, and the risk of collision with neighboring ships. The stranding was evaluated based on the relation between the estimated UKC owing to the vertical motions and water depth. The damaging accidents were evaluated based on the existence of obstacles near the simulated ship position.

(3) The index for the risk of collision was evaluated based the factors such as the DCPA, TCPA, and SDOI. It was observed that the drifting of the ship strongly influenced the risk of collision. The risk of collision increased simultaneously if the drifted distance increased as the underestimated wave condition worsened. However, the risk of collision decreased for

one of the ships near the anchored ship, even if the underestimated wave height was 3 times higher. This indicated that the risk of collision depends on the relationship between time-varying anchored ship motions and the surrounding traffic situation.

(4) Anchored ships should be treated as drifting object when ships drift over the swing circle of anchoring. This should be considered in future studies on collision risk. Furthermore, it is necessary to apply the methodology of this study to other ship types and sea areas to develop optimal ship routing.

Publication List

[Journal Papers]

1. Lee, S-.W., Sasa, K., Aoki, S., Yamamoto, K. and Chen, C., 2021. New evaluation of ship mooring with friction effects on mooring rope and cost-benefit estimation to improve port safety. *International Journal of Naval Architecture and Ocean Engineering*. Vol. 13, pp. 306-320. https://doi.org/10.1016/j.ijnaoe.2021.04.002.

2. Lee, S-.W., Sasa, K., Chen, C., Waskito, K. T. and Cho, I-.S., 2022. Novel safety evaluation technique for ships in offshore anchorage under rough seas conditions for optimal ship routing. *Ocean Engineering*. Vol. 253, 111323. https://doi.org/10.1016/j.oceaneng.2022.111323.

[Proceedings of International Conference]

1. Lee, S-.W., Cho, J-.W., and Cho, I-. S., 2018. A study on the proposal for probability of exceedance for the berthing velocity by measured data analysis. *Proceedings of International Association of Institutes of Navigation World Congress (IAIN) 2018*. Chiba, Japan.

References

ATSB (Australian Transport Safety Bureau), 2008. Independent investigation into the breakaway and grounding of the Hong Kong registered bulk carrier Creciente at Port Hedland, Western Australia on 12 September 2006. Canberra. https://www.atsb.gov.au/publications/investigation_reports/2006/mair/mair232/.

Bae, C. H., Lee, S. K., Lee, S. E. and Kim, J. H., 2008. A Study of the Automatic Berthing System of a Ship Using Artificial Neural Network. Journal of Navigation and Port Research, Vol. 32, No. 8, pp. 589-596.

Beckett Rankine, 2010. Berthing velocities and Brolsma's curves. London, United Kingdom.

Black, K., Banfield, S.J., Flory, J.F., Ridge, I.M.L., 2012. Low-Friction, Low-Abrasion Fairlead Liners. In: Proc. OCEANS 2012 IEEE/MTS. USA, 1–11. http://doi.org/10.1109/OCEANS.2012.6405022.

Booij, N. and Holthuijsen, L. H., 1987. Propagation of ocean waves in discrete spectral wave models. *Journal of Computational Physics*. Vol. 68, No. 2, pp. 307–326. https://doi.org/10.1016/0021-9991(87)90060-X.

Bossolini, E., Nielsen, O.W., Oland, E., Sørensen, M.P., Veje, C., 2016. Thermal properties of Fiber ropes. Paper presented at European Study Group with Industry, Denmark. https://orbit.dtu.dk/en/publications/thermal-properties-of-fiber-ropes.

Bowers, E. C., 1989. The mathematical formulation of non-linear wave forces on ships. *Report no. SR193. Hydraulic Research Limited*, Wallingford, p. 48

British Standards Institution, 2014. Code of Practice for design of fendering and mooring systems: BS6349 Part 4. BSI.

Brolsma, J. U., Hirs, J. A., and Langeveld, J.M., 1977. On fender design and berthing velocities. Proc. International Navigation Congress, Section II, Subject 4, pp. 87-100.

Burmeister, H. C., Walther, L., Jahn, C., Toter, S. and Froese, J., 2014. Assessing the frequency and material consequences of collisions with vessels lying at an

anchorage in line with IALA IWrap MkII. *TransNav, the International Journal on Marine Navigation and Safety of Sea Transportation*. Vol. 8, No. 1, pp. 61–68. https://doi.org/10.12716/1001.08.01.07.

Campos, R. M. and Guedes Soares, C., 2016. Comparison of HIPOCAS and ERA wind and wave reanalyses in the North Atlantic Ocean. *Ocean Engineering*. Vol. 112, pp. 320–334. https://doi.org/10.1016/j.oceaneng.2015.12.028.

Chai, T., Weng, J. and Xiong, D., 2017. Development of a quantitative risk assessment model for ship collisions in fairways. *Safety Science*. Vol. 91, pp. 71–83. https://doi.org/10.1016/j.ssci.2016.07.018.

Chen, C., Sasa, K., Ohsawa, T., Kashiwagi, M., Prpić-Oršić, J. and Mizojiri, T., 2020. Comparative assessment of NCEP and ECMWF global datasets and numerical approaches on rough sea ship navigation based on numerical simulation and shipboard measurements. *Applied Ocean Research*. Vol. 101., 102219. https://doi.org/10.1016/j.apor.2020.102219.

Chen, C., Sasa, K., Prpić-Oršić, J. and Mizojiri, T., 2021. Statistical analysis of waves' effects on ship navigation using high-resolution numerical wave simulation and shipboard measurements. *Ocean Engineering*. Vol. 229., 108757. https://doi.org/10.1016/j.oceaneng.2021.108757.

Chen, S. T. and Wang, Y. W., 2020. Improving coastal ocean wave height forecasting during typhoons by using local meteorological and neighboring wave data in support vector regression models. *Journal of Marine Science and Engineering*. Vol. 8, No. 3., 149. https://doi.org/10.3390/jmse8030149.

Cho, I. S., Cho, J. W., and Lee, S. W., 2018. A basic study on the measured data analysis of berthing velocity of ships. Journal of Coastal Disaster Prevention, Vol.5, No.2,pp. 61-71. (in Korean)

CNN. 2021. Everything you're waiting for is in these containers. https://edition.cnn.com/2021/10/20/business/la-long-beach-port-congestion-problem-national-impact/index.html. (accessed on 31 May 2022).

Coldwell, T. G., 1983. Marine traffic behaviour in restricted waters. *Journal of Navigation*. Vol. 36, No. 3, pp. 430–444. https://doi.org/10.1017/S0373463300039783.

Corbett, J. J., Winebrake, J., Endresen, O., Eide, M., Dalsøren, S., Isaksen, I. S. and Sørgård, E., 2010. International Maritime Shipping: The impact of globalisation on activity levels, in Globalisation, Transport and the Environment, *OECD Publishing*, Paris, pp.55-80. https://doi.org/10.1787/9789264072916-5-en.

Cummins, W. E., 1962. The impulse response function and ship motions. *Schiffstechnik*, *Bd.* 9, *Heft* 47, pp.101-109.

Debnath, A. and Chin, H., 2016. Modelling collision potentials in port anchorages: Application of the Navigational Traffic Conflict Technique (NTCT). *Journal of Navigation*. Vol. 69, No. 1, pp. 183–196. https://doi.org/10.1017/S0373463315000521.

Du, W., Li, Y., Zhang, G., Wang, C., Chen, P. and Qiao, J., 2021. Estimation of ship routes considering weather and constraints. *Ocean Engineering*. Vol. 228, 108695. https://doi.org/10.1016/j.oceaneng.2021.108695.

Ducruet, C., 2020. The geography of maritime networks: a critical review, *Journal of Transport Geography*. Vol. 88, 102804. https://doi.org/10.1016/j.jtrangeo.2020.102824.

EMSA (European Maritime Safety Agency), 2020. Annual Overview of Marine Casualties and Incidents, Lisbon, Portugal, 147p. https://www.emsa.europa.eu/newsroom/latest-news/item/4266-annual-overview-of-marine-casualties-and-incidents-2020.html.

Figuero, A., Sande, J., Peña, E., Alvarellos, A., Rabuñal, J. R. and Maciñeira, E., 2019. Operational thresholds of moored ships at the oil terminal of inner port of A Coruña (Spain), *Ocean Engineering*. Vol. 172, pp. 599–613. https://doi.org/10.1016/j.oceaneng.2018.12.031.

Foster, G.P., 2002. Advantages of Fiber Rope over Wire Rope. J. Ind. Text. 32 (1), 67–75.http://doi.org/10.1106/152808302031656.

Fujii, J. and Tanaka, K., 1971. Traffic capacity. *Journal of Navigation*, Vol. 24, No. 4, pp.543-552. https://doi.org/10.1017/S0373463300022384.

Gao, X. and Makino, H., 2017. Analysis of anchoring ships around coastal industrial complex in a natural disaster. *Journal of Loss Prevention in the Process Industries*. Vol. 50, Part B, pp. 355–363. https://doi.org/10.1016/j.jlp.2016.12.003.

Girolamo, P. D., Risio, M. D., Beltrami, G. M., Bellotti, G. and Pasquali, D., 2017. The use of wave forecasts for maritime activities safety assessment. *Applied Ocean Research*. Vol. 62, pp. 18–26. https://doi.org/10.1016/j.apor.2016.11.006.

González-Marco, D., Sierra, J.P., Fernández de Ybarra, O., Sánchez-Arcilla, A., 2008. Implications of Long Waves in Harbor Management: The Gijón Port Case Study. Ocean Coast Manag. 51, 180–201. https://doi.org/10.1016/j.ocecoaman.2007.04.001.

Hansen, M., Jensen, T., Lehn-Schioler, T., Melchild, K., Rasmussen, F. and Ennemark, F., 2013. Empirical ship domain based on AIS data. *Journal of Navigation*. Vol. 66, pp. 931–940. https://doi.org/10.1017/S0373463313000489.

Hashimoto, N., Kawaguchi, K., 2003. Statistical forecasting of long period waves based on weather data for the purpose of judgment of executing cargo loading. In: Proc. 13th Int. Soc. Offshore Polar Eng. Conf. Honolulu, USA, 697–704. https://www.onepetro.org/conference-paper/ISOPE-I-03-302.

Hearle, J.W.S., Parsey, M.R., Overington, M.S., Banfield, S.J., 1993. Modelling the Long-Term Fatigue Performance of Fibre Ropes. In: Proc. 3th Int. Soc. Offshore Polar Eng. Conf. Singapore, 377–383. https://www.onepetro.org/conference-paper/ISOPE-I-93-152.

Hobbs, R.E., Burgoyne, C.J., 1991. Bending Fatigue in High-Strength Fibre Ropes. Int. J. Fatigue. 13 (2), 174–180. http://doi.org/10.1016/0142-1123(91)90011-m.

Ikeda, H., Yasuda, D., Yoneyama, H., Otake, Y., Hiraishi, T., 2011. Development of mooring system to reduce long-period motions of a large ship. In: Proc. 21th Int. Soc. Offshore Polar Eng. Conf. Hawaii, USA, 1214–1221. https://www.onepetro.org/conference-paper/ISOPE-I-11-317.

Im, N. and Luong T. N., 2019. Potential risk ship domain as a danger criterion for real-time ship collision risk evaluation. *Ocean Engineering*. Vol. 194, 106610. https://doi.org/10.1016/j.oceaneng.2019.106610.

Inoue, K., 1981. An investigation on reducing cable tension caused by swing motion of ship moored at single anchor in wind-I: On the factors affecting the magnitude of cable tension. *The Journal of Japan Institute of Navigation*. Vol. 65, pp. 1–12. https://doi.org/10.9749/jin.65.1. (In Japanese).

Jing, Q., Sasa, K., Chen, C., Yin, Y., Yasukawa, H. and Terada, D., 2021. Analysis of ship maneuvering difficulties under severe weather based on onboard measurements and realistic simulation of ocean environment. *Ocean engineering*. Vol. 221., 108524. https://doi.org/10.1016/j.oceaneng.2020.108524.

John, F., 1950. On the motion of floating bodies II. *Communications on Pure and Applied Mathematics*. Vol. 3, No. 1, pp. 45–101. http://doi.org/10.1002/cpa.3160030106.

Karnoski, S.R., Liu, F.C., 1988. Tension and Bending Fatigue Test Results of Synthetic Ropes. In: Proc. Annual Offshore Tech. Conf. Houston, USA, 343–350. http://doi.org/10.4043/5720-ms.

Kearon, J., 1977. Computer programs for collision avoidance and traffic keeping, *Conference on Mathematical Aspects on Marine Traffic*, London, United Kingdom, pp.229-242.

Kikutani, H., Tsuruta, S., Fukutani, T., 1983. Experimental and analytical study on the dynamic tension of mooring chain. *The Journal of Japan Institute of Navigation.* Vol. 69, pp. 17–23. https://doi.org/10.9749/jin.69.17. (In Japanese).

Korea Maritime Safety Tribunal, 2015. Special Investigation Report on the Contact Accidents of M/T WU YI SAN. (in Korean)

Kwak, M., Moon, Y., Pyun, C., 2012. Computer Simulation of Moored Ship Motion Induced by Harbor Resonance in Pohang New Harbor. In: Proc. 33rd Conf. Coast. Eng. Spain. http://doi.org/10.9753/icce.v33.waves.68.

Kubo, M., Barthel, V., 1992. Some Considerations How to Reduce the Motions of Ships Moored at an Open Berth. J. Japan Inst. Nav. 87, 47–58. http://doi.org/10.9749/jin.87.47.

Kubo, M., Sakakibara, S., 1999. A Study on Time Domain Analysis of Moored Ship Motion Considering Harbor Oscillations. In: Proc. 9th Int. Soc. Offshore Polar Eng. Conf. France, 574–581. https://www.onepetro.org/conference-paper/ISOPE-I-99-309.

Liu, D. and Shi, G., 2020. Ship collision risk assessment based on collision detection algorithm. *IEEE Access*. Vol. 8, pp. 161969–161980. https://doi.org/10.1109/ACCESS.2020.3013957.

Liu, Z., Wu, Z. and Zheng, Z., 2019. A novel framework for regional collision risk identification based on AIS data. *Applied Ocean Research.* Vol. 89, pp. 261–272. https://doi.org/10.1016/j.apor.2019.05.020.

Liu, Z., Wu, Z. and Zheng, Z., 2020. A novel model for identifying the vessel collision risk of anchorage. *Applied Ocean Research*. Vol. 98, 102130. https://doi.org/10.1016/j.apor.2020.102130.

Lee, S. W., Sasa, K., Aoki, S., Yamamoto, K. and Chen C., 2021. New evaluation of ship mooring with friction effects on mooring rope and cost-benefit estimation to improve port safety. *International Journal of Naval Architecture and Ocean Engineering*. Vol. 13, pp. 306–320. https://doi.org/10.1016/j.ijnaoe.2021.04.002.

López, M., Iglesias, G., 2014. Long Wave Effects on a Vessel at Berth. J. Appl. Ocean Res. 47, 63–72. http://doi.org/10.1016/j.apor.2014.03.008.

Lu, L. F., Sasa, K., Sasaki, W., Terada, D., Kano, T. and Mizojiri, T., 2017. Rough wave simulation and validation using onboard ship motion data in the southern hemisphere to enhance ship weather routing. *Ocean Engineering*. Vol. 144, pp. 61–77. https://doi.org/10.1016/j.oceaneng.2017.08.037.

Lu, Y. and Bai, C., 2015. Dragging anchor event and theoretical verification of single mooring ship. *Proceedings of the 9th International Conference on Frontier of Computer Science and Technology, FCST 2015*, pp. 209–213. https://doi.org/10.1109/FCST.2015.16.

Luong, T. N., Hwang, S. and Im, N., 2021. Harbour Traffic Hazard Map for real-time assessing waterway risk using Marine Traffic Hazard Index. *Ocean Engineering*. Vol. 239, 109884. https://doi.org/10.1016/j.oceaneng.2021.109884.

MAIA (Marine Accident Inquiry Agency), 2006. Collection of Maritime Disaster Typhoon and Maritime Disaster, 131p. http://www.mlit.go.jp/jtsb/kai/bunseki/bunsekikohosiryo/no6_taihu/taihutokainantop.htm. (In Japanese).

McKenna, H.A., Hearle, J.W.S., O'Hear, N., 2004. Handbook of Fibre Rope Technology. Cambridge: Woodhead Publishing.

Ministry of Oceans and Fisheries, 2014. Harbour and fishery design criteria. (in Korean)

MLIT (Ministry of Land, Infrastructure, Transport and Tourism), 2009. Technical standards and commentaries for port and harbour facilities in Japan. Translated and edited by The Overseas Coastal Area Development Institute of Japan, Tokyo. http://ocdi.or.jp/en/technical-st-en.

Murakami, K., Takenobu, M., Miyata, M., and Yoneyama, H., 2015. A Fundamental Analysis on the Characteristics of Berthing Velocity of Ships for Design of Port Facilities. Technical note of National Institute for Land and Infrastructure Management, No.864. (in Japanese)

Nabijou, S., Hobbs, R.E., 1995. Frictional Performance of Wire and Fibre Ropes Bent over Sheaves. J. Strain Anal. Eng. 30 (1), 45–57. http://doi.org/10.1243/03093247V301045.

Nakajima, T., Motora, S. and Fujino, M., 1982. On the dynamic analysis of multi-component mooring lines. *Proceedings of the Annual Offshore Technology Conference*. pp. 105–110. https://doi.org/10.4043/4309-MS.

National Institute for Land and Infrastructure Management (NILIM), 2015. A fundamental analysis on the characteristics of berthing velocity of ships for design of port facilities. Techinical note of national institute for land and infrastructure management, Japan:NILIM. (in Japanese)

Natskår, A., Moan, T. and Alvær, P., 2015. Uncertainty in forecasted environmental conditions for reliability analyses of marine operations. *Ocean Engineering*. Vol. 108, pp. 636–647. https://doi.org/10.1016/j.oceaneng.2015.08.034.

Ning, F., Li, X., Hear, N.O., Zhou, R., Shi, C., Ning, X., 2019. Thermal Failure Mechanism of Fiber Ropes When Bent over Sheaves. Text. Res. J. 89 (7), 1215–1223. http://doi.org/10.1177/0040517518767147.

Nguyen, P. H. and Jung, Y. C., 2007. Automatic Berthing Control of Ship Using Adaptive Neural Networks. International Jouranl of Navigation and Port Research, Vol. 31, No. 7, pp. 563-568.

OCIMF (Oil Companies International Marine Forum), 2018. Mooring Equipment Guidelines. 4th ed. London: Oil Companies International Marine Forum.

Overington, M.S., Leech, C.M., 1997. Modelling Heat Buildup in Large Polyester Ropes. Int. J. Offshore Polar Eng. 7 (01), 63–69. https://www.onepetro.org/journal-paper/ISOPE-97-07-1-063.

Park, S. H., Cho, D.J. and Oh, S. W., 2006. A Study on Pseudolite-augmeted Positioning Method for Automatic Docking. Jouranl of Korean Navigation and Port Research, Vol. 30, No. 10, pp. 839-845.

Perkovic, M., Gucma, M., Luin, B., Gucma, L. & Brcko, T., 2017. Accomodating larger container vessels using an integrated laser system for approach and berthing. Microprocessors and Microsystems, Vol. 52, pp.106-116.

PIANC (World Association for Waterborne Transport Infrastructure), 1995. Criteria for movements of moored ships in harbor: A practical guide. Brussels: PIANC General Secretariat.

PIANC (World Association for Waterborne Transport Infrastructure), 2002. Guidelines for the design of fenders systems. Report of working group 33 of the MARITIME NAVIGATION COMMISSION.

PIANC (World Association for Waterborne Transport Infrastructure), 2017. Berthing velocities and fender design, Report of working group 145 of the MARITIME NAVIGATION COMMISSION.

Pietrzykowski, Z. and Uriasz, J., 2009. The ship domain – A criterion of navigational safety assessment in an open sea area. *Journal of Navigation*. Vol.62, pp. 93–108. https://doi.org/10.1017/S0373463308005018.

Pietrzykowski, Z. and Wielgosz, M., 2021. Effective ship domain – Impact of ship size and speed. *Ocean Engineering*. Vol. 219, 108423. https://doi.org/10.1016/j.oceaneng.2020.108423.

Plessas, T., Kanellopoulou, A., Zaraphonitis, G., Papanikolaou, A. and Shigunov, V., 2018. Exploration of design space and optimisation of RoPax vessels and containerships in view of EEDI and safe operation in adverse sea conditions. *Ocean Engineering*. Vol. 162, pp. 1–20. https://doi.org/10.1016/j.oceaneng.2018.05.022.

Qiang, Z., Guibing, Z., Xin, H. and Renming, Y., 2019. Adaptive neural network auto-berthing control of marine ships. Ocean Engineering, Vol. 177, pp. 40-48.

Qinetiq, Lloyd's Register, and Univ. of Strathclyde, 2013. Global marine trends 2030. pp. 1–144.

Ridge, I.M.L., Wang, P., Grabandt, O., O'Hear, N., 2015. Appraisal of Ropes for LNG Moorings. In: Proc. OIPEEC Conf. 5th Int. Stuttgart Rope days, Stuttgart, Germany. https://oipeec.org/products/appraisal-of-ropes-for-lng-moorings.

Roubos, A., L. Groenewegen, and D.J. Peters, 2017. Berthing velocity of large seagoing vessels in the ports of Rotterdam. Marines Structures, vol. 51, pp. 202-219.

Roubos, A., D. J. Peters, L. Groenewegen, and R. Steenbergen, 2018. Partial safety factors for berthing velocity and loads on marine structures. Marines Structures, vol. 58, pp. 73-91.

Sakakibara, S., Kubo, M., 2009. Initial Attack of Large-Scaled Tsunami on Ship Motions and Mooring Loads. J. Ocean Eng. 36 (2), 145–157. http://doi.org/10.1016/j.oceaneng.2008.09.010.

Sasa, K., Kubo, M., Shiraishi, S., Nagai, T., 2001. Basic research on frequency properties of long period waves at harbour facing to the Pacific Ocean. In: Proc. 11th Int. Soc. Offshore Polar Eng. Conf. Stavanger, Norway, 593–600. https://www.onepetro.org/conference-paper/ISOPE-I-01-322.

Sasa, K. and Incecik, A., 2012. Numerical simulation of anchored ship motions due to wave and wind forces for enhanced safety in offshore harbor refuge. *Ocean Engineering*. Vol. 44, pp. 68–78. https://doi.org/10.1016/j.oceaneng.2011.11.006.

Sasa, K., Chen, C., Shiotani, S., Ohsawa, T., and Terada, D., 2014. Numerical analysis of failed forecasts of waves under low pressures from viewpoint of ship operation, *Proceedings of the 33rd International Conference on Ocean, Offshore and Arctic Engineering*, *OMAE2014*, pp. 1–8. https://doi.org/10.1115/OMAE2014-23876.

Sasa, K., 2017. Optimal Routing of Short-Distance Ferry from the Evaluation of Mooring Criteria. In: Proc. Int. Conf. Offshore Mech. Arct. Eng. OMAE, 6 (2), 1–8. http://doi.org/10.1115/OMAE201761077.

Sasa, K., Mitsui, M., Aoki, S. and Tamura, M., 2018. Current analysis of ship mooring and emergency safe system. *Journal of Japan Society of Civil Engineers, Ser. B2 (Coastal Engineering).* Vol.74, No.2, pp.1399-1404. http://doi.org/10.2208/kaigan.74.I_1399. (In Japanese).

Sasa, K., Aoki, S., Fujita, T. and Chen, C., 2019. New evaluation for mooring problem from cost-benefit effect. *Journal of Japan Society of Civil Engineers, Ser. B2 (Coastal Engineering)*. Vol. 75, No. 2, pp. 1243–1248. http://doi.org/10.2208/kaigan.75.I_1243. (In Japanese).

Sasa, K., Chen, C., Fujimatsu, T., Shoji, R. and Maki, A., 2021. Speed loss analysis and rough wave avoidance algorithms for optimal ship routing simulation of 28,000-DWT bulk carrier. *Ocean Engineering*. Vol. 228, 108800. https://doi.org/10.1016/j.oceaneng.2021.108800.

Sharpey-Schafer, J. M., 1954. Anchor Dragging. *Journal of Navigation*. Vol. 7, No. 3, pp. 290–300. https://doi.org/10.1017/S0373463300020968.

Shin, C. S., 2007. Evaluation techniques on collision force between ship and port structure. Journal of the Korean Society of Civil Engineers, vol. 25, pp. 111-118, (in Korean)

Shiraishi, S., Kubo, M., Sakakibara, S. and Sasa, K., 1999. Study on numerical simulation method to reproduce long-period ship motions. *Proceedings of the 9th International Offshore and Polar Engineering Conference*, France, pp. 536–543. https://www.onepetro.org/conference-paper/ISOPE-I-99-304.

Shiraishi, S., 2009. Numerical simulation of ship motions moored to quay walls in long-period waves and proposal of allowable wave heights for cargo handling in a port. In: Proc. 19th Int. Soc. Offshore Polar Eng. Conf. Japan, 1109–1116. https://www.onepetro.org/conference-paper/ISOPE-I-09-232.

Sloan, F., Nye, R., Liggett, T., 2003. Improving Bend-over-Sheave Fatigue in Fiber Ropes. In: Proc. OCEANS 2003 IEEE/MTS, USA, 1054–1057. http://doi.org/10.1109/oceans.2003.178486.

Stopa, J. E. and Cheung, K. F., 2014. Intercomparison of wind and wave data from the ECMWF Reanalysis Interim and the NCEP Climate Forecast System

Reanalysis. *Ocean Modelling*. Vol. 75, pp. 65–83. https://doi.org/10.1016/j.ocemod.2013.12.006.

Sugomori, M., 2010. An empirical study on the need for anchor operation education and training. *World Maritime University Dissertations*. 418, http://commons.wmu.se/all_dissertations/418.

Tam, C. and Bucknall, R., 2010. Collision risk assessment for ships. *Journal of Marine Science and Technology*. Vol. 15, No. 3, pp. 257–270. https://doi.org/10.1007/s00773-010-0089-7.

The New York Times. 2021. 'I've Never Seen Anything Like This': Chaos Strikes Global Shipping. https://www.nytimes.com/2021/03/06/business/global-shipping.html. (accessed on 03 Feb 2022).

Tolman. H. L., 1989. The numerical model WAVEWATCH: a third-generation model for hindcasting of wind waves on tides in shelf seas. Faculty of Civil Engineering, Delft University of Technology.

Tolman. H. L., 2014. User manual and system documentation of WAVEWATCH III, Version 4.18, p. 282, *National Oceanic and Atmospheric Administration/National Weather Service/National Centers for Environmental Prediction (NOAA/NWS/NCEP)*. Technical Note.

Trelleborg, 2016. Fender application design manual. Trelleborg Marine Systems.

TTI and Noble Denton, 1999. Deepwater Fibre Moorings: an Engineers' Design Guide. Ledbury.

Ueda, S., Hirano, T., Shiraishi, S., and Yamase, S., 2002. Reliability design method of fender for berthing ship. Proc. Of the 30th PIANC, pp. 692-707.

UNCTAD (United Nations Conference on Trade and Development), 2020. Review of maritime transport. New York; Geneva, 146p. https://doi.org/10.18356/9789210052719.

Ura, T. and Toshim, T, 1980. A basic study on the transient behaviors of moored structures on the sea. *Journal of the Society of Naval Architects of Japan*. Vol. 148, pp. 121–127. https://doi.org/10.2534/jjasnaoe1968.1980.148_121. (in Japanese).

Van der Molen, W., Monárdez, P., van Dongeren, A.P., 2006. Numerical Simulation of Long-Period Waves and Ship Motions in Tomakomai Port, Japan. Coast. Eng. J. 48 (1), 59–79. http://doi.org/10.1142/S0578563406001301.

Van der Molen, W., Scott, D., Taylor, D., Elliott, T., 2015. Improvement of Mooring Configurations in Geraldton Harbour. J. Mar. Sci. Eng. 4 (3). http://doi.org/10.3390/jmse4010003.

Van Essen, S., Van der Hout, A., Huijsmans, R., Waals, O., 2013. Evaluation of Directional Analysis Methods for Low-Frequency Waves to Predict LNGC Motion Response in Nearshore Areas. In: Proc. Int. Conf. Offshore Mech. Arct. Eng. OMAE 2013. https://doi.org/10.1115/OMAE2013-10235.

Ventikos, N. P., Koimtzoglou, A. and Louzis, K., 2015. Statistics for marine accidents in adverse weather conditions. Maritime Technology and Engineering – Guedes Soares & Santos (Eds). Taylor & Francis Group, London. pp. 243–251. https://doi.org/10.1201/b17494

Villa-Caro, R., Carral, J.C., Fraguela, J.Á., López, M., Carral, L., 2018. A review of ship mooring systems. Brodogradnja 69 (1), 123–149. http://doi.org/10.21278/brod69108.

Walton, T. S. and Polachek, H., 1960. Calculation of transient motions of submerged cables. *Journal of Mathematics of Computation*. Vol.14, No.69, pp.27–46. https://doi.org/10.2307/2002982.

Wang, Y. and Chin, H., 2016. An empirically-calibrated ship domain as a safety criterion for navigation in confined waters. *Journal of Navigation*. Vol. 69, pp. 257–276. https://doi.org/10.1017/S0373463315000533.

Yamamoto, K., Kubo, M., Asaki, K., Kanuma, Y., 2004. An Experimental Research on Internal Stress of Ropes Under Repeated Load. J. Japan Inst. Nav. 112, 353–359. http://doi.org/10.9749/jin.112.353. [in Japanese].

Yamamoto, K., Kubo, M., Asaki, K., 2006. Comparison between Numerical Calculation and Experimental Results of Temperature Rise on Rope under Repeated Load. J. Japan Inst. Nav. 116, 269–275. http://doi.org/10.9749/jin.116.269. [in Japanese].

Yamamoto, K. 2007. Basic research on preventing breakage of mooring ropes. PhD diss., Kobe University. [in Japanese].

Yamase, S., Ueda, S., Okada, T., Arai, A., and Shimizu, K., 2013. Characteristics of measured berthing velocity and the application for fender design of berthing ship. Annual Journal of Civil Engineering in the Ocean, JSCE Vol.69, pp. 67-72. (in Japanese)

Yeo, G. T., Roe, M. and Soak, S. M., 2007. Evaluation of the marine traffic congestion of north harbor in Busan port. *Journal of Waterway, Port, Coastal, and Ocean Engineering*. Vol.133, No.2, pp.87-93. https://doi.org/10.1061/(asce)0733-950x(2007)133:2(87)

Yoneyama, H., Minemura, K., Moriya, T., 2017. A study on calculation methods of allowable wave heights of a moored ship in remote island ports. J. Japan Soc. Civ. Eng. 73(2), 803–808. http://doi.org/10.2208/jscejoe.73.I_803. [in Japanese].

Zhang, C., Zhang, D., Zhang, M. and Mao, W., 2019. Data-driven ship energy efficiency analysis and optimization model for route planning in ice-covered Arctic waters. *Ocean Engineering*. Vol.186, 106071. https://doi.org/10.1016/j.oceaneng.2019.05.053.

Zhang, P. and Zhao, J., 2013. The obligations of an anchored vessel to avoid collision at sea. *Journal of Navigation*. Vol. 66, No. 3, pp. 473–477. https://doi.org/10.1017/S0373463313000088.

Zhao, Y., Li, W. and Shi, P., 2016. A real-time collision avoidance learning system for Unmanned Surface Vessels. *Neurocomputing*. Vol. 182, pp. 255–266. https://doi.org/10.1016/j.neucom.2015.12.028.

Zhen, R., Riveiro, M. and Jin, Y., 2017. A novel analytic framework of real-time multi-vessel collision risk assessment for maritime traffic surveillance. *Ocean Engineering*. Vol. 145, pp. 492–501. https://doi.org/10.1016/j.oceaneng.2017.09.015.

Zou, Y., Shen, C. and Xi, X., 2012, Numerical simulations on the motions of anchored capesize ships. *Journal of Navigation*. Vol. 65, No. 1, pp. 145–158. https://doi.org/10.1017/S0373463311000580.

Acknowledgement

This work would not have been possible without the support and encouragement of many people. It has been challenging to finish this work after leaving the shipping company in Korea. This acknowledgement is an attempt to express my gratitude and sincere appreciation to those who supported my efforts.

In the beginning, I would like to express my deepest gratitude to my supervisor, Professor Kenji Sasa for giving excellent guidance, valuable ideas and suggestions, constant support and encouragement during these years. His considerable help and advice could be of great help to my life in Japan. I was able to learn not only academic knowledge, but also attitude as a researcher, sincerity towards students, and responsibility for assigned tasks. I will keep his teachings in my heart for the rest of my life.

I thank Professor Teruo Ohsawa and Minoru Takeda from the bottom of my heart for invaluable feedback and insight to proof-reading and editing this work. In the process of feedback and discussion with them, I could feel the lack of my research, and I could learn how to proceed the next step in the progress of the research.

Additionally, I appreciate Professor Shin-ich Aoki of Osaka University and Professor Kazusei Yamamoto of Marine Technical College, who gave me constructive suggestions and assistant about the direction of research.

I would like to express appreciation to Professor Chen Chen of Wuhan University of Technology in China and Professor Kurniawan T. Waskito of Universitas Indonesia in Indonesia for interesting discussions and encouragement.

I am also grateful for the warmest support and encouragement from current and past members of our laboratory.

I am especially grateful to Professor Ik-Soon Cho of Korea Maritime and Ocean University, who served as my supervisor. I have been extremely lucky to have a supervisor who cared so much about my work, and responded to my questions and queries so promptly. I am deeply grateful to Professor Byeong-Deok Yea and Professor Joong-Woo Lee for their kindness and sincere advice. I wish to express my special thanks to all member in Maritime Data Mining Laboratory in Korea Maritime and Ocean University.

I also owe a different kind of debt to my family. My wife, Mina Park, was the strongest supporter of my life as she never doubted on my decision. Without her dedication, I could not have finished this graduation. I thank my parents for their reliable support on both mental and financial aspects. I cannot forget my parents-in-law as their love and support towards me was never less than those from my parents.

I owed too many people to write down all their names. Even though some names are not listed here, my appreciation towards them cannot be underestimated. Whether mentioned here or not, it is true that all of them made my Ph.D. years to be one of the happiest moments. Both my academic and personal accomplishments never could have come this far without their cheerful love and support. Thanks again for all the things that they have done to me.